October 2018

Evaluation of The Erodibility of Soft Clays and the Influence of Biopolymers

Pamela Judge
University of Massachusetts Amherst

Evaluation of The Erodibility of Soft Clays and the Influence of Biopolymers

A Dissertation Presented

by

PAMELA K. JUDGE

Submitted to the Graduate School of the
University of Massachusetts Amherst in partial fulfillment
of the requirements for the degree of

DOCTOR OF PHILOSOPHY

September 2018

Civil and Environmental Engineering

Evaluation of The Erodibility of Soft Clays and the Influence of Biopolymers

A Dissertation Presented

by

PAMELA K. JUDGE

Approved as to style and content by:

_____

Don J. DeGroot, Co-Chairperson

_____

Guoping Zhang, Co-Chairperson

_____

Jonathan D. Woodruff, Member

_____

Richard N. Palmer, Department Head
Civil and Environmental Engineering Department

DEDICATION

To my aunt Prof. Barbara M. Schaedler

for teaching me when I fall to just pick myself up, dust myself off, and try again

and

my earth science teacher Mrs. Esther C. Klein

for teaching me the key to good science is to keep asking good questions.

ACKNOWLEDGEMENTS

This research was primarily supported by the Sustainable Adaptive Gradients in the Coastal Environment (SAGE) National Science Foundation (NSF) Research Collaboration Network (RCN), project**:** Sustainable Adaptive Gradients in the Coastal Environment (SAGE): Reconceptualizing the Role of Infrastructure in Resilience, Award Number: ICER-1338767. Any opinions, findings, and conclusions or recommendations expressed in this paper are those of the authors and do not necessarily reflect the views of the NSF. Additional sources of funding which made this research possible include: The Boston Society of Civil Engineers Section (BSCES) of the American Society of Civil Engineers (ASCE) Leo Casagrande Memorial Scholarship, and several sources of support provided by the University of Massachusetts Amherst such as the Graduate School Dissertation Research Grant, Charles Perrell Fellowship, and Edith Robinson Fellowship.

Thank you to Ms. Jing Peng for her efforts of computational fluid dynamics, and index testing of soils. Thank you to Dr. Yongkang Wu, and Mr. Shengmin Lou for their assistance with X-ray Diffraction testing. Special thanks to Ms. Martha Harris and Ms. Xianxiu Xie for their assistance with biopolymer sample preparation and Liquid Limit testing. Thank you to Ms. Siyan Lin for infrared sensor and circuit board prototyping.

Thank you to Dr. Gregory Hendricks (Laboratory Manager, University of Massachusetts Medical School (UMMS)) for his assistance with the Scanning Electron Microscope (SEM). Regarding the SEM work: "The project described was supported by Award Number S10RR021043 from the National Center for Research Resources. The authors are solely the responsibility for the content of this paper and do not necessarily represent the official views of the National Center for Research Resources or the National Institutes of Health."

I would also like to acknowledge and thank the following people for helping make this research possible: Dr. Don DeGroot, advisor and mentor, for his belief in me and dedication to teaching; Dr. Guoping Zhang for serving on my committee and introducing me to the exciting topic of biogeotechnics; and Dr. Jon Woodruff for serving as my interdisciplinary committee member; Mr. Lenny Czerwonka for his machining work; Dr. Elisabeth Hamin for her devoted work to the SAGE network; Ms. Rebecca Fricke and Ms. Jodi Ozdarski for their administrative assistance; past and present graduate student for all their support; my family for their encouragement; my son Jeffrey who was my little sidekick throughout much of this dissertation; and last but certainly not least my husband Aaron who has always supported my professional goals and was a constant friend and mentor throughout my PhD program.

ABSTRACT

EVALUATION OF THE ERODIBILITY OF SOFT CLAYS AND THE INFLUENCE OF BIOPOLYMERS

SEPTEMBER 2018

PAMELA K. JUDGE, B.S., COLORADO SCHOOL OF MINES

M.S., UNVERSITY OF CALIFORNIA BERKELEY

Ph.D., UNIVERSITY OF MASSACHUSETTS AMHERST

Directed by: Professor Don J. DeGroot

Erosion of silts and clays is less well understood than erosion of sands. Further, current and anticipated climate change impacts along coastlines compel consideration of new approaches to coastal protection measures; seawalls and breakwaters designs now include natural and nature-based measures.

The first research topic consists of the Adaptive Gradients Framework which was a theoretically-informed facilitation tool. The framework was intended to aid a collaborative and interdisciplinary decision-making process to encourage inclusion of natural and nature-based measures in coastal protection planning and design. This research is the culmination of a series of workshops and fieldtrips executed by the Sustainable Adaptive Gradients in the Coastal Environment (SAGE) network.

Biopolymers could prove an effective nature-based means of stabilizing the upper portion of soft clay. Therefore, the second phase of this research investigated changes in strength, micromorphology, and microstructure for a variety of soils amended by four biopolymers (xanthan gum, guar gum, carrageenan and dextran), and then used this information to infer biopolymer-soil interactions. Test methods included liquid limit (LL), fall cone (FC), and environmental scanning electron microscopy (ESEM). Fall cone results

demonstrated both an immediate strength gain, and a time-dependent strength gain to the biopolymer-soil mixtures. Some of the biopolymers demonstrated a saturation point. Finally, the results showed that the guar and carrageenan behave fundamentally differently than xanthan and dextran. Advantages and limitations of different biopolymers were compared.

The final phase of research included design and construction of the UMass Amherst Flume (UMAF). The UMAF was built to observe erosion of very soft cohesive soils under varying tidal flow rates. Final design included an infrared sensor and sampling port. Computational fluid dynamics modeling was performed to quantify the applied stress of the fluid flow at the soil-water interface for varying speeds. The flume was validated through a series of laboratory tests including fine- and coarse-grained soils and biopolymer-soil mixtures. Results of this investigation indicate that soils with similar index properties and similar undrained shear strengths may erode at different critical erosion shear stresses. Results also indicate that biopolymers have the potential to increase critical erosion shear stress for very soft cohesive soils.

CONTENTS

Page

LIST OF TABLES

LIST OF FIGURES

LIST OF SYMBOLS AND ABBREVIATIONS

English Symbols

C_s	roughness constant
Cu	coefficient of uniformity
Cc	coefficient of curvature
cm	centimeter
D	diameter of agitator
d_{50}	mean soil grain diameter
El.	Elevation
g	grams
ha	hectare
in	inch
K	von Karmen constant
k	kinetic energy
kg	kilogram
kPa	kilo-Pascale
K_s	roughness height
k_s	effective bed roughness
L	liter
$LL_{0\%}$	Liquid Limit (no biopolymer added; control)
LL_B	Liquid Limit (biopolymer only; no soil)
m	meter
meq	miliqauvilent
MHz	MegaHertz

min	minute
mL	milliliter
mm	millimeter
N	rotational velocity of paddles
nm	nanometers
Pa	Pascale
R_e	Reynolds number
R_e^*	rougness Reynolds number
RPM	rotational speed [rotations/min]
s	second
SSC	suspended sediment concentration [g/L]
s_u	undrained shear strength
$s_{u,t0}$	undrained shear strength, at t = 0
t	time
U	average current velocity [m/s]
u	velocity at height (z) above the bed
$u*$	critical shear (frictional) velocity [m/s]
u_c^*	critical shear (frictional) velocity at the critical erosion threshold
V	volts
z	height above bed of interest
z_0	roughness length

Greek and Miscellaneous Symbols

ε	turbulent energy

ρ	density of fluid [kg/m^3]
τ_0	bed shear stress [Pa]
τ_{0max}	maximum bed shear stress [Pa]
τ_c	critical erosion shear stress [Pa]
ν	kinematic viscosity
μ	viscosity of fluid
μm	micrometer
%	percentage
<	less than
70K30M	soil consisting of 70% Prestige and 30% Pure Gold Gel, by mass
85K15M	soil consisting of 85% Prestige and 15% Pure Gold Gel, by mass
100K0M	soil consisting of 100% Prestige, by mass

Acronyms

ADV	Acoustic Doppler Velocimeter
AF	Annular Flume
CEC	Cation Exchange Capacity
CEE	Civil and Environmental Engineering
CET	Critical Erosion Threshold
CF	Clay Fraction
CL	Lean Clay
CFD	Computational Fluid Dynamics
CSM	Cohesive Strength Meter
DI	Deionized (water)

EIS	Environmental Impact Statement
EPA	Environmental Protection Agency
EPS	Extracellular Polymeric Substances
ESEM	Environmental Scanning Electron Microscope
FC	Fall Cone
IPCC	Intergovernmental Panel on Climate Change
IR	Infrared Light
LL	Liquid Limit
MAF	Mini-Annular Flume
MCDA	Multicriteria Decision Analysis
MIT	Massachusetts Institute of Technology
MLF	Motorized Lab Vane
MRF	Multiple Reference Frame
NACCS	North Atlantic Coast Comprehensive Study
NNBF	Natural and Nature-Based Features
NSF	National Science Foundation
NYC	New York City
PI	Plasticity Index
PL	Plastic Limit
PML	Plymouth Marine Laboratory
OBS	Optical Backscatter Sensor
RCN	Research Collaboration Network
SAGE	Sustainable Adaptive Gradients in the Coastal Environment
SEM	Scanning Electron Microscope
SSA	Specific Surface Area

TKE	Turbulent Kinetic Energy
UMAF	UMass Amherst Flume
UMass	University of Massachusetts
UMMS	University of Massachusetts Medical School
USACE	United States Army Corps of Engineer
USCS	Unified Soil Classification System
XRD	X-Ray Diffraction

CHAPTER 1

INTRODUCTION

Natural and nature-based coastal infrastructure (including wetlands, dunes, and oyster reefs) present an environmentally benign technique to protect coastlines from flooding and erosion due to storms and extreme tidal inundation. In some instances, natural and nature-based features (NNBF) are more cost effective that traditional structural measures for coastal protection (such as seawalls and breakwaters.) However, little remains known regarding quantitative information for NNBF for the purposes of engineering design.

The overarching objective of this research is to increase the uptake of natural and nature-based infrastructure within the coastal civil engineering community, while providing quantitative information for natural and nature-based coastal protection techniques. Specifically, this research addresses preservation of cohesive intertidal mudflat soils. Intertidal mudflats could prove beneficial to the engineering community as a means of providing space for attenuation of wave energy, and protection of near shore properties and businesses in the event of potential flood inundation. Further, if an area within intertidal mudflats is identified has having high erosion potential, it may be desirable for a community or property owner to invest resources into decreasing the erosion hazard through mitigation using a natural or nature-based approach.

Specific research objectives of this research were: (1) develop a framework for evaluating coastal protection measures in a collaborative and interdisciplinary process, (2) investigate the use of biopolymers as a potential NNBF approach to reducing erosion of cohesive intertidal mudflat soils, and (3) design and develop an annular flume for testing cohesive coastal intertidal mudflat soils.

The research is organized as follows:

Chapter 2 presents a background into the array of infrastructure measures currently available including structural, non-structural, and nature and nature-based features. Each method is clearly defined in accordance with the US Army Corp of Engineers. An introduction to the concepts of resiliency and eco-system goods and services is also provided.

Chapter 3 presents “The Adaptive Gradients Framework,” which is a facilitation tool (framework) intended to aid a community in performing a collaborative and interdisciplinary decision-making process, and ultimately select a full array of coastal protection measures. This research is the culmination of a series of extensive literature reviews, workshops, and fieldtrips executed by the Sustainable Adaptive Gradients in the Coastal Environment (SAGE) network. This chapter has been accepted for publication in the Journal *Sustainability: Sustainable Use of the Environment and Resources,* Special Issue on *Social-Ecological Restoration for Coastal Sustainability.* The paper title is "Pathways to coastal resiliency: the Adaptive Gradients Framework" with co-authors Elisabeth M Hamin, Yaser Abunnasr, Max Roman Dilthey, Pamela Judge, Melissa A Kenney, Paul Kirshen, Thomas C Sheahan, Don J DeGroot, Robert L Ryan, Brian G McAdoo, Leonard Nurse, Jane Buxton, Ariana Sutton-Grier, Elizabeth A Albright, Marielos Arlen Marin, and Rebecca Fricke. The Lead Author of the paper is the Principal Investigator of the US National Science Foundation grant: Research Collaboration Network (RCN), Science, Engineering and Education for Sustainability (SEES), "Sustainable Adaptive Gradients in the Coastal Environment (SAGE): Reconceptualizing the Role of Infrastructure in Resilience." The Author is the fourth author and together with

the third Author (Max Dilthey) were the lead PhD students on the project. The Author's key contributions to development of the Adaptive Gradients Framework and preparation of the journal paper included: conceptualization, methodology, validation, and manuscript writing, reviewing and editing. For the workshops and field trips that were the basis for development of the framework, the Author was either the lead or co-lead graduate student for five SAGE workshops (and accompanying field trips to coastal restoration projects) held in New York City (2014), Jamaica (2015), Boston (2016), Barbados, (2017) and Maryland (2018). The Author was the lead person in charge of incorporation of engineering considerations within the framework. The Author was also a Teaching Assistant for the 1st Short Course on SAGE held at Northeastern University in June 2018, where the Author demonstrated implementation of the Adaptive Gradients Framework to graduate students.

Chapter 4 then investigates biopolymers as a means of increasing soil strength, and hence, potentially reducing soil erosion. Biopolymers are naturally occurring soil binders and may prove a useful soil enhancement additive for reducing coastal erosion, increasing undrained shear strength of clay soils. This research presents the results of a series of laboratory investigation into four biopolymers (xanthan gum, guar gum, carrageenan, and dextran), and their effect on cohesive soil properties. Test methods included liquid limit, fall cone, and environmental scanning electron microscopy. Results indicate there is both an immediate and time-dependent strength gain to biopolymer-soil mixtures. Results also indicated that some biopolymers may demonstrate a saturation point, above which additional biopolymer does not provide an improvement in soil properties. Finally, results indicate that guar and carrageenan behave fundamentally differently than xanthan and dextran, likely due to the high viscosity of guar and carrageenan solutions.

Recommendations for future studies are provided, such as investigating variations in salt concentration, gaining a better understating of biopolymers under remolded conditions, and determining the best methods to incorporate biopolymers into soil on a large field scale. This paper will be submitted to the journal *Applied Clay Science*. Coauthors on this paper are expected to include Zhang, G and DeGroot, D.J.

Chapter 5 presents the design and construction of an annular flume intended to observe soft cohesive sediment erosion at varying flow rates, as well as numerical modeling to quantify applied shear stress at the soil-water interface at the time of critical erosion. The flume was validated by testing a series of very soft cohesive soils, coarse grained soils, and biopolymer-soil mixes. Results indicate that soils with similar undrained shear strength and soil index properties may have different critical erosion threshold shear stress, likely due to differences in minerology. Results also indicate that biopolymers have the potential to increase the critical erosion threshold shear stress for very soft cohesive soils. Recommendations for future studies are provided, such as testing cohesive soils and higher undrained shear strength, testing the flume on naturally occurring mudflats to examine its suitability for field testing, and determining the best methods to incorporate biopolymers into soil on a large field scale. This paper will be submitted to the American Society of Civil Engineers *Journal of Geotechnical and Geoenvironmental Engineering.* Coauthors on this paper are expected to include Peng, J., DeGroot, D.J. and Zhang, G.

Chapter 6 is the closing chapter that summarizes the original contributions of this research and provides recommendations for further study.

CHAPTER 2

BACKGROUND

2.1 Recent Coastal Flooding and Weather-Related Events

Coastal flooding due to extreme weather events and sea level rise is of growing global concern, and increasing coastal resilience to these threats is a priority for many countries. There were 11 weather and climate disaster events across the United States in 2012, including Hurricane Sandy. Nationally, these disaster events cumulatively caused 377 deaths and over $110 billion in damages (Sutton-Grier et al. 2015). Hurricane Sandy (October 29, 2012) alone flooded nearly 50 square miles of New York City (NYC), and caused tremendous damage in the city, as well as in Long Island, New Jersey, and other coastal communities. Sandy was the most destructive storm in the New York City region's history. Smaller nor'easters and tropical storms regularly cause coastal flooding and erosion, and will continue to do so. Flooding from high tides alone affects portions of New York City today (NYC 2013).

Sea levels in the New York City region have risen by roughly a foot in the last century. Middle range projections for sea level rise in New York City range from 4 to 8 inches by the 2020s and 11 to 24 inches by the 2050s (NYC 2013). As sea levels rise, the lowest-lying areas of the city will gradually become more vulnerable to regular flooding from daily and monthly high tides. Unreinforced shorelines and weakened shoreline structures will become more vulnerable to erosion. Sea level rise will mean that coastal storms will create higher storm surges that will flood larger areas, and changes in storm activity will lead to a greater number of the most intense hurricanes (NYC 2013).

2.2 Role of Coastal Ecosystems in Reducing Storm and Erosional Impacts

More and more, coastal communities are moving away from post-storm crisis response towards more proactive planning initiatives to prepare for disasters in advance to ensure their community's future existence in the dynamic coastal landscape. These communities are trying to improve their "community resiliency." Community resilience is the capability to anticipate risk, limit impact, and bounce back more rapidly through survival, adaptability, evolution, and growth in the face of turbulent change (USACE 2013).

There is an increased effort to include coastal ecosystem protection and restoration as part of coastal adaption strategies. This is due, in part, to the increased attention from the U.S. federal government and a growing interest among coastal planners at state and local level to consider natural (or "green") infrastructure, along with build infrastructure, in protecting our coastlines and communities. Thus, as the U.S. re-envisions how to increase the resilience of its coastal communities, there is a significant potential for coastal ecosystems to play an important role in reducing storm and erosional impacts (Sutton-Grier et al. 2015). In addition to providing protection from extreme weather events, coastal ecosystems strengthen resilience to chronic flooding. As sea level continues to rise, the ability of natural infrastructure to absorb chronic impacts may become even more important (Sutton-Grier et al. 2015).

2.3 USACE Recommendations

One of the predominate stakeholders in coastal protection is the United States Army Corps of Engineers (USACE). The USACE is a U.S. federal agency under the Department

of Defense and is one of the world's largest public engineering, design, and construction management agencies. Its primary responsibilities include, although are not limited to, planning, designing, building, and operating locks and dams, flood control, beach nourishment, dredging for waterway navigation, design and construction of flood protection systems through various federal mandates, and environmental regulation and ecosystem restoration. The following section describes recent recommendations provided by the USACE as it pertains to natural infrastructure for coastal protection. Many of these recommendations came out of reviewing and analyzing the impact Hurricane Sandy had on the NYC region.

United States Army Corps of Engineers (USACE) Natural and Nature-Based Features (NNBF) Final Report was a product of the North Atlantic Coast Comprehensive Study (NACCS) and was designed to support post-Hurricane Sandy recovery efforts. According to the USACE, coastal systems are increasingly vulnerable to flooding due to combined influence of coastal storms, development and population growth, geomorphic change, and sea level rise. This reality has increased efforts to make greater use of ecosystem-based approaches to reduce risk from coastal storms, approaches which draw from the capacity of wetlands, beaches, and dunes, biogenic reefs, and other natural features to reduce the impacts of storm surge and waves. The NNBF report offers details regarding the use of NNBF to improve coastal resilience. The USACE suggests an integrative framework which focuses on classifying NNBF, characterizing vulnerability, developing performance matrices, incorporating regional sediment management, monitoring and adaptively managing from a system perspective, and addressing key policy changes (USACE 2013).

2.3.1 Full Array of Measures

"Nature," "nature-based," "nonstructural," and "structural" are terms used to describe the full array of measures that can be employed to support coastal resilience and risk reduction (USACE 2013). By definition, natural features are created and evolve over time through the actions of physical, biological, geologic, and chemical processes operating in nature. Conversely, nature-based features are those that may mimic characteristics of natural features, but are created by human design, engineering, and construction to provide specific services such as coastal risk reduction. Structural measures can be designed to decrease shoreline erosion or reduce coastal risks associated with wave damage and flooding. Traditional structures include levees, storm surge barrier gates, seawalls, revetments, groins, and nearshore breakwaters (USACE 2013).

Nonstructural measures, on the other hand, include structure acquisitions or relocations, flood proofing of structures, implementing flood warning systems, flood preparedness planning, establishment of land use regulations, development restrictions within the greatest flood hazard areas, and elevated development. Nonstructural measures are most often under the jurisdiction of state and local governments which develop, implement, and regulate these measures for the community at large (USACE 2013).

USACE planning supports an integrated approach to reducing coastal risks and increasing human and ecosystem community resilience through the full array of natural, nature-based, nonstructural, and structural measures, including combinations of measures. The built components of the system include nature-based and other structures that support a range of objectives including erosion control and storm risk reduction (e.g., sea walls,

levees) as well as infrastructure providing economic and social functions (e.g., navigation channels, ports harbors, residential housing). An integrated approach to coastal resilience and risk reduction will employ a full array of measures (USACE 2013).

Structural measures are the most effective coastal protection measure, but also the most expensive. Natural and nature-based measures, on the other hand, are less effective but also less expensive. Therefore, using a hybrid approach, which consists of both natural (or nature-based) features, and structural measures, has the potential to protect the coast while keeping design, construction, and maintenance costs at a minimum (TRS 2014).

2.3.2 Ecosystem Goods and Services

It is important to recognize that the benefits of natural approaches are not limited to the value of coastal protection; they provide other benefits as well (Sutton-Grier et al. 2015). Natural, nature-based and/or structural features produce socially valued benefits that can be utilized either directly or indirectly to promote human well-being; these benefits are referred to as "ecosystem goods and services". Examples of ecosystem goods and services include, but are not limited to: aesthetics, biodiversity, carbon sequestration, clean water protection, habitat for fish and wildlife, maintenance of sediment levels, sources for raw materials, recreational venues, and tourism revenue (USACE 2015). Society determines the value or worth of these benefits. Shifts in these perceived values can be driven by any number of factors including the state of the economy as well as the dynamics of supply and demand on the goods and services themselves. Paramount to successful implementation of NNBF is the ability to create, enhance or preserve ecosystem features

and associated processes, structure and function, which ultimately culminate in the expression of goods and services (Sutton-Grier et al 2015).

2.4 Challenges with Nature and Nature-Based Features

One of the key questions about natural infrastructure is the value of the benefits provided by these systems. In other words, do these systems provide a measurable amount of storm protection benefits? As highlighted by Sutton-Grier et al. (2015), coastal wetlands in the US were estimated to provide $23.2 billion per year in storm protection services. Further, a loss of 1 ha of wetland increased average storm damages by as much as $33,000 for some storms. Another estimate for southeast Louisiana determined that coastal wetlands reduced storm surge: a 0.1 increase in the ratio of wetland to open water resulted in saving three to five properties – avoiding damages estimated between $590,000 and $792,000 for a given storm (Sutton-Grier et al. 2015).

That said, there are relatively few studies that have quantified the value of natural ecosystem for storm and erosion protection Sutton-Grier et al. (2015). This is further compounded by the challenge that there is an increased pressure from the public for engineers to consider natural and nature-based features in coastal erosion mitigation and design. To date, civil engineers are extremely limited in their professional experience designing natural and nature-based features in conjunction with (or instead of) more traditional structural engineering features. This begs the question: Is there enough available information to guide an engineer's decisions to "stamp" the drawings and plans? The professional engineer may be conflicted: not wanting to take on an excessive amount of risk in design, while at the same time wanting to meet the changing demands of society.

2.5 References

NYC (2013). "Coastal climate resilience: urban waterfront adaptive strategies." *Department of City Planning, City of New York,* June 2013, www.nyc.gov/uwas.

TRS (2014). "Resilience to extreme weather." *The Royal Society, Science Policy Center*, London, Report 02/14, Chapter 3.

Sutton-Grier, A. E.; Wowk, K.; Bamford, H. Future of our coasts: The potential for natural and hybrid infrastructure to enhance the resilience of our coastal communities, economies and ecosystems. *Environ. Sci. Policy* 2015, *51*, 137–148.USACE, 2013.

USACE (2013). "Coastal risk reduction and resilience: using the full array of measures." *Directorate of Civil Works, US Army Corps of Engineers*, CWTS 2013-3.

USACE (2015). "Use of Natural and Nature-Based Features (NNBF) for Coastal Resilience, Final Report." *Engineer Research and Development Center, US Army Corps of Engineers*, ERDC-SR-15-1.

CHAPTER 3

PATHWAYS TO COASTAL RESILIENCY: THE ADAPTIVE GRADIENTS FRAMEWORK

3.1 Preface

The following chapter presents the paper "Pathways to coastal resiliency: the Adaptive Gradients Framework" which is a cross-case analysis to encourage uptake of resilient and sustainable coastal infrastructure. This chapter was accepted for publication in the Journal *Sustainability: Sustainable Use of the Environment and Resources,* Special Issue on *Social-Ecological Restoration for Coastal Sustainability.* This work was performed by the National Science Foundation (NSF) "Sustainable Adaptive Gradients in the coastal Environment" (SAGE) Research Collaboration Network (RCN) on resilient coastal infrastructure. This research is the culmination of a series of extensive literature reviews, workshops, and fieldtrips executed by the SAGE network. The Principal Investigator for this project was Elisabeth Hamin (UMass Amherst, Regional Planning), and Co-Principal Investigators include: Don DeGroot (UMass Amherst, CEE), Melissa Kenney (University of Maryland, Decision Science), and Thomas Sheahan (Northeastern, CEE). This paper was written by an interdisciplinary committee of authors, of which the author of this dissertation was fourth author: By E Hamin, Y Abunnasr, M Dilthey, P Judge, M Kenney, P Kirshen, T. Sheahan, D DeGroot, RL Ryan, B McAdoo, L Nurse, J Buxton, E Roper, E Albright, M Buchanan, M Marin, R Fricke.

The Author of this dissertation is an active member in SAGE, having participated in five SAGE workshops: 2014 (New York, in person), 2015 (Jamaica, in person), 2016 (Boston, via Skype), and 2017 (Barbados, via Skype), and 2018 (Maryland, in

person). The Author photo-documented the 2014 and 2015 workshop field trips and wrote Field Trip Summary reports, available to the public at: http://www.resilient-infrastructure.org/sage-2015-workshop.html. The Author's efforts supporting this paper predominantly included providing technical language and definitions on the current standard of practice for coastal infrastructure within the professional civil engineering community. The Author participated in numerous webinars, case study analyses, literature reviews, figure preparation, and document formatting. The Author also attended monthly meetings with the UMass Amherst Landscape Architecture and Regional Planning (LARP) Department to help LARP graduate students understand more technical and civil engineering related aspects of their dissertation or masters research. The Author's primary contribution was command of core civil engineering; the Author summarized engineering literature and design codes (such as those provided in the US Army Corps of Engineers or Uniform Building Codes) and described them in straight forward terms non-engineers could understand and implement into this interdisciplinary work.

The Author presented a seminar talk on "Pathways to coastal resiliency: the Adaptation Gradients Framework ~ or ~ SAGE from a Civil Engineering Perspective" to the UMass Amherst Civil and Environmental Engineering Geotechnical Group in November 2017. The Author also presented a poster talk on SAGE at the National Counsel for Science and the Environment (NCSE) 18th National Conference and Global Forum on Science Policy and the Environment: The Science, Business, and Education of Sustainable Infrastructure in Arlington Virginia, January 2018. Finally, the Author was a Teaching Assistant for the first SAGE Short Course offered at Northeastern

University in June 2018 where the author demonstrated implementation of the Adaptive Gradient Framework to graduate students.

3.2 Abstract

Current and future climate-related coastal impacts such as catastrophic and repetitive flooding, hurricane intensity, and sea level rise necessitate a new approach to developing and managing coastal infrastructure. Traditional "hard" or "grey" engineering solutions are proving both expensive and inflexible in the face of a rapidly changing coastal environment. Hybrid solutions that incorporate natural, nature-based, structural, and non-structural features may better achieve a broad set of goals such as ecological enhancement, long-term adaptation, and social benefits, but broad consideration and uptake of these approaches has been slow. One barrier to the widespread implementation of hybrid solutions is the lack of a relatively quick but holistic evaluation framework that places these broader environmental and societal goals on equal footing with the more traditional goal of exposure reduction. To respond to this need, the Adaptive Gradients Framework was developed and pilot-tested, with the goal of making it easier for communities to understand, evaluate, and potentially select more diverse kinds of infrastructural responses, including natural, nature-based, and regulatory/cultural approaches, as well as hybrid designs combining multiple approaches. The framework is a theoretically-informed facilitation tool based on a collaborative and interdisciplinary evaluation process. It enables rapid expert review of project designs based on technical and economic fitness as well as social benefits, ecological enhancement, greenhouse gas reduction, and institutional capacity. The article

presents the framework and a pilot test of its application, along with resources that would enable wider application of the framework by practitioners and theorists.

3.3 Introduction

The many and varied recent coastal disasters highlight the importance of creating more resilient coastal areas. Climate change is exacerbating the impact of these events, along with the increased concentration of people and assets in urban areas. Some impacted areas will be abandoned through retreat. Others will be rebuilt, and new lands will continue to be urbanized, bringing opportunities to re-envision infrastructure designs. The stakes are high – one study found that protecting seaports across the globe from climate change will require about 49 million metric tons of concrete alone [1] if traditional construction methods are used; globally, 271 million people are at risk from coastal flooding, and that number will rise to 345 million by 2050 [2]. The risks for small island developing states are particularly high [3,4], as 2017 hurricanes Irma and Maria in the Caribbean have shown. All of these threats and concerns due to climate change are leading communities to re-consider approaches for coastal protection. More socially and ecologically beneficial coastal resiliency actions are necessary given the continuing build-up of coastlines and the interdependence of ecosystems and social-ecological resilience [5].

Recent years have seen significant advances in developing a wider range of options for coastal restoration and protection [6], and projects now include approaches that go beyond traditional infrastructure. The range of choices includes natural, nature-based, and non-structural measures such as living shorelines [7], revised building codes, zoning, and community disaster preparedness [8]. Here, we define hybrid designs as those that include

non-structural interventions such as zoning changes and local capacity building alongside green and grey approaches (see Figure 3.1). Current research suggests that hybrid projects may provide the greatest potential for improving resilience to climate impacts [9–12], with different components working together to create mutually supportive conditions. When compared to traditional methods, this broader portfolio of coastal adaptation options can achieve social and environmental objectives alongside exposure reduction, and may achieve change across multiple criterion [13,14], as recommended in the Intergovernmental Panel on Climate Change (IPCC) Fifth Assessment Report [15].

Despite the strong research into theory and design innovations in coastal adaptation, adoption of hybrid projects has been slow, albeit increasing [18]. One of the challenges of hybrid approaches is that they require holistic consideration of biophysical, engineering, economic, legal and sociocultural components. These projects bridge across discipline-specific practices and terminology, posing logistical and methodological challenges for policy-makers and designers [19]. Nordenson & Seavitt [20] find that coastal land use decisions and planning would be greatly improved with a clear identification and articulation of a broad potential range of goals such as ecosystem support and co-benefits for impacted communities. A interdisciplinary approach that utilizes a diversity of expertise, experience, and perspectives across multiple stakeholders from the practitioner, academic, and public domains would assist in overcoming this barrier.

To address this need, a network of North American and Caribbean researchers, the Sustainable Adaptive Gradients in the coastal Environment (SAGE) network, developed the Adaptive Gradients Framework as a means of improving the visibility and facilitating the discussion of multiple goals for coastal systems projects, including social, ecological,

and technical aspects. In this article we detail this Adaptive Gradients framework and provide a case study, demonstrating how this Framework can highlight the range of goals these more complex, hybrid projects may achieve.

3.3.1 Gradients

Many, if not most, natural processes exist along a continuum defined by fairly constant (but sometimes steep) gradients. The concept of a gradient informs the design of the Adaptive Gradients Framework, by suggesting the consideration of different aspects of coastal resiliency along sliding scales. Gradients describe the range of conditions in a particular system, placed along some scale (e.g. temporal, spatial, biofunctional, etc.) that will allow comparison across cases [21]. For instance, climate tends to vary along a longitudinal gradient from hot, moist equatorial regions to cold, dry polar regions, and historically, biological systems are fairly well adapted to the temperatures and weather patterns along this gradient. However, this adaptation is being challenged by climate-change induced changes, such as droughts and extreme weather events. Many regional socio-economic characteristics can be conceptualized along gradients as well, such as population density, income inequality, or population health. However, not all characteristics are gradual. Physical factors for hazard risk can change quite abruptly, such as types of offshore soils, and social characteristics like ethnic self-identification can be quite distinct in adjacent regions. This gradient concept informs the intellectual foundation of the Adaptive Gradients framework.

3.3.2 Current Frameworks and Barriers to Hybrid or Greener Designs

The IPCC frameworks on risk provide a baseline language for resilience planning [22]. The IPCC finds that disaster risk is based on physical conditions amplified by anthropogenic contributions to climate change, using socially-framed impact parameters. More precisely, risk from climate change is defined as a function of hazards, exposure and vulnerability. Hazard is the climate-related physical event, including storms, droughts, landslides, increased disease vectors, etc., with climate change as an exacerbating factor. Vulnerability is defined as the level of susceptibility to harm, while exposure is the people, assets, and ecosystems that may be affected by a hazard event. Applying these to a hurricane yields this basic form of analysis: what is the seriousness of the hurricane (the hazard); how many people, which ecosystems, and what value or social importance of buildings and other assets will likely be affected (the exposure), and how well the systems and people are likely to recover (the vulnerability). At the local level, projects may reduce hazard through such actions as reducing wave height and energy. They may also ameliorate exposure by moving or protecting the people, species, and ecological, social, and economic resources in at-risk areas. This reduces vulnerability [23]. Other definitions of risk take a more probabilistic approach, with risk being defined as the probability of an event (the hazard) times the consequences (the vulnerability). [24,25]

Structural/grey infrastructure interventions, as the defacto baseline for many coastal projects, are often well suited to addressing exposure. These traditional grey approaches may, however, also encourage maladaptation, in which projects intended to improve resilience also increase greenhouse gas emissions, burden the most vulnerable, or create other social issues while pursuing the stated mission [26]. Particular organizational norms

may strongly orient to structural interventions, such as the use of benefit-cost analysis for Environmental Impact Statement (EIS) by the U.S. Environmental Protection Agency (EPA) and/or structured decision-making practices used by the U.S. Geological Survey for environmental management [27,28] or the US Army Corps of Engineers. Even when agencies seek to expand beyond these traditional measures (see, e.g., [16]), they may be challenged by the complexity of social and environmental dimensions of resilience such as the technical challenge of an uncertain climate future [29], and difficulty in effectively addressing aspects of justice and public participation in decision-making under complexity [30]. As climate change impacts increase across the globe, well-established prescriptive approaches for identifying initial or preferred protection solutions [29] have been criticized for being too restrictive, often failing to encompass socioeconomic realities and plurality in stakeholder values and objectives [32]. This leaves prescriptive, unidimensional approaches inadequate for long-term resilience [33].

Among the barriers for uptake of infrastructure innovations is that most institutions experience path dependence, which Mathews et al [34] define as "situations where institutions become used to responding to specific issues and are consequently reluctant to respond to new imperatives when they manifest." Minor incremental change is easier than major shifts in organizational culture. Deeply held social norms such as a preference for knowledge stability (comfort in knowing what we know, rather than the challenge of admitting what we don't know) and predictability may work against the kinds of innovative and novel practices required for climate change adaptation planning and policies [35]. For green infrastructure, path dependence tends to lead to adding multiple goals as secondary considerations within existing planning frameworks, rather than undertaking more

substantive change [34]. Path dependence exists at the project scale as well. Once design alternatives are identified and significant dollars are spent on modeling those alternatives, an organization is less likely to consider significant changes to a design. To overcome these issues, it may be helpful to influence processes early in the development of a project, before significant resources (financial, as well as institutional and reputational) are invested in a particular, and likely more traditional, approach.

Beyond the challenge of path dependence, a range of other barriers to the adoption of more innovative resilient infrastructure has been identified. In adaptation more generally, identified barriers can be categorized as a lack of leadership, lack of resources, challenges in communication and information, and conflicting deeply held values and beliefs [36]. Lack of information is a critical problem, as planners and decision-makers are often asked to implement adaptation measures without adequate information about local-scale impacts, vulnerabilities, or the long-term consequences of an intervention [37]. This is particularly challenging in situations which lack officially accepted projections or institutional mandates for using projections that do exist [38,39]. The breadth of disciplinary knowledge required for hybrid designs is another informational challenge; a decision framework that supports hybrid designs will need to supplement typical engineering expertise with ecological, social, land use, policy and participatory process knowledge.

An important response to these challenges has been to complement traditional engineering effectiveness and benefit-cost analysis with a focus on the benefits of projects that go beyond their contributions to exposure reduction, central as that remains (see, e.g., [40]). The term co-benefits is defined in some contexts as complementarity between

mitigation and adaptation [41]; here, we use a broader definition that describes how project outcomes achieve locally-desired goals outside of primary hazard reduction, such as health benefits from particulate reduction through urban greening, provision of locally desired public space, or restoration of local fisheries through erosion control [42]. A just distribution of benefits is an important theme in research and practice of climate adaptation because less-resourced communities tend to experience greater environmental risk [43,44]. Given the challenges and conflicting priorities facing local governments, it can be politically and practically helpful to publicly and clearly define these anticipated co-benefits [45].

Based on current literature, infrastructure planning and evaluation should incorporate concepts of resilience and vulnerability[46-48], address climate adaptation [36,49], establish indicator systems [50], and utilize monitoring and assessment as integral to the project [51]. A more inclusive process may help communities make better infrastructure decisions [52]. It is also good practice to include local knowledge of biophysical, socio-economic, and community components of resilient infrastructure, at both local and regional scales [53]. This local knowledge helps communities find solutions that work well for their particular needs.

Research finds that generalizable approaches to project assessment may be effective and appropriate [54]. While theory is well developed, the applications of theory in practice is under-represented in academic literature [37]. Despite a portfolio of adaptation measures to choose from, planners may feel left without the resources necessary to confidently make decisions, particularly for innovative and complex projects. Based on the literature above as well as perspectives developed through the process described in the

section below, we believe that a structured facilitation tool for the development of resilient infrastructure should be used early in a decision process in order to clearly identify co-benefits, integrate a range of disciplines, facilitate a range of technical and social objectives, and promote a transparent process with the potential for high levels of stakeholder participation. These observations underlie the Adaptive Gradients Framework that is proposed in this study.

3.4 Methods

These findings were reached through a collaborative four-year process undertaken by the SAGE network. SAGE is a NSF-funded network of thirty academics and practitioners across the domains of engineering, ecology, and social science, and includes representation from the US Northeast and the Caribbean, with several members from Europe. The project's webpage is http://www.resilient-infrastructure.org, where details of our process and background data for this paper can be found. The goal of the network was to enable cross-disciplinary and cross-geographic learning, with the particular goal of encouraging the adoption of greener, more resilient, and more just infrastructure practices. Early meetings focused on identifying barriers to the uptake of green infrastructure. A key problem that members identified was the lack of a holistic way to evaluate projects, one which would directly recognize a wider range of potential project goals early in project design. Such an approach could be most useful after initial project scoping and idea development but before issuing a full Request for Proposals, so that the RFP criteria can identify broader project goals and opportunities. This evaluation is straightforward enough to be easily explained to decision-makers and politicians, and quick and inexpensive

enough to be done in less-resourced communities and countries as well as more developed ones.

To be systematic about responding to the need for more holistic infrastructure evaluation, the SAGE network undertook a holistic, collaborative, iterative theory-building research project, and began building a case study data bank (see Figure 3.2). The first phase began in 2014 with an online survey asking SAGE network participants from the US and Caribbean (n=28) to identify the most important factors for enabling greener infrastructure. Survey participants included social scientists, civil engineers, ecologists, and policy experts in both public and private sectors, including NGO's, planning organizations, universities, and government, representing the breadth of the SAGE research network (see acknowledgements section for a list of network members). Survey participants were deliberately selected to ensure that the foundational data for the framework was representative of an interdisciplinary and holistic perspective.

All subjects gave their informed consent for inclusion before they participated in the study. The study was conducted in accordance with the Declaration of Helsinki, and the protocol was approved by the Ethics Committee of the University of Massachusetts, Amherst (2013-1734). The survey asked research participants two overarching questions:

- What are the most important factors that should, or do, influence decisions regarding particular types of coastal infrastructure will be chosen for a particular site?
- What are the greatest barriers to using 'greener' types of infrastructure choices?

Results for this first research phase were inductively coded, categorized, and re-checked with respondents at a following workshop to assure categorization was considered valid. A wide range of barriers and factors were identified.

For phase 2 of the research, a second survey was sent to network participants asking them to prioritize the factors they thought were most important to assess coastal infrastructure projects. The top factors that influence the choice of coastal infrastructure identified in this phase were (in alphabetical order): ethical and policy fitness, including whether the project could be managed by the entities, and whether it achieved justice goals; financial effectiveness; whether there was sufficient information about an intervention type to make decisions; fit to local community and social goals; and combined technical and ecological fitness. In surveys one and two short answer responses included nuanced explanation. When respondents chose information as a key barrier, for instance, they discussed it in three ways -- whether there was sufficient information to evaluate a project, whether the public would understand it, and how the project dealt with uncertainty. Survey findings were discussed at SAGE workshops and site visits in 2014, 2015 and 2017 with local and national decision-makers in the US Northeast, Jamaica, and Barbados, respectively.

Given the short answers to the surveys supplemented through discussions during the workshops with SAGE network members and practitioners in these locations, we refined and expanded the gradient scope, as follows. The complexity in responses indicated the initial five gradients were likely not sufficient for a full evaluation. For example, ecology and technical fitness each needed their own category; information as a category was too broad and it was difficult to evaluate what we do not know; regulatory

and political feasibility needed to be separate from issues of justice; benefits to local communities were not necessarily the same as a participatory process; a project's ability to contribute to reductions in greenhouse gases was not covered in other items. These findings lead to the eight gradients which make up the Adaptive Gradients Framework: exposure reduction, cost efficiency, institutional capacity, ecological enhancement, adaptation over time, greenhouse gas reduction, participatory process, and social benefits, as defined and further described in the results section.

Discussions among the overall group carefully considered ways to visualize the gradients and the data to support the gradient findings. The importance of clear, communicative visuals is supported by research, which suggests that the abstract nature of climate change, predicted to take place in distant locations in the distant future, contributes to challenges in thinking about, communicating about and caring about the issue [55,56]. Beyond knowledge transfer, communicating about climate change to engage the audience in seeking change can be challenging [57]. Network members who work closely with policymakers stressed the importance of a one-page summary with a graphic of findings that can be shown to high level politicians to generate discussion and support for change. An example of this is shown in Figure 3.4. Members also highlighted the value of using graphic visualization tools to engage discourse with decision makers and co-produce understanding about climate change priorities. In the end we felt that the most visually compelling but easy to produce graphic was the 'spider diagram' shown in Figure 3.5.

Phase three tested the case study protocol and underlying Adaptive Gradients Framework. The SAGE network developed a case study protocol where data could be organized in a replicable and comparable form, available on our website. The use of a

rigorous case study template is a core feature of the process, providing a reproducible path for data collection and analysis. The Network developed four extensive case studies of community coastal interventions: Harlem River Park redevelopment in New York City, Palisados Boardwalk in Jamaica; East Boston coastal protection project in Boston, USA; Ferry Point living shoreline in Maryland. Two of these are already built (Harlem River, Palisados) while two are in design (East Boston, Ferry Point). One case study (Harlem River) is detailed in Figure 3.4; for brevity we could not present the full detail of the other case studies here, but all are included on our project website. The data for these case studies was gathered through document analysis, except for Palisados which we also visited, and organized into the case study protocol. In 2016 and 2017, the SAGE group applied the Adaptive Gradient Framework to these cases in an iterative refinement process. The steps for each included:

1. Lead researcher and assistant use secondary documents to prepare case study while also providing secondary documents to whole panel
2. Panel members collaboratively discuss the case study to identify and solidify basic information;
3. Individual panel members use the Adaptive Gradients Framework to evaluate the project;
4. Researcher collates the individual evaluations;
5. Full panel discussion of ratings to identify where differences were from varying interpretations of data or gradient framework, and which were basic differences in evaluation

6. Revisions to case study and framework to reflect uncertainties uncovered in the panel discussion
7. Reranking of the case study by individual panel members based on new information and collaborative discussion of results.

At the workshop in summer 2017 we undertook proof-of-concept testing by evaluating a site proposal in the British Virgin Islands with government officials from there. By this point the evaluation was fast -- two days total -- the gradient definitions were judged sufficient for rating by the workshop attendees, and the feedback from the client was positive about the Framework's worth. Later, a practitioner's guide was also developed and is available on our website (http://www.resilient-infrastructure.org/practitioners-guide.html). This provides very plain language description of the gradients and the process, referring to this paper as the intellectual support for the report.

3.5 Results

The eight gradients developed using the surveys, workshop, and case study are identified and explained below, including some example considerations that could be asked in a particular evaluation. Each of these provides an important element to include for evaluation of a coastal resiliency project or proposal. Different projects will of course have slightly different questions for each gradients, based on the context of the project and the proposed interventions. The gradients and their relationship to infrastructure projects is summarized in Figure 3.3. Applying the Adaptive Gradient Framework is further explained following the discussion of the individual gradients.

- **Exposure Reduction**

Exposure reduction can be defined as the ability to successfully reduce impacts to at-risk populations or assets when a hazard occurs. Exposure reduction is often the primary goal of infrastructure projects evaluated with existing engineering methods. The amount of exposure reduction will also be relative to the assets (population, buildings, etc.) at risk. Some factors that are particularly important to consider for the Exposure Reduction category include how well the project design will function under different kinds of storm events (such as Nor-Easters or hurricanes). If the project is using built infrastructure such as jetties or seawalls, was consideration given to whether these hardened structures would increase vulnerabilities or other problems such as erosion to adjacent shorelines beyond the immediate project area? Project proposals that are highly rated on this gradient are judged to be technically likely to reduce the impact of hazards.

- **Cost Efficiency**

Actions taken need to demonstrate efficient use of funds and resources, typically measured through standard or extended benefit-cost analysis. It is important to consider both construction and maintenance costs in this category. Some green infrastructure, such as living shorelines, may have lower maintenance costs than grey infrastructure, as the reefs, dunes and marshes have the potential to improve and adapt with time. Green infrastructure is not without maintenance cost, however, as regular monitoring, waste removal and replanting are often required. The incorporation of new and innovative funding practices like climate finance and green financial institutions may increase cost efficiency when compared to traditional loans and financing options. A highly rated

project will represent a good/low-cost use of money from sources that suit the local situation.

- **Institutional Capacity**

Projects that are highly rated on this gradient will be a good match to the responsible agency's ability to both fund and maintain the project. The administrative unit's ability to fund the project will impact its implementation, so that available bonding capacity and funding record for that scale of project is important. During the design and construction phase, some factors to consider in this gradient include the experience of the design and construction team(s), their success rate with similar projects, and the diversity of the skills sets on the team(s). Also important to consider are how well the project team is going to work with local, regional and national level governments to facilitate the permitting process, to ensure that project designs will be well-received and are likely to receive regulatory approval. Partnerships with other local companies, NGOs, and academic institutions may be able to provide help with data collection and monitoring or input on design and implementation to facilitate a successful project. Post-construction institutional capacity matters as well. Projects focusing on changing zoning will require the ability of the government to enforce regulations. Green infrastructure, for instance, as a distributed system that may be located on both public and private lands may require more maintenance staff and administration than a more centralized grey system [58]. Projects focusing on changing zoning will require the ability of the government to enforce regulations. At the same time, a project may assist in building capacity in the agencies responsible. For this

gradient we define institutional capacity as the match to governmental or non-governmental strengths, attributes, and resources that reduce impacts, mitigate harm, and ensure future resilience [59,60]. This is reflected in the IPCC model which suggests explicit consideration of socio-economic development pathways and assuring that institutions have the capacity to lead change and respond to risk [61]. A strong match of institutional capacity to the particular challenges of the project being evaluated will bring a high rating on this gradient.

- **Ecological Enhancement**

Given the high level of biodiversity in coastal areas along with the essential economic resources provided by coastal habitat, projects should be evaluated on how effectively they support or improve the health of local ecosystems. Analysis of this gradient is likely to vary depending on site and regional conditions – rural areas typically offer greater opportunity for ecological preservation due to low development density, while urban areas offer increased potential for innovative or resource-intensive solutions that support remaining coastal habitats. This gradient considers how much ecological "uplift" or improvement a project is going to achieve. If an area has lost beach or wetland habitat, for example, and the project aims to restore as much or more habitat than the amount lost, then this project will have an overall ecological benefit to the area. In order to effectively quantify this benefit, however, it is important to have baseline data on what habitats have been lost or degraded or what habitat features have become degraded (such as decreases in water quality or fishery production or wildlife usage). It may be important for project design teams to include ecological expertise in order to ensure that ecological

enhancements occur and to be able to accurately measure these enhancements in comparison to baseline (pre-project) conditions. Additionally, it is important to balance the anticipated long-term ecological benefits with any project impacts to score the overall ecological enhancement of the project. Average rated projects may contribute to sustaining the current ecology, while highly rated projects are expected to contribute to improving local and regional ecologies over the long term.

- **Adaptation Over Time**

Solutions should also be effective over time, as social and particularly climatic conditions change. A coastal dune system, for instance, may become more effective at hazard reduction over time as plantings grow, while a seawall may become less effective if sand is scoured from its base over the years. Fitness to projected climate change should also be considered in this gradient. An example of designing for adaptability is to include expected climate change impacts into project plans, such as requiring wider setbacks from the shore to anticipate sea level rise. Well designed projects may indicate different steps to take over time as conditions change, such accommodating flooding now and retreating from the shoreline as sea levels rise. This can be conceptualized as adaptation pathways [62,63], creating windows of opportunity for matching infrastructural needs to emerging conditions [64]. Adaptation over time does not necessarily mean getting it right the first time, but instead planning via regular monitoring and funding to implement adaptive management as needed to assure that the project functions well despite landscape and socio-economic changes. Plans for monitoring and assessment will also support this gradient, particularly if those plans are binding and properly funded. One important

consideration for coastal projects is how much is sea level predicted to rise in the project area over the next 100 years. With these estimates, projects can actually plan to accommodate sea level rise in the design. For example, if marsh habitat is being restored, it is possible to design the elevation of the marsh to include more high marsh species and area which will eventually become low marsh habitat as sea levels rise. It may also be possible to build into the project design forested or other habitat behind the marsh which will not be marsh in the present conditions but will allow the marsh to migrate inland as sea level rises such that the total amount of marsh habitat may be able to stay constant despite sea level rise. Consideration of projected population and land use changes is equally important to consider in resilient designs. Thus, a project that explicitly considers climate and socio-economic projections, builds in flexibility or technical capacity to match expected future conditions, and/or enables flexible responses to future changes would receive a high score for adaptation over time.

- **Greenhouse Gas (GhG) Reductions**

Projects can be evaluated on whether they represent more or less embodied energy and/or carbon sequestration. Embedded energy is considered to be the sum total of energy used to extract or mine raw materials, manufacture the raw materials into a product, and transport that product to market, while carbon sequestration means the long-term storage of carbon in plants, soils and the like. Typically, concrete has a high embodied energy because it takes a great deal of energy to produce, while living shorelines have low embodied energy and also provide a carbon sink. Plantings in general and coastal wetlands in particular tend to sequester carbon, so project designs that include a substantial amount

of living material will usually result in fewer GHG emissions. Projects can also be evaluated on whether they provide long-term energy efficiency, such as including wind turbines in a design. General principles of sustainability, such as use of local or recycled material, can be considered here. This gradient encourages intention in design, so that GHG-reducing strategies are more readily adopted into adaptation practices as they scale upwards over time. Currently, few projects include explicit GhG calculations. Including explicit discussion of GhG in the design or the request for proposals will be contribute to higher ratings on this gradient, as will a lower overall accounting of greenhouse gases associated with the project's construction and operation.

- **Participatory Process**

A participatory process evaluation asks whether the process was transparent, who was included in the decision-making, and whether participants had enough power in the process so that their perspectives made a difference in the final design of the project [65,66]. Collaborative processes that engage stakeholders in deliberations are common in participatory processes [67]. Diverse groups should be engaged, including those who may not as readily come to community meetings, and participatory processes should influence the final design of a project [68–70]. Factors to include in evaluation of this gradient are whether multiple mechanisms of engagement were used before, during, and after the project implementation, and to the extent that it can be determined, the level of enthusiasm of the participants and their assessment of the inclusivity of diverse perspectives and consideration of stakeholder goals. A high ranking on this criterion will come from having processes that represent the diverse publics affected by the project, a strong institutional

history of engaging diverse publics and directing projects toward achieving expressed stakeholder goals, and a demonstration that the public participation and expressed stakeholder goals changed the design of the project.

- **Social Benefits**

This category addresses both distributive equity and co-benefits. Regardless of participatory process, the actual or anticipated outcomes of a project can contribute to a more equitable and fair balance of benefits and costs and may redress old harms; conversely, projects can have unanticipated negative distribution of consequences, thereby continuing patterns of injustice [39,71]. A particular concern is that climate risk is unevenly distributed, as is the ability to pay for protection and recovery from hazard. Thus, projects that are scored highly in this gradient should benefit community members in historically disadvantaged groups. They may provide indirect social community benefits, such as jobs, recreation opportunities, and healthy accessible environments for a broad population. Specific evaluation of the co-benefits of a project will help to operationalize this issue – are there clear advantages, such as recreational access or improved air quality, for disadvantaged populations? If the investment is likely to increase property values and thus has the potential to bring in new development pressure, has consideration been given to gentrification possibilities? Highly rated projects should appropriately distribute benefits and costs and build a more equitable society through improving the position of those most affected by economic and environmental injustice [72,73].

3.5.1 The Framework, Applied to Harlem River Park

In Figure 3.4, we demonstrate the application of the adaptive gradients using one case study, Harlem River Park in New York City. This tidal strait was strongly affected by Hurricane Sandy. The project is an early example of integrating green and grey infrastructure to achieve social benefits, and is intended to illuminate the use of the gradients rather than to be a representative coastal case study. Figure 3.5 presents a diagram of results from the case study

3.6 Discussion and Conclusions

3.6.1 Implementation of the Adaptive Gradients Framework

The Adaptive Gradients Framework outlines the process an expert review panel can use for a fairly rapid assessment of general project designs. Because it is context specific, it is designed for use in one site at a time with a host who provides information and can use the results, rather than as a cross-case comparison tool. It will be useful in comparing proposed design packages early in the determination of a project. Analysis through the Adaptive Gradients Framework could also occur in different phases of a project's life, for assessment at intervals along the planning and post-construction timeline for a particular project. Time up front is required for working with the host to gather information and discuss evaluation goals and then for the panel leader to develop a case study following the protocol identified above. At the site, two or three days would likely suffice. It is important that evaluation teams include technical experts from a range of disciplines.

The philosophy behind the scoring process is that knowledge is built collaboratively and through shared development of understanding. Scoring is done by the whole team on all gradient categories to enable discussion about differences in evaluation. The gradient definitions are standard as shown above, but their application may vary by individual panel member and individual site, which is why a team approach is necessary. We have found it helpful to have individuals do their own scoring first, and then to discuss those ratings collaboratively to come to a consensus evaluation. Confidence in analyses is increased with multiple iterations of scoring and discussion, helping to create a consistent scale interpretation across disciplines and individuals. Evaluations are descriptive, qualitative, and highly contextual, which is why we believe that non-numeric ranking is best (eg., 'low' to 'high'). The role of the panel is not to weight the importance of different gradients. Instead, the host can compare results to their own goals and hopes for the project. A low score in some categories may be fine in any particular situation, depending on project goals and stakeholder mission.

Based on our pilot tests of the framework, we envision that an agency or city using the Adaptive Gradients process for a proposed site will proceed as follows:

1. The initiating organization develops basic case study materials organized along gradients, with multiple design options.
2. A panel is chosen including technical experts plus representatives of a diverse stakeholder group.
3. Pre-scoring is conducted by each member of the panel based on case study materials.

4. Ideally, a site visit with meetings with stakeholders is conducted, but this could be done remotely to save travel time.
5. Panelists discuss their preliminary scoring of the project to highlight differing perspectives; individuals may choose to change their own scoring based on the discussion. Any needed further information is gathered.
6. A final score or score range for each gradient is agreed upon by the group. Where consensus on a score is not reached, the range of scores that individual panel members endorse is included in the final report.
7. Finally, results are placed into the 'spider diagram', a simple visual summary which helps inform policy-makers regarding different policy goals achieved by different proposals.
8. An optional step is for the evaluating team to make recommendations for improving the project based on the analysis done in the steps above.

3.6.2 Limitations

The Adaptive Gradients process framework is designed as a discussion tool, providing a holistic approach to project and proposal evaluation. It does not take the place of a full Environmental Impact Statement, and engineering reviews will still be necessary; in fact these studies will often form the basis of the information used to do the Gradients analysis. The qualitative rankings are intended to encourage a more interdisciplinary and holistic approach to the decision-making process. The inclusion of qualitative data and more elusive concepts like participation and process is necessary, but is challenging for

scoring. The more technical members of each team (e.g., engineers) found qualitative scoring particularly difficult. Similarly, scoring the effectiveness of exposure reduction, for instance, was challenging for social scientists on the team. For both of these cases, collaborative discussion of results led by experts from the appropriate topic area was beneficial. This points to the necessity of cross-disciplinary teams and discussion amongst members to create a valid outcome. The visual of the gradients can be construed as an argument that each gradient should be equally weighted; rather, each situation will have goals that are most important, and thus gradients will be differentially important in different contexts. Given that we did not want to pre-decide weighting, we felt the even presentation was the most valid, but a local implementation should consciously discuss weighting as part of their analysis. Smaller projects may be constrained in ways that prevent high achievement across all the gradients, while more complex and larger projects or a portfolio of smaller projects may be expected to perform better across all gradients.

3.6.3 Conclusions

Current and anticipated acute and chronic climate change impacts such as catastrophic and repetitive flooding, sea level rise, and other challenges of climate change along coastlines are resulting in communities becoming more interested in considering new approaches to make their communities more resilient to these threats. However, to help broaden the suite of solutions being considered by communities, and in particular to make those solution options more holistic and inclusive, it is very important that communities consider a wider range of objectives when discussing alternative solutions. This includes considering factors such as social equality or ecological benefits of projects which have

typically not been considered when only traditional, built approaches to deal with coastal protection (such as sea walls or levees) are the only available options.

It is essential that research and practice reduce knowledge gaps across disciplines and between academics and policymakers, enabling the adoption of infrastructural solutions that meet a wide range of goals, supporting adaptation decisions that increase resilience to climate change. The Adaptive Gradients Framework proposed here meets this criteria through the explicit qualitative evaluation of eight Adaptive Gradients covering the most relevant socio-economic and biophysical variables in a multi-day, interdisciplinary process. Our case study of Harlem River Park illustrates that the evaluation method can be implemented and led us to design an eight step process for it to be carried out by an evaluation team. This was supported by testing with three other case studies.

The next step in the research is for our research team to analyze results from implementing the process in a range of settings. To facilitate this process we are undertaking workshops in Maryland and Puerto Rico to test the process of applying the gradients to project proposals. We also see opportunities for application of the Adaptive Gradients Framework by public and private sector entities with responsibility for choosing coastal resilience interventions and will be seeking feedback about the effectiveness of the framework in these applications. While our focus is coastal projects, there is no reason that the framework needs to be limited to coastal application – holistic solutions are needed in a range of ecological and social settings. We invite others to use the case study template and contribute case study data, and to utilize the framework for collaborative inquiry and decision-making; together, this will build a stronger evidence-basis for understanding the goals and mechanisms that lead to more resilient coastal infrastructure. We hope the

Adaptative Gradients Framework will become a useful tool for communities to help expand the set of solutions being considered as communities make investments to increase their resilience, and encourage practitioners to download the Practical Guide to Collaborative Project Evaluation (Fricke and Hamin, 2017), available on our website.

The challenges of planning in the face of changing climates is extremely critical in coastal settings which are already being severely impacted by rising sea-levels and extreme weather events. The Adaptive Gradients Framework provides a unique and innovative approach to address these hazards while at the same time strengthening social, economic, and ecological resilience to these challenges. As described by Kelman et al. [74], "those most vulnerable to one challenge tend to be most vulnerable to other challenges," creating a condition of multiple exposure to hazards. The framework allows planners to help vulnerable communities address a range of challenges that are exacerbated by coastal flooding and other disaster events. Building climate change resilience requires addressing the range of issues facing a community beyond engineering and technical solutions, and will assist communities in creating projects with benefits now and into the future.

3.7 Supplementary Materials

The following are available on line at http://www.resilient-infrastructure.org:

1. Case study protocol
2. Practical Guide to Collaborative Project Evaluation
3. Harlem River case study
4. Ferry Point case study
5. Palisados case study

6. East Boston case study

3.8 Author Contributions

All authors contributed to concept development both at in-person meetings and asynchronously. All authors co-wrote draft or final sections. Y Abunnasr and B McAdoo developed figures. EM Hamin developed web survey. E Hamin and MA Kenney supervised development of case studies. Y Abunnasr, P Judge, P Kirshen, JA Buxton, L Nurse, EA Albright, RL Ryan, AE Sutton-Grier and MA Marin co-wrote or edited sections. E Hamin, D DeGroot, T Sheahan, B McAdoo, and MA Kenney developed initial SAGE project concepts. R Fricke managed the research project and contributed to concept development.

3.9 Other SAGE Network Member Acknowledgements

Other SAGE members contributed to overall development of the project and the ideas and implementation of the gradients concept. These include Allison Baer, Maya Buchanon, Angela Burnett, Barbara Carby, John Charlery, Carter Craft, David Dodman, Fernando Gilbes, Mervin Hastings, Lorna Inniss, Lianna Jarecki, James Kostaris, David Kriebel, Ainsley Lloyd, Kim Penn, Rob Pirani, Tim Randhir, Cynthia Rolli, Steven Scyphers, Kevin Smith, Bhaskar Subramanian, Robert Walker, Dale Webber, Mona Webber, and Robert Weiss.

3.10 Funding

This project is supported by the NSF Research Collaboration Network (RCN): Science, Engineering and Education for Sustainability (SEES), Project title: Sustainable Adaptive Gradients in the Coastal Environment (SAGE): Reconceptualizing the Role of Infrastructure in Resilience Award Number: ICER-1338767 and USDA Massachusetts Agricultural Experiment Station Grant MAS00458. In-kind support was also provided by the Jamaican Government and the University of the West Indies and Pratt University. We gratefully acknowledge the time shared with us by Hurricane Sandy recovery stakeholders in New York City.

3.11 Conflicts of Interest:

The authors declare no conflict of interests. The funding sponsors had no role in the design of the study; in the collection, analyses, or interpretation of data; in the writing of the manuscript; and in the decision to publish the results.

3.12 Figures

NATURAL AND NATURE-BASED (or "Green")

Ecosystem-services based approaches which may be preserving long-standing natural processes or creating/recreating such systems through human intervention

EXAMPLES: Dunes and Beaches, Vegetated Features, Oyster and Coral Reefs, Barrier Islands, and Constructed wetlands and floodable parks

Sand Dune Replenish-ment, post-Sandy

New York City, USA
SAGE Field Trip,
2014 Workshop

STRUCTURAL (or "Grey")

Designed to decrease shoreline erosion or reduce coastal risks associated with wave damage and flooding

EXAMPLES: Levees, Storm Surge Barriers, Seawalls and Revetments, Groins, and Detached Breakwaters

Groins for wave reduction

New York City, USA
SAGE Field Trip,
2014 Workshop

NONSTRUCTURAL

Modifications in public policy, management practices, regulatory policy, and pricing policy to achieve resilience goals.

EXAMPLES: Floodplain Policy and Management, Increasing coastal building setbacks, Inter-agency recovery planning, Community organization for disaster safety, and Flood insurance rate management

Emergency Housing Planning shipping container prototype

New York City, USA

SAGE Field Trip, 2014 Workshop

(continued on next page)

INTEGRATED (or “Hybrid”)

Draws from the full array of coastal risk reduction measures, considers the engineering attributes of the component features and the dependencies and interactions among these features over both the short and long term with a focus on effectiveness.

EXAMPLES: Combinations of Examples Listed Above

Replenishing Sand, Riprap, and Planting Mangroves

Palisadoes Tombolo, Jamaica

SAGE Field Trip, 2015 Workshop

TRANSFORMATIVE

Recognized through its aspirations for broader social and ecological change. Portfolio projects that integrate effectiveness goals along with local benefits, ecological improvement, and a just and transparent process.

EXAMPLES: Coastal defenses providing locally desired play space - Renters insurance subsidies along with integrated infrastructure - Hybrid design of dune nourishment, boardwalk development, removal of at-risk structures, local fisheries protection and shoreline access developed through participatory process.

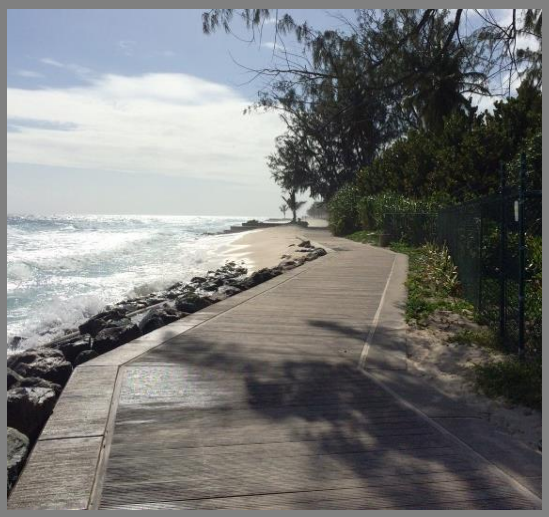

Boardwalk, replenished sand & costal vegetation for tortoise habitat, and aesthetics for hotel redevelop-ment

Barbados

SAGE Site visit, 2016

Figure 3.1: Defining infrastructure and intervention types.

This figure synthesizes language used across several disciplines around types of coastal resilience measures, particularly engineering, policy, and landscape architecture, to ensure interdisciplinary accuracy in conversation. The first panel presents nature-based engineering and ecosystem approaches; the second panel focuses on traditional built forms such as seawalls; the third panel identifies alternative approaches that focus on regulations and culture to change coastal resiliency; and the final panel defines the integration of these three as fully hybrid approaches. Sources:[8,16,17]. Photos: SAGE Workshop Field Trips and site visits; 2014-2016. Photo credit: Rebecca Fricke.

Phase 1	Network survey 1: Relevant factors & barriers
Objective	• Identify the universe of factors that influence infrastructure decisions
Action	• Categorize responses, eliminate duplicates, unify terminology (surveys = 28); completed May 2015. Result is 38 factors that influence infrastructure project decisions.
Validation	• Workshop Discussion: Generating the categories -- group discussion of survey 1 results.
Results	• Assure that categories represent participant views (participants = 31); completed June 2015.

Phase 2	Network survey 2: Ranking the factors
Objective	• Identify the most important factors that influence infrastructure decisions; use this to develop initial gradients
Action	• Retain items selected by at least 50% of experts and categorize; completed August 2015. Results in 5 factors / gradients.
Validation	• Workshop Discussion: Testing the categories -- group discussion of survey 2 results with input from policymakers in network.
Results	• Gradients expanded to 7 for clarity, preliminary defintions developed for each category.

Phase 3	Gradients applied to case studies
Objective	• Test and refine gradient framework
Action	• Prepare case study protocol based on gradients defined in phase 2
Validation	• Case study tests: 4 project cases prepared using case study protocol; In-person writing workshop tests preliminary gradients by evaluating case studies.
Results	• Refine gradients definitions and add Greenhouse Gas Reduction (completed February 2018). • Final test: BVI case study with hosts.

Figure 3.2: Phases of the Adaptive Gradient Framework development and testing process

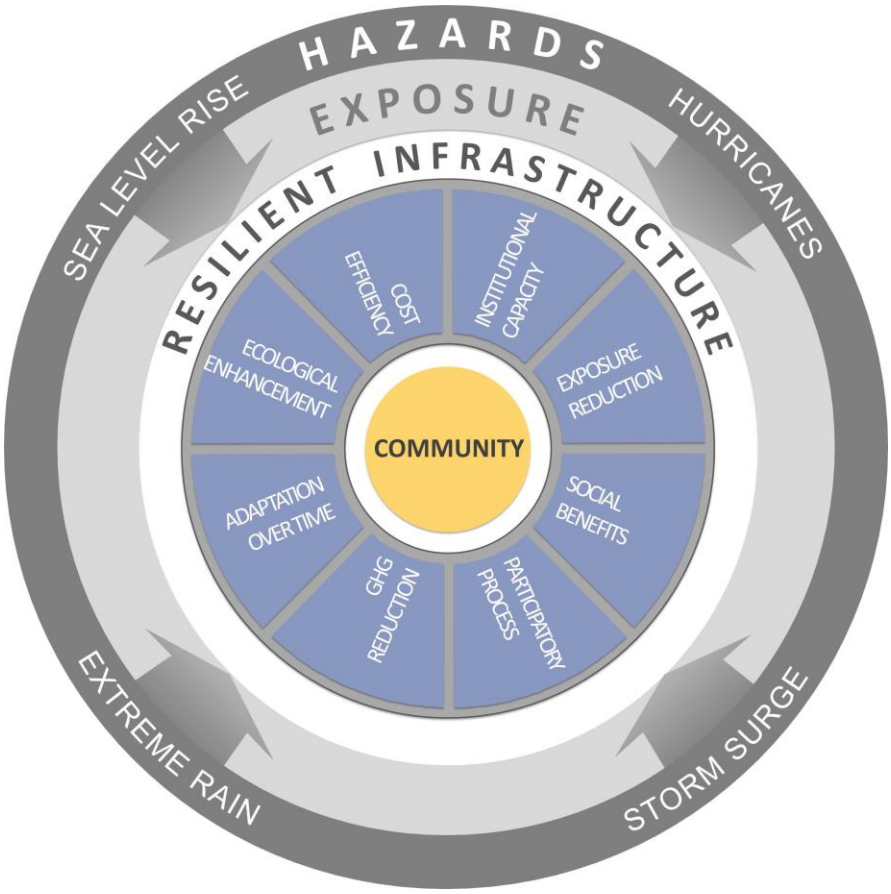

Figure 3.3: Adaptive Gradients as dimensions of holistic project assessment.

Resilient infrastructure protects coastal communities from current and future hazards by reducing exposure while achieving multiple goals. Emerging practices focus on hybrid projects, which may include green (ecosystem based), grey (traditional built infrastructure), and non-structural (zoning, building codes, governance) components. The Adaptive Gradients, shown as the inner wheel, summarize the various dimensions of project success. Outcomes can be measured by contributions to exposure reduction, institutional capacity, cost efficiency, ecological enhancement, adaptation over time, greenhouse gas reduction, participatory process, and social benefits. Investing in the expansion of coastal defenses and incentivizing collaboration between integrated spheres of influence results in better buffering of the community from hazards and uplift to other goals. Evaluation across all these measures will encourage adoption of more complete and community appropriate resiliency interventions, both currently and as climate changes over time.

Case Study Box: Harlem River Park, New York

BACKGROUND: The Harlem River Park is a 20-acre linear park on a dense urban riverfront between the busy Harlem River Parkway and the Harlem River between 132nd and 145th streets, on the north-east coastline of Manhattan New York. Harlem River Park serves a dense urban environment with vulnerable populations of which 49% live in poverty, 10% are immigrants, 87% of housing units are rentals, and the median household income is $31,105 (U.S Census Bureau, 2016). Risks include flooding from coastal as well as inland sources. Original site conditions include degraded hard shorelines, rip-rap, bulkhead and revetment (HRNEER, 2015).

THE PROJECT: The Harlem River Park revitalization was a three-phase community initiated project aimed to keep the coastline from eroding into the water. Designs were strongly influenced by community activism. Completed in 2009, the $14.3M project was funded by a combination of state and city funding and a $40,000 NY State "Designing the Edge" grant, to research and include habitat-friendly alternatives for water access. This grant enabled the installation of alternatives to standard infrastructure such as porous sea-walls of stacked green walls, flexible gabions, and tide pools. The site also features a focus on native vegetation (HRNEER, 2015).

RESULTS: As a pilot test of the Gradients theory we synthesized existing documents into a case study template which provides both a narrative of the case and data organized to match the gradients. This was sent to a peer panel of seven SAGE experts for evaluation along the gradients from a range of fields including engineering, coastal science, landscape architecture, and planning. Results of the panel are presented in the table below to give a sense of what the pilot study found. Note that the review ratings varied across experts and fields, particularly in areas with less information and/or subjective topics such as equitable outcomes, social capacity or GHG emissions.

Gradient	Rating	Representative Comments from Different Expert Panel Members
Exposure	Medium-low	The project performed well during Hurricane Sandy. With the project there, less debris was reported built up after the hurricane. Good spaces for flooding.
Institutional Capacity	Medium-high	Scored high because of grant funding. I thought about the time it took for the project and the steps taken over the years.
Cost Efficiency	Medium-high	I scored this high because I think it cost less than if they had used all grey infrastructure. I think the maintenance costs/longterm costs are uncertain.
Ecological Enhancement	Medium-high	Vegetation is doing well. They are still figuring out the tree growth/maintenance. I didn't give a 3 because they used gray (walls) and not a lot of green.
Adaptation over Time	Medium	The project creates tidal pool areas and new volumes of space for water. The vegetation has room to migrate. If the sea rises will this need to be raised? The project should include an analysis of how it would hold up with sea level rise.
Greenhouse Gas Reduction	Medium-low	Green space is better than concrete. I would need to know where the materials and vegetation was grown and what kind of lighting is used. GHG emissions weren't considered in the design process. Even on small projects, consideration of GHG reduction sets a standard for future. development.
Participatory Process	High	Community was the one who sparked the project and involvement lasted the whole process. The outcome was changed as a result of community participation.
Equitable Outcomes	High	The neighborhood is relatively poor so investment there brings a good score. I scored it high because the project improved the overall environmental quality and program options for the area.

Foot Notes: Based on a neighborhood defined as New York County Census tract 210 (Census, 2016) which is a 0.08 Sq mile residential bedroom community with a population of 7,144. • Greenwalls – sea walls fostering plant growth of various sizes from the "Verdura System," with small plantable pockets, suitable for vines, grasses and small plants the "Evergreen Wall" which is suitable for trees (2). • Gabion – a mesh container filled with heavy materials such as rock, or broken concrete used in the construction of dams, retaining wall, etc (8).

Figure 3.4: Harlem River case study

This demonstrates the application of the Adaptive Gradients framework, summarizing the findings from the case study template and results from a collaborative peer-review process.

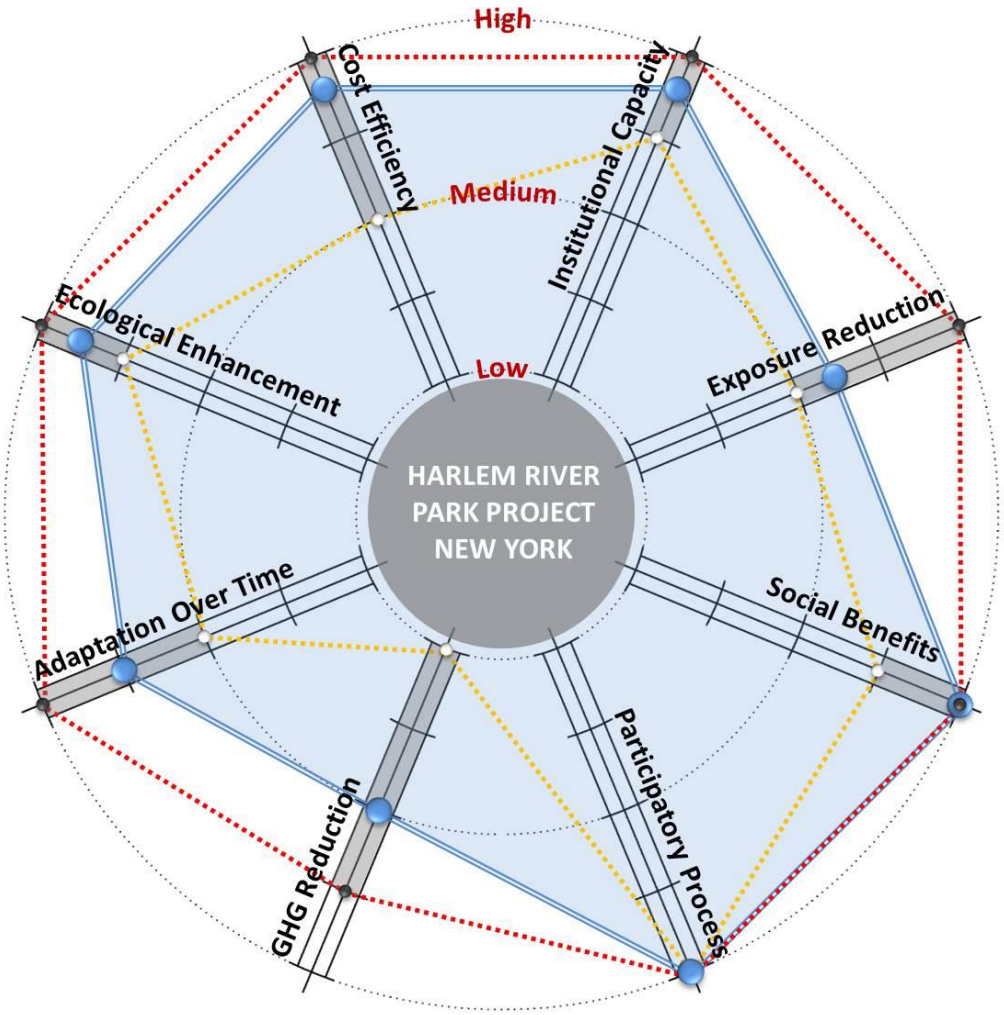

Figure 3.5: Adaptive Gradients 'Spider Diagram' for Harlem River Park case study

The relative outcomes for the Harlem River case study are presented along the eight Adaptive Gradients. Blue buttons are the average of the scores, red line shows the maximum for each assessment by individuals on the peer review panels, and yellow the minimum scored outcome by a panel member. The grey bar represents the range of evaluations by the peer panel. Note that evaluation is on a qualitative scale from low to high, rather than numerical, to highlight the important role that judgement plays in each person's score. In this case we scored a built project to test its actual outcomes.

3.13 References

1. Becker, A.; Chase, N. T. L.; Fischer, M.; Schwegler, B.; Mosher, K. A method to estimate climate-critical construction materials applied to seaport protection. *Glob. Environ. Change* **2016**, *40*, 125–136.
2. Jongman, B.; Ward, P. J.; Aerts, J. C. J. H. Global exposure to river and coastal flooding: Long term trends and changes. *Glob. Environ. Change* **2012**, *22*, 823–835.
3. Mycoo, M. Sustainable tourism, climate change and sea level rise adaptation policies in Barbados. *Nat. Resour. Forum* **2013**, *38*, 47–57.
4. Pelling, M.; Uitto, J. I. Small island developing states: natural disaster vulnerability and global change. *Global Environmental Change Part B: Environmental Hazards* **2001**, *3*, 49–62.
5. Adger, W. N.; Hughes, T. P.; Folke, C.; Carpenter, S. R.; Rockström, J. Social-ecological resilience to coastal disasters. *Science* **2005**, *309*, 1036–1039.
6. Sandifer, P. A.; Sutton-Grier, A. E.; Ward, B. P. Exploring connections among nature, biodiversity, ecosystem services, and human health and well-being: Opportunities to enhance health and biodiversity conservation. *Ecosystem Services* **2015**, *12*, 1–15.
7. NOAA *Guidance for Considering the Use of Living Shorelines*; National Oceanic and Atmospheric Administration, U.S. Department of Commerce, 2015;.
8. Sutton-Grier, A. E.; Wowk, K.; Bamford, H. Future of our coasts: The potential for natural and hybrid infrastructure to enhance the resilience of our coastal communities, economies and ecosystems. *Environ. Sci. Policy* **2015**, *51*, 137–148.
9. Chen, L.C., Liu, Y.C., & Chan, K.C. Integrated Community-Based Disaster Management Program in Taiwan: A Case Study of Shang-An Village. Nat Hazards Natural Hazards. *Journal of the International Society for the Prevention and Mitigation of Natural Hazards* **2006**, *37*, 209–223.
10. Allen, K. M. Community-based disaster preparedness and climate adaptation: local capacity-building in the Philippines. *DISA Disasters,* **2006**, *30*, 81–101.
11. Muttarak, R.; Pothisiri, W. The role of education on disaster preparedness: case study of 2012 Indian Ocean earthquakes on Thailand's Andaman Coast. *Ecology & Society*

2013, *18*, 1–16.

12. Lutz, W.; Muttarak, R. Forecasting societies' adaptive capacities through a demographic metabolism model. *Nat. Clim. Chang.* **2017**, *7*, 177–184.
13. Neuman, M. Infiltrating infrastructures: On the nature of networked infrastructure. *Journal of Urban Technology* **2006**, *13*, 3–31.
14. Brown, H. *Next generation infrastructure : principles for post-industrial public works*; Island Press: Washington; Covelo; London, 2014;.
15. Klein, R. J. T.; Midgley, G. F.; Preston, B. L.; Alam, M.; Berkhout, F. G. H.; Dow, K.; Shaw, M. R. Adaptation opportunities, constraints, and limits. In *Climate Change 2014: Impacts, Adaptation, and Vulnerability. Part A: Global and Sectoral Aspects. Contribution of Working Group II to the Fifth Assessment Report of the Intergovernmental Panel on Climate Change*; Field, C.B., V.R. Barros, D.J. Dokken, K.J. Mach, M.D. Mastrandrea, T.E. Bilir, M. Chatterjee, K.L. Ebi, Y.O. Estrada, R.C. Genova, B. Girma, E.S. Kissel, A.N. Levy, S. MacCracken, P.R. Mastrandrea, and L.L. White, Ed.; Cambridge University Press, 2014; pp. 899–943.
16. Bridges, T. S.; Burks-Copes, K. A.; Bates, M. E.; Collier, Z. A.; Fischenich, J. C.; Piercy, C. D.; Russo, E. J.; Shafer, D. J.; Suedel, B. C.; Gailani, J. Z.; Rosati, J. D.; Wamsley, T. V.; Wagner, P. W.; Leuck, L. D.; Vuxton, E. A. *Use of natural and nature-based features (NNBF) for coastal resilience*; U.S. Army Engineer Research and Development Center, Environmental Laboratory, Coastal and Hydraulics Laboratory: Vicksburg, MS, 2015;.
17. National Research Council; Division on Earth and Life Studies; Board on Atmospheric Sciences and Climate; America's Climate Choices: Panel on Adapting to the Impacts of Climate Change *Adapting to the Impacts of Climate Change*; National Academies Press, 2011; ISBN 9780309145916.
18. Zaidi, A.; Timothy, D. T. M. Incorporating Natural Infrastructure and Ecosystem Services in Federal Decision-Making Available online: https://www.whitehouse.gov/blog/2015/10/07/incorporating-natural-infrastructure-and-ecosystem-services-federal-decision-making (accessed on Nov 20, 2016).
19. Kenney, M. A.; Hamin, E. M.; Sheahan, T. C. Reconceptualizing the Role of Infrastructure in Resilience. *Eos Trans. Amer. Geophys. Union* **2014**, *95*, 298–298.

20. Nordenson, G.; Seavitt, C. Structures of coastal resilience: Designs for climate change. *Soc. Res.* **2015**, *82*, 655–671.
21. Brown, C.; Ghile, Y.; Laverty, M.; Li, K. Decision scaling: Linking bottom-up vulnerability analysis with climate projections in the water sector. *Water Resour. Res.* **2012**, *48*.
22. IPCC *Climate Change 2014: Synthesis Report. Contribution of Working Groups I, II and III to the Fifth Assessment Report of the Intergovernmental Panel on Climate Change*; Core Writing Team, R.K. Pachauri and L.A. Meyer., Ed.; IPCC: Geneva, Switzerland, 2014;.
23. IPCC *Climate Change 2014: Impacts, Adaptation, and Vulnerability Summaries, Frequently Asked Questions, and Cross-Chapter Boxes, A Contribution of Working Group II to the Fifth Assessment Report of the Intergovernmental Panel on Climate Change*; Field, C.B., V.R. Barros, D.J. Dokken, K.J. Mach, M.D. Mastrandrea, T.E. Bilir, M. Chatterjee, K.L. Ebi, Y.O. Estrada, R.C. Genova, B. Girma, E.S. Kissel, A.N. Levy, S. MacCracken,P.R. Mastrandrea, and L.L. White, Ed.; World Meteorological Organization, Geneva, Switzerland, 2014;.
24. Di Risio, M., Bruschi, A., Lisi, I., Pesarino, V., & Pasquali, D. (2017). Comparative Analysis of Coastal Flooding Vulnerability and Hazard Assessment at National Scale. Journal of Marine Science and Engineering, 5(4), 51.
25. Silva, S.F.; Martinho, M.; Capitão, R.; Reis, T.; Fortes, C.J.; Ferreira, J.C. An index-based method for coastal-flood risk assessment in low-lying areas (Costa de Caparica, Portugal). Ocean Coast. Manag. 2017, 144, 90–104.
26. Barnett, J.; O'Neill, S. Maladaptation. *Glob. Environ. Change* **2010**, *20*, 211–213.
27. EPA Guidelines for Preparing Economic Analyses Available online: https://www.epa.gov/environmental-economics/guidelines-preparing-economic-analyses#download (accessed on Oct 3, 2017).
28. USGS Structured Decision Making for Management of Warm-Water Habitat of Manatees Available online: https://www.usgs.gov/centers/wetland-and-aquatic-research-center-warc/science/structured-decision-making-management-warm?qt-science_center_objects=1#qt-science_center_objects (accessed on Oct 3, 2017).
29. Hallegatte, S. Strategies to adapt to an uncertain climate change. *Glob. Environ.*

Change **2009**, *19*, 240–247.

30. Ellen, I. G.; Yager, J.; Hanson, M.; Bosher, L. Planning for an Uncertain Future Can Multicriteria Analysis Support Better Decision Making in Climate Planning? *Journal of Planning Education and Research* **2016**, *36*, 349–362.
31. CEQ *Revised Draft Guidance for Federal Departments and Agencies on Consideration of Greenhouse Gas Emissions and the Effects of Climate Change in NEPA Reviews*; Council on Environmental Quality, 2014; Vol. 79;.
32. Serban Scrieciu, S.; Belton, V.; Chalabi, Z.; Mechler, R.; Puig, D. Advancing methodological thinking and practice for development-compatible climate policy planning. *Mitig Adapt Strateg Glob Change* **2014**, *19*, 261–288.
33. Jones, L.; Champalle, C.; Chesterman, S.; Cramer, L.; Crane, T. A. Constraining and enabling factors to using long-term climate information in decision-making. *Clim. Policy* **2016**, *17*, 551–572.
34. Matthews, T.; Lo, A. Y.; Byrne, J. A. Reconceptualizing green infrastructure for climate change adaptation: Barriers to adoption and drivers for uptake by spatial planners. *Landsc. Urban Plan.* **2015**, *138*, 155–163.
35. Moser, S. C.; Dilling, L. *Creating a Climate for Change: Communicating Climate Change and Facilitating Social Change*; Cambridge University Press, 2007; ISBN 9781139461085.
36. Moser, S. C.; Ekstrom, J. A. A framework to diagnose barriers to climate change adaptation. *Proc. Natl. Acad. Sci. U. S. A.* **2010**, *107*, 22026–22031.
37. Mimura, N.; Pulwarty, R. S.; Duc, D. M.; Elshinnawy, I.; Redsteer, M. H.; Huang, H. Q.; Nkem, J. N.; Sanchez Rodriguez, R. A. Adaptation Planning and Implementation. In *Climate Change 2014: Impacts, Adaptation, and Vulnerability. Part A: Global and Sectoral Aspects. Contribution of Working Group II to the Fifth Assessment Report of the Intergovernmental Panel on Climate Change*; Field, C.B., V.R. Barros, D.J. Dokken, K.J. Mach, M.D. Mastrandrea, T.E. Bilir, M. Chatterjee, K.L. Ebi, Y.O. Estrada, R.C. Genova, B. Girma, E.S. Kissel, A.N. Levy, S. MacCracken, P.R. Mastrandrea, and L.L. White, Ed.; Cambridge University Press, 2014; pp. 869–898.
38. Hamin, E. M.; Gurran, N.; Emlinger, A. M. Barriers to municipal climate adaptation: examples from coastal Massachusetts' smaller cities and towns. *J. Am. Plann. Assoc.*

2014, *80*, 110–122.

39. Shi, L.; Chu, E.; Anguelovski, I.; Aylett, A.; Debats, J.; Goh, K.; Schenk, T.; Seto, K. C.; Dodman, D.; Roberts, D.; Roberts, J. T.; VanDeveer, S. D. Roadmap towards justice in urban climate adaptation research. *Nat. Clim. Chang.* **2016**, *6*, 131–137.
40. Raymond, C. M.; Frantzeskaki, N.; Kabisch, N.; Berry, P.; Breil, M.; Nita, M. R.; Geneletti, D.; Calfapietra, C. A framework for assessing and implementing the co-benefits of nature-based solutions in urban areas. *Environ. Sci. Policy* **2017**, *77*, 15–24.
41. Duguma, L. A.; Minang, P. A.; van Noordwijk, M. Climate Change Mitigation and Adaptation in the Land Use Sector: From Complementarity to Synergy. *Environ. Manage.* **2014**, *54*, 420–432.
42. Younger, M.; Morrow-Almeida, H. R.; Vindigni, S. M.; Dannenberg, A. L. The built environment, climate change, and health: opportunities for co-benefits. *Am. J. Prev. Med.* **2008**, *35*, 517–526.
43. Hallegatte, S.; Corfee-Morlot, J. Understanding climate change impacts, vulnerability and adaptation at city scale: an introduction. *Clim. Change* **2011**, *104*, 1–12.
44. Cutter, S. L.; Finch, C. Temporal and spatial changes in social vulnerability to natural hazards. *Proc. Natl. Acad. Sci. U. S. A.* **2008**, *105*, 2301–2306.
45. Heltberg, R.; Siegel, P. B.; Jorgensen, S. L. Addressing human vulnerability to climate change: Toward a “no-regrets” approach. *Glob. Environ. Change* **2009**, *19*, 89–99.
46. Smit, B.; Wandel, J. Adaptation, adaptive capacity and vulnerability. *Glob. Environ. Change* **2006**, *16*, 282–292.
47. Cutter, S. L.; Boruff, B. J.; Shirley, W. L. Social vulnerability to environmental hazards. *Soc. Sci. Q.* **2003**, *84*, 242–261.
48. Cutter, S. L.; Barnes, L.; Berry, M.; Burton, C.; Evans, E.; Tate, E.; Webb, J. A place-based model for understanding community resilience to natural disasters. *Glob. Environ. Change* **2008**, *18*, 598–606.
49. Moser, S. C.; Boykoff, M. T. *Successful Adaptation to Climate Change: Linking Science and Policy in a Rapidly Changing World*; Routledge, 2013; ISBN 9781135071301.
50. Kenney, M. A.; Janetos, A. C.; Lough, G. C. Building an integrated U.S. National

Climate Indicators System. *Clim. Change* **2016**, *135*, 85–96.

51. Ahern, J. From fail-safe to safe-to-fail: Sustainability and resilience in the new urban world. *Landsc. Urban Plan.* **2011**, *100*, 341–343.
52. Mendoza, G. A.; Martins, H. Multi-criteria decision analysis in natural resource management: A critical review of methods and new modelling paradigms. *For. Ecol. Manage.* **2006**, *230*, 1–22.
53. Bierbaum, R.; Smith, J. B.; Lee, A.; Blair, M.; Carter, L.; Chapin, F. S.; Fleming, P.; Ruffo, S.; Stults, M.; McNeeley, S.; Wasley, E.; Verduzco, L. A comprehensive review of climate adaptation in the United States: more than before, but less than needed. *Mitig Adapt Strateg Glob Change Mitigation and Adaptation Strategies for Global Change : An International Journal Devoted to Scientific, Engineering, Socio-Economic and Policy Responses to Environmental Change* **2013**, *18*, 361–406.
54. McDaniels, T.; Chang, S.; Cole, D.; Mikawoz, J.; Longstaff, H. Fostering resilience to extreme events within infrastructure systems: Characterizing decision contexts for mitigation and adaptation. *Glob. Environ. Change* **2008**, *18*, 310–318.
55. Scannell, L.; Gifford, R. Climate Change Engagement Questionnaire. *PsycTESTS Dataset* 2013.
56. Boulton, E. Climate change as a “hyperobject”: a critical review of Timothy Morton’s reframing narrative. *WIREs Clim Change* **2016**, *7*, 772–785.
57. Aragon, C., Hamin, E. & Buxton, J. The Role of Landscape Installations in Climate Change Visualization (Manuscript) 2017.
58. Keeley, M.; Koburger, A.; Dolowitz, D. P.; Medearis, D.; Nickel, D.; Shuster, W. Perspectives on the Use of Green Infrastructure for Stormwater Management in Cleveland and Milwaukee. *Environ. Manage.* **2013**, *51*, 1093–1108.
59. Aldrich, D. P.; Meyer, M. A. Social Capital and Community Resilience. *Am. Behav. Sci.* **2015**, *59*, 254–269.
60. Smith, J. B.; Klein, R. J. T.; Huq, S. *Climate change, adaptive capacity and development*; Imperial College Press: London, 2003;.
61. IPCC *Managing the Risks of Extreme Events and Disasters to Advance Climate Change Adaptation. A Special Report of Working Groups I and II of the Intergovernmental Panel on Climate Change*; Field, C.B., V. Barros, T.F. Stocker, D.

Qin, D.J. Dokken, K.L. Ebi, M.D. Mastrandrea, K.J. Mach, G.-K. Plattner, S.K. Allen, M. Tignor, and P.M. Midgley, Ed.; IPCC: Cambridge, United Kingdom and New York, NY, USA, 2012;.

62. Haasnoot, M.; Kwakkel, J. H.; Walker, W. E.; ter Maat, J. Dynamic adaptive policy pathways: A method for crafting robust decisions for a deeply uncertain world. *Glob. Environ. Change* **2013**, *23*, 485–498.
63. Rosenzweig, C.; Solecki, W. Hurricane Sandy and adaptation pathways in New York: Lessons from a first-responder city. *Glob. Environ. Change* **2014**, *28*, 395–408.
64. Abunnasr, Y.; Hamin, E. M.; Brabec, E. Windows of opportunity: addressing climate uncertainty through adaptation plan implementation. *J. Environ. Planning Manage.* **2015**, *58*, 135–155.
65. Arnstein, S. R. A Ladder Of Citizen Participation. *J. Am. Inst. Plann.* **1969**, *35*, 216–224.
66. Collins, K.; Ison, R. Jumping off Arnstein's ladder: social learning as a new policy paradigm for climate change adaptation. *Environmental Policy and Governance* **2009**, *19*, 358–373.
67. Innes, J. E.; Booher, D. E. *Planning with Complexity: An Introduction to Collaborative Rationality for Public Policy*; Routledge, 2010; ISBN 9781135194277.
68. Meadow, A. M.; Ferguson, D. B.; Guido, Z.; Horangic, A.; Owen, G.; Wall, T. Moving toward the Deliberate Coproduction of Climate Science Knowledge. *Weather, Climate, and Society* **2015**, *7*, 179–191.
69. Head, B. W. Community Engagement: Participation on Whose Terms? *Aust. J. Polit. Sci.* **2007**, *42*, 441–454.
70. Cornwall, A. Unpacking "Participation": models, meanings and practices. *Community Dev. J.* **2008**, *43*, 269–283.
71. Adger, W. N. Place, well-being, and fairness shape priorities for adaptation to climate change. *Glob. Environ. Change* **2016**, *38*, A1–A3.
72. Goodin, R. E. *Utilitarianism as a public philosophy*; Cambridge University Press: Cambridge; New York, 1995;.
73. Rawls, J. *A Theory of Justice*; Harvard University Press: Cambridge, MA, 2009;.
74. Kelman, I.; Gaillard J C Lewis; Mercer, J. Learning from the history of disaster

vulnerability and resilience research and practice for climate change. *Nat. Hazards* **2016**, *82*, S129–S143.

CHAPTER 4

EFFECTS OF BIOPOLYMERS ON THE LIQUID LIMIT AND UNDRAINED SHEAR STRENGTH OF SOFT CLAYS

This chapter presents the strength, micromorphology, and microstructure of a variety of soft clays amended by four biopolymers (including xanthan gum, guar gum, carrageenan, and dextran) and then discusses the biopolymer-clay interactions. Tests soil minerology is predominantly kaolin with lesser amounts of montmorillonite. The effectiveness of different biopolymers and their interactions with different clay minerals are assessed over a range of biopolymer concentrations. The adopted test methods include liquid limit (LL) measurement, fall cone (FC) penetration, and environmental scanning electron microscope (ESEM). The effects of biopolymer-clay interactions on the temporal development of intact strength and the remolded strength are investigated. Fall cone results demonstrate both an immediate strength gain and a time-dependent strength gain induced by biopolymers for the clay samples studied. Some of the biopolymers demonstrate a saturation point. Finally, the results show guar and carrageenan behave fundamentally differently than xanthan and dextran. The advantages and limitations of the potential applications of four biopolymers in terms of effectiveness, costs, and ease of application are compared.

4.1 Introduction

Preservation of cohesive soils on intertidal mudflats proves beneficial to the engineering community as a means of providing a buffer zone for attenuation of wave and surge energy and protecting the nearshore properties and infrastructure in the events of potential flood inundation. Once areas of high erosion potential are identified, it is

desirable for a community or property owner to invest resources into decreasing the erosion hazard through mitigation measures and technologies. Biopolymers occur naturally in a wide range of soil environments (e.g., coastal areas, lake deposits), and may prove a useful soil enhancement additive for reducing coastal erosion and increasing the undrained shear strength of clayey soils.

Given the challenges in directly measuring the erosion resistance of cohesive soils, numerous investigators have tried to develop empirical correlations between erosion resistance and other physical and mechanical properties such as grain size characteristics, plasticity, and undrained shear strength. Of these efforts, correlating erodibility with undrained shear strength seems the most promising (e.g., Partheniades 1971, Watts et al. 2003, and Meng et al. 2012) and reasonable since both parameters are a function of interparticle forces. As the void ratio decreases in a soil, the particles become closer together and the interparticle forces have a greater impact on binding the soil together. Therefore, increasing undrained shear strength was considered a proxy means for improved erosion resistance throughout this investigation.

Bacteria respond to alterations in soil hydration status with a diverse set of physiological mechanisms. While these responses can be intracellular and individual, the most successful ones are probably those that occur at a communal level, such as synthesis and secretion of extracellular polymeric substances (EPS), which form protective coatings for the embedded microcolonies. The EPS layer, in turn, can affect the physical characteristics of the host medium through the reduction of available pore spaces for water flow and alteration of water retention and mechanical properties (Or et al. 2007). Most biopolymers possess a high tensile strength (Chang et al. 2016) and high molecular weight

(Nugent et al. 2009). Formation of microbial colonies on sediment surfaces impacts soil microstructure, primarily through the formation of polymer bridges that bind soil particles. Prior scanning electron microscopy (SEM) observations demonstrate that EPS in soil environments is closely associated with the surrounding clay particles (Chenu 1993).

In general, most biopolymers, including EPS (e.g., xanthan gum) and some analogs (e.g., guar gum) can be an effective means of stabilizing the surface layers of soft clay sediments, and likewise decreasing the erosion of intertidal soft clays. EPS analogs have been used to increase the crop yield by reducing erosion in the agriculture industry (Abu-Zreig 2006). Biogeotechnics will likely become part of the mainstream geotechnical engineering in the future (DeJong 2015). Biopolymers present an alternative to traditional cement-based additives for soil improvement with a lower carbon footprint. Further, cement-based soil improvement is mostly permanent, whereas biopolymer-improved soil can be more easily removed or reversed in the event of demolition. Finally, cement presents challenges with increased runoff, whereas biopolymers do not present these runoff concerns because of their water-retention properties (Chang 2016).

The study of biopolymers and their interactions with clay minerals may even prove useful beyond traditional geotechnical engineering purposes. They are currently being investigated in the fields of biology and medicine. Specifically, they are being studied for their potential in medicine distribution, gene therapy, and bionanocomposites. Studies on the adsorption and binding of biopolymers by clay minerals may also help the understanding of the origin of life (Yu et al. 2013).

Many engineering properties of biopolymer-bearing soils, particularly cohesive soils, remains unknown. First, there are many different types of biopolymers, each with

different chemical properties (e.g., polarity), functional groups, and molecular structures. Second, little is known regarding the long-term effectiveness of specific biopolymers, especially considering a range of other interrelated factors, such as interactions with different types of clay minerals, cations, and other organic substances, variable biopolymer concentrations, and the degree of soil disturbance (remolding). These factors may act together making it challenging to recommend a specific biopolymer type (and respective concentrations) as a viable improvement technique to a specific soil and site condition. Therefore, a better understanding of the impact of various biopolymers on soft clays under varied conditions is of key importance and is beneficial to the coastal community.

This paper presents results from an investigation of the changes in the strength, micromorphology, and microstructure of clayey soils consisting of three kaolinite-montmorillonite mixtures induced by four biopolymers. The effectiveness of different biopolymers for soil improvement was assessed via liquid limit over a range of biopolymer concentrations. Their interactions with different clay minerals was also assessed. The effect of biopolymer-clay interactions on the undrained shear strength and its temporal development, and the undrained shear strength resistance to disturbance (remolding) was investigated. Finally, this chapter compares the advantages and limitations of different biopolymers in terms of effectiveness, costs, and ease of application. Ideally, this research will aid the decision-making process for the coastal and geotechnical engineers to determine which (if any) of the tested biopolymers presents a cost-effective soil improvement additive for reducing the erosion of coastal cohesive soils.

4.2 Materials and Methods

Four different biopolymers, including xanthan gum, guar gum, carrageenan, and diethylaminoethyl-dextran chloride form (DEAE-Dextran, referred to hereafter as "dextran") were studied. Different soil minerals were considered, consisting predominantly of kaolinite, with varying amounts of montmorillonite. Test methods included liquid limit measurement by Casagrande method, fall cone penetration, and environmental scanning electron microscopy.

4.2.1 Clay Minerology

This section presents a brief background on clay mineralogy pertaining to kaolinite and montmorillonite, which were the two clay minerals used in this work. Typical values for some important properties of kaolinite and montmorillonite are summarized in Table 4.1.

Clay minerals are usually very small-sized (i.e., <2 μm) particles. Because of crystal defects such as isomorphous substitutions, their surfaces possess charges and hence are chemically active, with permanent negative charges on the face surface and pH-dependent charges on the edge surface, enabling their interactions with other chemically active or charged particulate matter as well as dissolved ions and molecules. Their very large aspect ratio (i.e., the ratio of diameter to thickness typically ranges from 10 to 100) results in a very large specific surface area (SSA), augmenting the interactions occurring on clay surfaces (Zhang et al. 2013).

Kaolinite consists of stacked 1:1 layers that consist of one tetrahedral (silica) sheet and one octahedral (alumina) sheet. The two sheets join together in such a way that the

apical oxygen atoms of the silica sheet and the hydroxyls of the octahedral sheet are shared to form a single 1:1 layer (Figure 4.1a). This basic layer is about 0.72 nm thick and extends infinitely in the other two directions (i.e., planar dimensions). A kaolinite crystal, then, consists of a stack of many basic 1:1 layers. Successive layers in the crystal are held together by hydrogen bonds between the hydroxyls of the octahedral sheet and the oxygens of the tetrahedral sheet. Since the hydrogen bond is relatively strong, it prevents hydration (or water molecules from entering the interlayer) and allows the layers to stack up to make a rather large crystal (Holtz et al. 2011).

Montmorillonite, on the other hand, is a 2:1 mineral (Figure 4.1b). It has a thickness of ~0.96 nm and extends infinitely in the other two directions. The interlayer bonding includes primarily Coulomb forces and secondary van der Waals' forces. There is a net negative charge deficiency in the octahedral sheet. Water and exchangeable cations can readily enter the interlayer space and hence expand the structure. Thus, montmorillonite crystals have a very strong attraction for water and are expandable (Holtz et al. 2011).

In addition to cation exchange and electrostatic forces, the presence of a "hydrophobic region" and a "hydrophilic region" on a clay mineral surface is also responsible for adsorption of molecules by clay minerals. Clay minerals are capable of binding polar molecules since the octahedral surface is hydrophilic while the tetrahedral surface with the hydroxyl groups is hydrophobic (Yu et al. 2013). The exchangeable cations in the interlayer space balancing the charge deficit of the layers have a hydrophilic character, while the uncharged regions between charge sites present a partial hydrophobic character (Yu et al. 2013). Different clay minerals have different adsorption sites (Figure 4.2) available for molecule adsorption (Yu et al. 2013). The adsorption sites on kaolinite

are only external surfaces due to their non-expanding layers. Montmorillonite is an expanding layer silicate and thus has extensive internal and external surfaces for adsorption. For montmorillonite, adsorption of molecules occurs at both interlayer and external surfaces, while for kaolinite, it always occurs at the external surfaces (Yu et al. 2013).

4.2.2 Materials

Four different biopolymers were investigated, including xanthan gum, guar gum, carrageenan, and dextran. These biopolymers were specifically selected to cover a range of variable chemical properties, including net charge (polarity), molecular shape, and molecular weight. They also encompassed a variety of biological origins, unit costs, and solubility properties. All biopolymers were reagent graded and ordered through the Fisher Scientific, Inc. Each of the biopolymers are discussed briefly below, and important properties are summarized in Table 4.2. Molecular weights for biopolymers tend to be very high because they are large sugar molecules. However, exact molecular weights may vary based on the precise bacterial strains (as applicable) and/or physiological environment used during production (Nugent et al. 2009). Therefore, the molecular weights provided in Table 4.2 are for general comparison purposes only. Chemical structures for each of the studied biopolymers are presented in Figure 4.3

Xanthan gum is a polysaccharide produced by the bacteria, *Xanthomonas campestris,* and has an anionic (negative) charge (Nugent et al. 2009). It consists primarily of a cellulose chain (Dontsov and Bigham 2005) (Figure 4.3a) with a molecular weight of 0.9–1.6x10^6 g/mol (Nugent et al. 2009). Xanthan gum is commonly used as a food additive

(Chang et al. 2015). It is in the middle price range compared to the other biopolymers investigated. When xanthan is dissolved in water, the resulting solution is pseudoplastic, which means its viscosity decreases with increasing shear rate (Nugent et al. 2009).

Guar gum is a polysaccharide found in seeds of the plant *Cyamopsis tetragonoloba*. It has a neutral charge and contains numerous hydroxyl (-OH) groups for forming hydrogen bonds. Guar has a molecular weight of up to $2x10^6$ g/mol (Nugent et al. 2009) and consists mostly of linear polymannan with single galactose unit side chains (Whitcomb et al. 1980) (Figure 4.3b). It is the least expensive of the four tested biopolymers. When guar is dissolved in water, the resulting solution tends to be very viscous, making it commercially significant (Nugent et al. 2009); it is used as a thickening agent in foods, medicine, and drilling and fracking well operations. Like xanthan, guar solutions are pseudoplastic (Whitcomb et al. 1980, and Nugent et al. 2009).

Carrageenan is a naturally occurring, sulphated polysaccharide obtained from red seaweed through different extraction and purification methods. It is classified in three main structural forms: kappa (κ), iota (ι) and lambda (λ) (Herrera and Vasanthan 2018). The carrageenan used in this investigation consisted predominantly of κ-carrageenan with lesser amount λ-carrageenan. Therefore, the description of carrageenan provided hereinafter refers specifically to κ-carrageenan. The gelation of κ-carrageenan is generally believed to involve two steps: the coil-helix transition and subsequent aggregation of double helices (Figure 4.3c). Due to its excellent biodegradability and biocompatibility, κ-carrageenan is used in medical care, drug-controlled release and encapsulation. The gelation of κ-carrageenan is influenced by temperature, concentration, type and amount of metal salts, and the presence of food ingredients such as other sugars (Yang et al. 2018).

It has a neutral chemical charge (FAO 1965) and a molecular weight of about $0.2 – 0.4x10^6$ g/mol (McGill et al. 1977). It is in the middle price range, compared to the other investigated biopolymers.

Dextran is a cationic biopolymer, and therefore has a net positive charge. This polysaccharide is an FDA-approved branched polysaccharide composed of glucose units (Figure 4.3d). Dextran is synthesized from sucrose by certain lactic acid bacteria (Tabujew and Peneva 2015) and is highly water-soluble irrespective of the pH (Samal et al. 2012). The dextran used in these experiments had a molecular weight of $0.5x10^6$ g/mol. It is significantly more expensive than the other three polysaccharides investigated.

Three soils mixes were used for testing: kaolinite and two different kaolinite-montmorillonite mixtures.. The two ingredient soils were sourced from commercially available soils to minimize sample variability. The kaolinite soil is known commercially as "Prestige" (Unimin Corporation) and the montmorillonite source is known commercially as "Pure Gold Gel" (CETCO). These soils were specifically selected to investigate the influence of varying minerology and hence liquid limit on biopolymer-soil interactions.

Clay mineral composition was confirmed by X-ray diffraction (XRD) at the Massachusetts Institute of Technology (MIT). Quantitative XRD results indicate that the Prestige soil contained about 95% kaolinite and 5% anatase, while the Pure Gold Gel soil consisted of about 61% smectite (referred to herein as montmorillonite), 15% quartz, 15% illite, with lesser amounts of calcite, ettringite, and nordstrandite. Grain size distribution on the Prestige was determined by hydrometer tests, performed in general accordance to

ASTM D422 – 63. These results indicate that the Prestige soil contained 63% clay-sized and 37% silt-sized particles.

The kaolinite-rich soil consisted entirely of Prestige and was referred to as the 100K0M soil. The first kaolinite-montmorillonite soil mixture consisted of 85% Prestige and 15% Pure Gold Gel and was referred to as the 85K15M soil. The other kaolinite-montmorillonite soil mixture consisted of 70% Prestige and 30% Pure Gold Gel and was referred to as the 70K30M soil. The LL values of these soils (without any added biopolymer) were referred to as the $LL_{0\%}$ values and were 44%, 96%, and 175% for 100K0M, 85K15M, and 70K30M, respectively (Table 4.3).

4.2.3 Methods

The biopolymer mixed soil samples in this investigation were identified by biopolymer concentrations, where the concentration is defined by a mass ratio. For example, a 1% xanthan mix contained one gram of xanthan for every 100 grams of air-dried soil. The immediate impact of biopolymers on soil was investigated by liquid limit (LL) measurements. Changes in strength with time and resistance to remolding were investigated using Fall Cone (FC) penetration testing. Finally, the morphology of biopolymer-soil mixtures was observed using an environmental scanning electron microscope (ESEM).

Samples were generally prepared in a similar manner for all three types of tests (LL, FC, and ESEM). preparation started with first dissolving the biopolymer (dry powder) into deionized (DI) water to form a solution. This was accomplished by slowly adding the biopolymer to DI water and then stirring until it fully dissolved and the solution obtained

a uniform consistency (Figure 4.4a). While some solutions were mixed using a combination of magnetic stirring and hand-mixing, the solutions were generally too viscous for this to be effective, and in most cases an electrical Emersion blender was used. Next, the solution was introduced into air-dried soils using an electric mixer (Figure 4.4b).

The amount of solution initially combined with the soil was equal to that necessary to bring the soil to a water content equal to the $LL_{0\%}$. Finally, the sample was wrapped in plastic film to prevent moisture loss and allowed to rest overnight in a humid room (11 ^{o}C, RH > 85%) to ensure water equilibrium in the sample. Prior to testing, samples were then allowed to return to room temperature, as recommended by Nugent et al. (2009).

The dry biopolymer powder was dissolved into water to form a solution, and then the solution was incorporated into air dried soil, as suggested by Nugent et al. (2009). In the case of liquid limit testing, additional DI water was added to the biopolymer-soil mixture, prior to overnight conditioning for water equilibrium. This was accomplished by spot checking the consistency using a Casagrande cup, necessary to prepare the mixture near the actual LL of the respective soil mix; this spot checking was challenging likely due to the pseudoplastic behavior of aqueous biopolymer solutions. The liquid limit testing was performed in general accordance with the ASTM D4318 – 10. Liquid limit tests were performed at concentrations ranging between 0% and 8% mixes for xanthan, carrageenan, and dextran, for the 100K0M, 85K15M, and 70K30M soils. Guar presented difficulty in dissolving at higher concentrations. Therefore, guar mixes were tested for concentrations ranging between 0% and 4%.

Values of liquid limits for each pure biopolymer (without any soil) were also determined; these were referred to as the "biopolymer-only" tests, LL_B. This was

accomplished by combining a known mass of biopolymer and DI water by trial-and-error until the sample formed a uniform gel with a consistency that as spreadable with a spatula. While some attempts were made to confirm these results using a Casagrande device, this generally proved challenging due to issues of pseudoplasticity. Therefore, LL_B results were considered approximate and used for general comparison purposes only.

Fall Cone (FC) testing was performed in general accordance with ISO (2017) to measure the undrained shear strength of the biopolymer-soil mixtures over time. A large batch of biopolymer-soil mixture was prepared to a water content equal to the $LL_{0\%}$ of the respective soil, and then rested overnight in the humid room. Samples were then allowed to return to room temperature immediately prior to FC testing. Testing was accomplished by stirring the biopolymer-soil mixture vigorously and then portioned out into individual small glass jars. The first jar was tested immediately (as time = 0), and the remaining jars were wrapped with parafilm and sealed lids and submerged in a bucket of DI water to prevent moisture changes while aging. Further, the submerged jars were stored in a temperature control box which generally remained between 23 and 24 ^{o}C to minimize the effects of temperature variations while aging.

Fall cone tests were performed on 1% and 4% mixes of xanthan, guar, and dextran on both the 100K0M and 85K15M soils. (Carrageenan was not tested in FC because preliminary LL tests indicated guar and carrageenan demonstrated similar behavior, and guar was the less expensive of these two biopolymers.) Subsequent fall cone measurements were then obtained at the time of 3 hr, 6 hr, 1 day, 3 days, and 7 days. The 7-day sample was, after tested,mixed vigorously and tested again to determine the impact of remolding on biopolymer effectiveness (i.e., sensitivity). Controls of 100K0M and

85K15M (no biopolymer) were tested at the same time increments for comparison purposes.

Initial density and final water content values for each FC jar were tracked for quality control purposes. For the 100K0M mixes, water content ranged from 42% – 46% with an average final water content of 44 %. The density ranged from 1.54 – 1.71 g/cm^3 with an average density of 1.63 g/cm^3. For the 85K15M mixes, water content ranged from 95% - 99% with an average final water content of 97%. The density ranged from 1.33 – 1.42 g/cm^3 with an average density of 1.37 g/cm^3. It is important to note that the biopolymers remain stable in the oven due to their high molecular weight (Nugent et al. 2009). Therefore, these water content values were calculated by prorating out the mass of the biopolymers from the mass of solids, considering the initial biopolymer-soil mass ratios. In generally, the moisture content values associated with the remolded sample were slightly lower than the intact samples, likely due to additional time exposed to air during remolding.

Finally, the morphology of several biopolymer-soil mixtures was observed using an Environmental Scanning Electron Microscope (ESEM). The tests were performed using the FEI Quanta 200 FEG MKII ESEM located at the University of Massachusetts Medical School. ESEM observations do not require the samples to be preprocessed (e.g. dried, coated, or fixed). Five different 100K0M mixtures were observed under humidity of about 84% to 89%, to help prevent drying during imagining. Samples were also limited to more than one hour of exposure within the chamber, again to minimize drying of sample. During viewing, special attention was paid to clay particle aggregation, aggregate sizes, and the presence of biopolymer gels in pores. The five mixtures included: 0% (control), and 0.5%,

1%, 2%, and 4% xanthan mixtures. The 1% and 4% tests were directly comparable with the Fall Cone results (Time = 0 hr). The 0.5% and 2% xanthan mixtures were investigated to observe general transition of particle aggregation, aggregate size, and gel within the pores between the 0%, 1%, and 4% mixtures. This is generally similar in terms of process and materials studied in Nugent et al. (2009), although this investigation tested higher concentrations of biopolymer than Nugent et al. (2009), which only considered xanthan up to 1% concentration.

4.3 Analysis of Results

The following section presents the liquid limit, fall cone, and environmental scanning electron microcopy results.

4.4.1 Liquid Limit

The results of the LL_B values for the biopolymer-only tests are presented in Table 4.4. These results showed that the liquid limit of pure guar and carrageenan solutions is much higher than those of pure xanthan and dextran.

The LL values for the biopolymer-soil mixtures are presented in Figure 4.5. The LL results for guar and xanthan 100K0M mixes are generally similar to that presented by Nugent et al. (2009). Based on the results presented in Figure 4.5, guar and carrageenan showed a substantial increase in LL with increasing biopolymer concentration (regardless of soil type), reaching LL values of up to 150%. The results of xanthan and dextran behaved fundamentally different than the guar and carrageenan in two ways: First, the resulting LL values were much lower, remaining below 150%. Second, xanthan and

dextran did not necessarily increase the LL with an increase in biopolymer concentration. In fact, LL starts to decrease at high concentrations of xanthan and dextran for the 70K30M test. Note that the LL results of two of the biopolymers (xanthan and carrageenan) converged at a specific concentration for all soil types; xanthan LL values converged at about 100% at 8% concentration, whereas the carrageenan LL values converged at about 325% at 8% concentration (Figure 4.5). Finally, the results were normalized by the liquid limit of the control soil ($LL/LL_{0\%}$), as presented as Figure 4.6. The $LL/LL_{0\%}$ results indicate that the biopolymer was most effective at increasing LL for the 100K0M mixture (i.e. higher value of $LL/LL_{0\%}$).

4.4.2 Fall Cone

The results of the FC testing for the 100K0M and 85K15M mixes are presented in Figure 4.7a and Figure 4.8a, respectively. The control samples were expected to have an undrained shear strength near 2 kPa, because these were prepared to the liquid limit (Sharma and Bora 2003). The control samples were measured at the same time increments as the biopolymer-soil mixes, which allows for comparison of strength over time due solely to thixotropy (Mitchel 1960). The results were normalized by dividing the s_u at a given time, by the s_u at time zero (s_{ut0}) for the respective biopolymer type and biopolymer concentration. These normalized values (s_u/s_{ut0}) for 100K0M and 85K15M mixtures are presented in Figure 4.7b and Figure 4.8b respectively.

Based on the results of the 100K0M mixes, dextran and guar showed the highest gains, while xanthan strength gain was minimal. The guar and dextran both showed the 4% mixtures resulted in higher undrained shear strength than the respective 1% mixtures.

The 1% xanthan, on the other hand, demonstrated a higher undrained shear strength than the 4% concentration (Figure 4.7a). The biopolymer-soil mixtures generally demonstrated a substantial strength gain nearly instantaneously (at t= 0 reading). Then, the strength tended to increase gradually up to about 3 days, after which point the strength began to level off with time. Figure 4.7b presents the normalized results as a time-dependent strength gain factor. Thixotropy may not be sufficient to explain the time-dependent strength gain; some of the time-dependent strength gain could be associated with the biopolymer-soil interactions. Remolding the soil tended to decrease the undrained shear strength, indicating that the biopolymer-soil mixes were sensitive.

For the 85K15M mixtures (Figure 4.8), the undrained shear strength values were much lower than that of the 100K0M mixes. (Note that the scales on the y-axis for Figure 4.7 and Figure 4.8 are significantly different.) In fact, the 85K15M Xanthan 4% was lower than the control. Still, four general observations remained the same as the 100K0M mixtures: (1) Dextran and guar showed highest gains, while xanthan gain was minimal, (2) substantial strength gain was nearly instantaneous, (3) soils generally showed a continued increase in strength with time, and (4) remolded strength indicates some sensitivity.

4.3.3 ESEM

The results of the ESEM are provided in Figure 4.9. All samples consisted of 100K0M mix and were prepared to a water content of 44%. The 0%, 0.5% and 1% samples were scanned at about 5,000X magnification. For the higher xanthan concentrations (2% and 4%), it was helpful to observe the general soil matrix from a further perspective, so those were scanned closer to 1,000X magnification. Figure 4.9a is the control (100K0M,

0%) and is shown for comparison purposes. Note that a typical individual (primary) clay particle (without influence of biopolymers) has a size of around 2 μm (Zhang et al. 2013). It is clear from Figure 4.9a that primary clay particles were visible, the particle edges were angular and clearly defined, and the particles were generally hexagonal in shape which is typical for kaolin minerals.

Figure 4.9b presents the results for xanthan 0.5% which showed a general meshing of the soil matrix. Further, the edges of the clay particles were becoming less distinct (less angular). Figure 4.9c shows the results for the 1% mix in which the edges of clay particles were much less distinct than the control and stands of biopolymer began to form, which connected the clay particles. Flocculi on the order of 10 μm were visible in the 1% mix. Flocculi consist of strongly bound primary clay particles with a face-to-edge association via Coulomb attraction and have a size of typically 10 – 30 mm (Zhang et al. 2013). The results of Figure 4.9c are generally consistent with that of Nugent et al (2009). Note that additional strands were observed at the initiation of some scans, but the strands broke before the scan was completed.

Regarding the ESEM scans at higher xanthan concentrations, the results for the 2% and 4% mixes are shown in Figure 4.9d and Figure 4.9e, respectively. The 2% mix demonstrated well defined larger grains (microflocs) on the order of 100 – 200 μm. There were also biopolymer bridges connecting the microflocs forming macroflocs. According to Zhang et al. (2013), microflocs consist of flocculi and primary particles with a size range of 30–200 μm. Macroflocs are built up from microflocs, primary particles, and flocculi and have a size range of hundreds to thousands of micrometers. Finally, the 4% concentration

shows that the biopolymer solution has formed a film filling the void space between microflocs.

4.4 Interpretation and Discussion of Results

Clarification of the two principal forms of attraction, cohesion and adhesion, is essential to interpret the impact of biopolymers on soft clay properties. In chemistry, cohesion is used to describe the attraction between chemically similar molecules, particles or substances. This refers typically to the attraction of clays and colloids by electro-chemical forces, such as van der Waals forces and electrostatic attraction. Adhesion, on the other hand, is used to describe the attraction between dissimilar molecules, particles, and substances. In sediment research, the term "adhesion" refers to the binding of sediment particles by an additional inter-particle substance that is different from the sediment particles, such as biopolymers (Grabowski et al. 2011).

4.4.1 Liquid Limit Tests

Based on the liquid limit results, it is clear that guar and carrageenan behave fundamentally differently from xanthan and dextran. The substantial increase in LL for guar and carrageenan is likely due to an increase in the LL of the pore fluid (LL_B), rather than the increased cohesion of the clay particles directly (Table 4.4). In general, the higher the viscosity of the pore fluid, the greater the shearing stress required to cause the soil mass to deform and induce slip between soil particles; the biopolymers with high LL_B values were more viscous, and therefore increased the resistance to shearing.

Since clay particles usually have a net negative charge and hence can attract cations, it can be reasoned that dextran (the only cationic biopolymer used in this investigation) would have the greatest impact on increasing LL; diminished repulsive forces between particles should increase cohesion (particle-to-particle contact) due to reduction in double layer thickness. However, this effect was somewhat overshadowed by the exceptionally high LL_B of guar and carrageenan (Table 4.4). To better illustrate this point, the LL results were normalized by LL_B, as presented in Figure 4.10. Here dextran clearly has the highest impact of all four soil types.

Still, considering that xanthan had a lower LL_B than guar and carrageenan, and xanthan is anionic (could potentially increase repulsive forces of soil particle), it was a bit surprising that the LL results of xanthan were relatively similar to that of dextran. This leads one to consider there may be factors beyond just polarity, and LL_B, contributing to the changes in LL for biopolymer-soil mixtures. It is possible that the molecular size and shape, could also have an effect. In other words, the xanthan may have been less effective at increasing cohesion, but alternatively may provide more opportunities for adhesion, especially at higher concentrations. This seems reasonable considering the shape of biological molecules (e.g., DNA) have been shown to have an impact on how easily they bond to clay minerals (Yu et al. 2013).

Finally, the LL results indicate that there is a potential point of biopolymer-soil mixtures at which the impact of different soil types becomes negligible (the trendlines of 100K0M, 85K15M, and 70K30M all converged). In other words, there is a point at which adding additional biopolymer may no longer be cost effective as a soil additive for high LL soils. It is possible this point represents the concentration at which the soil is starting

to behave as a gel, and there is little to no particle-to-particle interactions. This is particularly true of xanthan at 8% (LL about 100%) and carrageenan at 8% (LL about 325%). In short, additional biopolymer above 8% would likely result in the same LL, regardless of soil type. Note that the results for dextran presented in Figure 4.5 appear to be starting to converge and the saturation point is likely above the maximum concentration of 8% tested in this investigation. The one exception to this behavior is for the 70K30M soil which the specimen with 4% guar does not match the convergence LL obtained for the 4% guar 100K0M and 85K15M specimens (note: this test was repeated twice and the same result was obtained). This likely represents two different behaviors, associated with two different soil consistencies. The lower values (LL about 200% for 100K0M and 85K15M soils) may be caused by a matrix supported mixture, with isolated macroflocs; the soil is being sheared through the more gel like matrix. The higher value (LL = 350% for 70K30M) maybe associated with a more uniform textured soil.

4.4.2 Fall Cone and ESEM

The results of this investigation indicate that Fall Cone testing is a better measure of biopolymer-soil behavior than liquid limit testing, for two reasons: First, the liquid limit test is inherently a dynamic test and biopolymer solutions often demonstrate pseudoplastic behavior. Therefore, the shearing of the pore fluid during liquid limit testing can have an impact on results, decreasing the LL (and likewise decreasing the apparent strength) of the mixture. Also, the Fall Cone results indicate that biopolymer-soil mixes demonstrate a sensitive time-dependent strength gain. Since liquid limit testing is performed on

thoroughly remolded soils, and represents a snapshot in time, it cannot adequately capture this time-dependent strength gain, especially on intact samples.

The immediate strength gain observed in the FC tests is likely a combination of increased viscosity of the pore fluid and increased cohesion of the clay particles (i.e., formation of flocs). The time-dependent strength gain is likely predominantly caused by an increase in adhesion between flocs by the formation of biopolymer bridges (formation of microflocs and macroflocs) over time as the soil matrix reorganizes. This was because the time-dependent strength gain was often somewhat, if not entirely, removed during remolding. Likewise, the time-dependent strength gain may represent an unstable situation (i.e., sensitivity). Traditional thixotropy (Mitchel 1960) alone was not enough to explain this strength gain, because the time-dependent strength gain of the biopolymer-soils well exceeded that of the control, particularly for the 100K0M mixtures.

The idea that increased cohesion and adhesion affected the soil at different rates, and with different degrees of sensitivity, was supported by the ESEM observations. During the ESEM testing, some biopolymer strands broke during scans, while the flocculi remained intact. In short, remolding the soil destroys biopolymer bridges, and in doing so breaks down microflocs and macroflocs into flocculi. The flocculi cannot be further broken down, and represents the immediate and permanent strength gain (in addition to that provided by increased viscosity of the pore fluid). Presumably, if the remolded soil was allowed to rest, some bridges might begin forming again with time, as the water and biopolymer redistribute throughout the void space in an arrangement approaching a new equilibrium.

Finally, the Fall Cone strength results for the 85K15M were much lower than that of the 100K0M mixtures. This may be because the water contents of the 85K15M samples were much higher (and the densities much lower) than the 100K0M samples, although both were prepared to their respective control LL. This difference resulted in more dilute biopolymer solutions, and likewise less viscous solutions, in the 85K15M mixtures. Also, because of the increased void space, the clay particles were inherently further away from each other. This decreased both cohesion and adhesion; the cohesion decreased because attractive forces were weaker over larger distances, and the adhesion decreased because it was difficult to form bridges across the larger void space. This interpretation is supported by the normalized results which showed similar s_u/s_{ut0} values.

It is interesting to note that the Fall Cone strength values for xanthan 4%-amended clays were less than those of the 1% mix, for both soil types. This raises a couple of important points. First, it is obvious that the strength gain was not necessarily proportional to the amount of added biopolymer. Also, the 100K0M mixes corresponded to two of the ESEM tests. The ESEM images of the 1% mix (Figure 4.9c) show the polymer strands that adhered to the soil particles, while in the 4% mix (Figure 4.5e) the biopolymer present as a film in the void space. This shows that the 4% mix may contain supersaturated (or excessive) biopolymer; the biopolymer solution was getting in the way of particle-to-particle cohesion forces. This rendered the biopolymer ineffective as a soil improvement additive.

4.4.3 Future Considerations

The biopolymers tested in this research covered a wide range of unit costs. Xanthan was moderately priced; however, it did not demonstrate a significant improvement of soil properties (relative to the other biopolymers tested). Therefore, xanthan may not provide significant improvement in field conditions. Dextran was the most expensive, and guar was the least expensive, per unit weight. Ironically, dextran, did not provide any significant increase in LL or undrained shear strength values as compared to guar. While this may suggest that that guar is the most cost-effective option, it is important to note that guar also produced a more viscous solution, and therefore required considerable effort both to dissolve into solution, and to incorporate that solution into the soil. Therefore, in terms of a soil improvement technique, unit cost of biopolymer chemical is only one part of cost-effectiveness; field mixing time and equipment should also be considered.

Moving forward, there remains much to be learned regarding biopolymers and their impact on clay soil properties. It is apparent from this investigation that chemistry plays an important role in biopolymer-soil interactions. Future investigations should consider the influence dissolved salt ions have on results, as this would better represent intertidal environmental conditions. Further studies are also required to better understand biopolymer-soil interactions upon remolding. It would be interesting to see if time-dependent strength gains are made following remolding, and the rate at which such gains might occur. This is particularly important when considering biopolymers as a soil improvement technique in areas with heavy traffic and, likewise, soil disturbance. Finally, additional studies are required to better understand the most efficient way to incorporate

biopolymer solutions into in situ soil for field placement and ground improvement purposes.

4.5 Summary and Conclusions

In summary, biopolymers act as soil binders and may prove to be an effective soil improvement additive for reducing coastal erosion, increasing undrained shear strength, and improving building foundation soils. Many factors affect soil strength and behavior when biopolymers are present in the pore fluid including the chemical properties of the soil and biopolymer, concentration of the biopolymer, water content and stiffness of the soil, elapsed time, and degree of remolding. Gaining a better understanding of the impact of various biopolymers on different soils, at different concentrations, and over a prolonged period of time, can be beneficial to further understanding their potential use for coastal restoration and protection effort.

This work tested three soils consisting predominantly of kaolin, with varying amounts of montmorillonite, mixed together within xanthan, guar, carrageenan and dextran in concentrations ranging from 1 to 8% by dry mass of soil. Tests included liquid limit, fall cone measurement of undrained shear strength, and environmental scanning electron microscope (ESEM).

Based on the liquid limit testing, it is clear that guar and carrageenan behave fundamentally differently from xanthan and dextran. The increased LL by guar and carrageenan is likely associated with their high LL_B values. Xanthan and dextran, on the other hand, have lower LL_B values. When the LL results are normalized by LL_B, it become apparent that cationic dextran has more pronounced effect on increasing the particle-to-

particle attraction. There may be factors beyond just LL_B, such as polarity, which may contribute to the changes in LL. It is possible that the molecule size and shape may affect the soil-biopolymer mixtures. Xanthan may be less effective in increasing cohesion, but alternatively may have provided more opportunities for adhesion, especially at higher concentrations. Finally, each biopolymer likely has a critical concentration at which the impact of different soil types becomes negligible, as the soil becomes saturated with biopolymer solution, and reduces particle-to-particle interactions.

The Fall Cone results demonstrated both an immediate strength gain up addition of a biopolymer to a soil, and a sensitive time-dependent strength gain. The immediate strength gain was likely a combination of increased viscosity of the pore fluid and increased cohesion of the clay particles (formation of flocculi). The time-dependent strength gain was likely predominantly caused by an increase in adhesion between flocs by the formation of biopolymer bridges (formation of microflocs and macroflocs) over time as the soil matrix reorganizes.

Since a liquid limit test is performed on thoroughly mixed soil, and represents a snapshot in time, it cannot adequately capture the time-dependent strength gain, especially for intact samples. Therefore, fall cone testing is preferred over liquid limit testing for quantifying biopolymer-soil interactions. Also, liquid limit tests may not accurately account the pseudoplastic behavior demonstrated by many biopolymer solutions.

The biopolymers tested in this research covered a wide range of unit costs. Xanthan was moderately priced; however, it did not demonstrate a significant improvement of soil properties (relative to the other biopolymers tested). Therefore, xanthan may not provide significant improvement in field conditions. Dextran was the most expensive, and guar

was the least expensive, per unit weight. Ironically, dextran, did not provide any significant increase in LL or undrained shear strength values as compared to guar. While this may suggest that that guar is the most cost-effective option, it is important to note that guar also produced a more viscous solution, and therefore required considerable effort both to dissolve into solution, and to incorporate that solution into the soil. Therefore, in terms of a soil improvement technique, unit cost of biopolymer chemical is only one part of cost-effectiveness; field mixing time and equipment should also be considered.

Moving forward, there remains much to be learned regarding biopolymers and their impact on clay soil properties. It is apparent from this investigation that chemistry plays an important role in biopolymer-soil interactions. Future investigations should consider the influence of dissolved ions on the behavior of soft clays, as this better represents the intertidal environments with saline or brine water. Further studies are also required to better understand biopolymer-soil interactions upon remolding. Finally, additional studies are required to better understand the most efficient way to incorporate biopolymer solutions into the in-situ soil for practical ground improvement.

4.6 Acknowledgments

The authors would like to thank Ms. Jing Peng for her help with the index testing of control soils. Thanks to Dr. Yongkang Wu and Mr. Shengmin Luo for their assistance with X-ray Diffraction testing. Thanks to Dr. Gregory Hendricks for his assistance with the Scanning Electron Microscopy (SEM). The project described was supported by Award Number S10RR021043 from the National Center for Research Resources. The authors are solely the responsibility for the content of this paper and do not necessarily represent the

official views of the National Center for Research Resources or the National Institutes of Health. Special thanks to Ms. Martha Harris and Ms. Xianxiu Xie for their assistance with biopolymer sample preparation and liquid limit testing. Finally, the authors want to thank Dr. Jon Woodruff for serving as an interdisciplinary PhD committee member.

The authors also want to acknowledge several sources of funding that made this research possible, including the Boston Society of Civil Engineers Section (BSCES) of the American Society of Civil Engineers (ASCE) Leo Casagrande Memorial Scholarship, the National Science Foundation Research Collaboration Network (RCN), Science, Engineering and Education for Sustainability (SEES) Grant: "RCN-SEES: Sustainable Adaptive Gradients in the Coastal Environment (SAGE): Reconceptualizing the Role of Infrastructure in Resilience," Award Number: ICER-1338767, and several sources of support provided by UMass Amherst such as the Graduate School Dissertation Research Grant, Charles Perrell Fellowship, and Edith Robinson Fellowship.

4.7 Tables

Table 4.1: Summary of Important Clay Mineral Properties (after Holtz et al. 2011)

Mineral	Typical Thickness (nm)	Typical Diameter (nm)	Specific Surface (km^2/kg)	CEC (meq/100 g)	Activity
Kaolinite	50 – 2000	300 – 4000	0.01 – 0.02	2 – 15	0.3 – 0.5
Montmorillonite	3	100 – 1000	0.7 – 0.84	80 – 150	4 – 7

Note: CEC = Cation exchange capacity

Table 4.2: Summary of Biopolymers

Biopolymer	Source	Polarity	Molecular Weight (X 10^6 g/mol)	Molecular Shape	Cost ($/100 g)
Xanthan	Bacteria	Anionic (negative)	0.9 – 1.6	cellulose chain	$40
Guar	Plant Seed	Neutral	2.0	linear chain with side units	$25
Carrageenan	Seaweed	Neutral	0.2 – 0.4	helix	$45
Dextran	Bacteria	Cationic (positive)	0.5	branched	$315

Table 4.3: Summary of the Liquid Limit, Clay Fraction and Minerology for the three test soils.

Soil	$LL_{0\%}$ (%)	CF (%)	Primary Clay Minerals	Secondary Clay Minerals
100K0M	44	63	kaolinite	-
85K15M	96	67	kaolinite	montmorillonite, illite
70K30M	175	71	kaolinite, montmorillonite	illite

Note: $LL_{0\%}$ = liquid limit (no biopolymer added), clay fraction (CF) = % < 0.002 mm, primary minerals comprise of at least 15% of soil by dry mass, secondary minerals comprise less than 15% of the soil by dry mass.

Table 4.4: Liquid limit results of biopolymer-only tests.
These consisted of biopolymer mixed with DI water. No soil was included.

Biopolymer	$LL_{B\,(\%)}$
Xanthan	720
Guar	3,200
Carrageenan	4,100
Dextran	40

Note: $LL_{B(\%)}$ = the liquid limit of the biopolymer only (no soil).

4.8 Figures

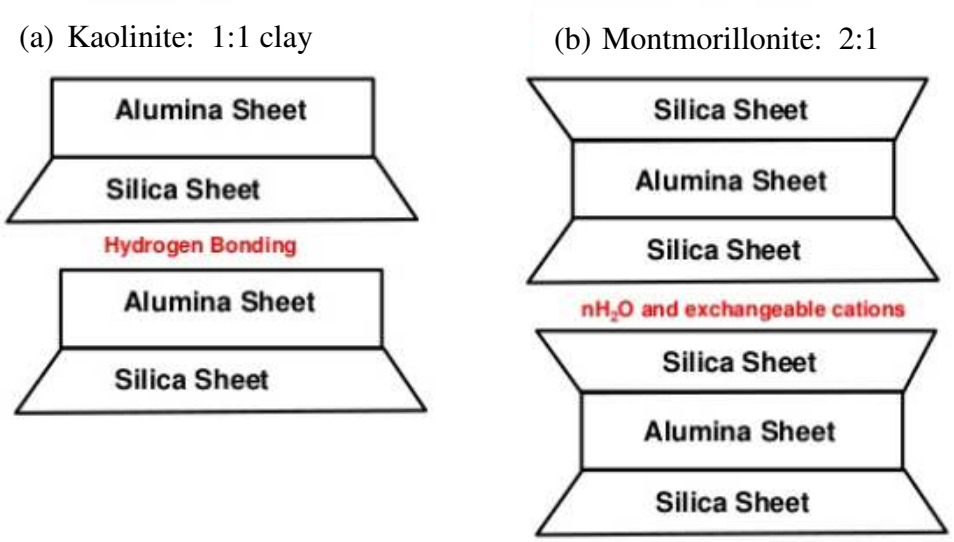

Figure 4.1: Clay Mineral Structure of (a) Kaolinite versus (b) Montmorillonite (after Holtz et al. 2011)

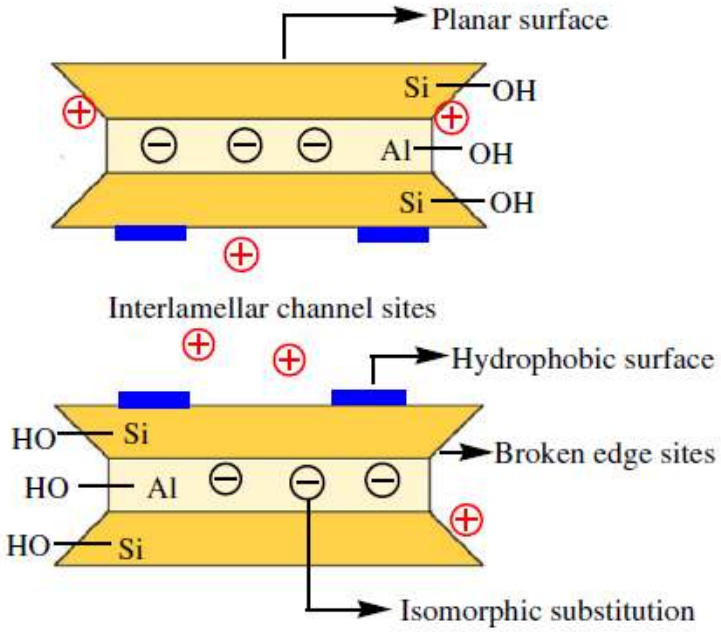

Figure 4.2: Main adsorption sites on clay minerals (Yu et al. 2013)

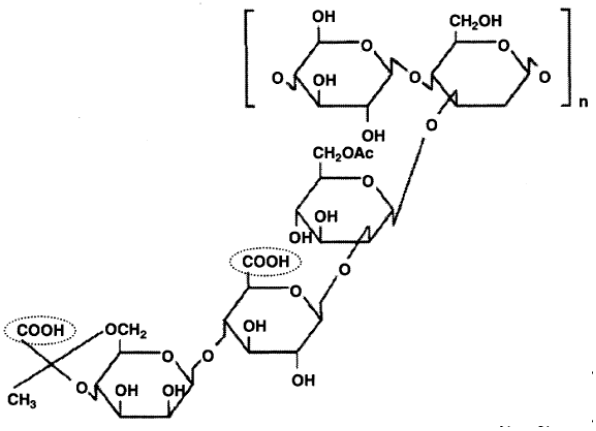

(a) Xanthan

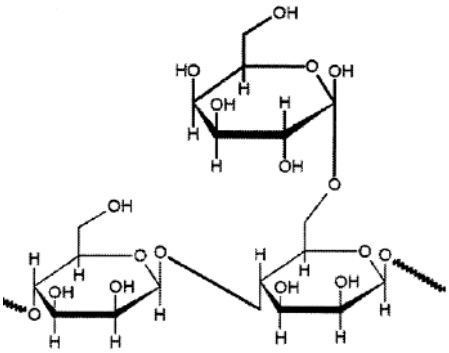

(b) Guar

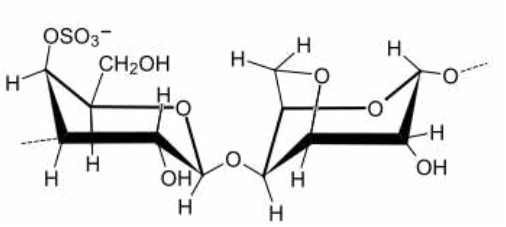

(c) κ-Carrageenan

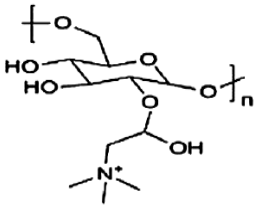

(d) Cationic Dextran

Figure 4.3: Chemical structure of each biopolymer: (a) Xanthan (after Nugent et al. 2009), (b) Guar (after Nugent et al. 2009), (c) κ -Carrageenan (FAO 1965), and (d) DEAE-Dextran (after Samal et al. 2012) (not to scale).

(a) (b)

Figure 4.4: Laboratory Preparation of Soil Samples: (a) Guar dissolved in DI water to form solution in 700 ml beaker and (b) 6-quart electric mixer used to incorporate biopolymer solution into soil.

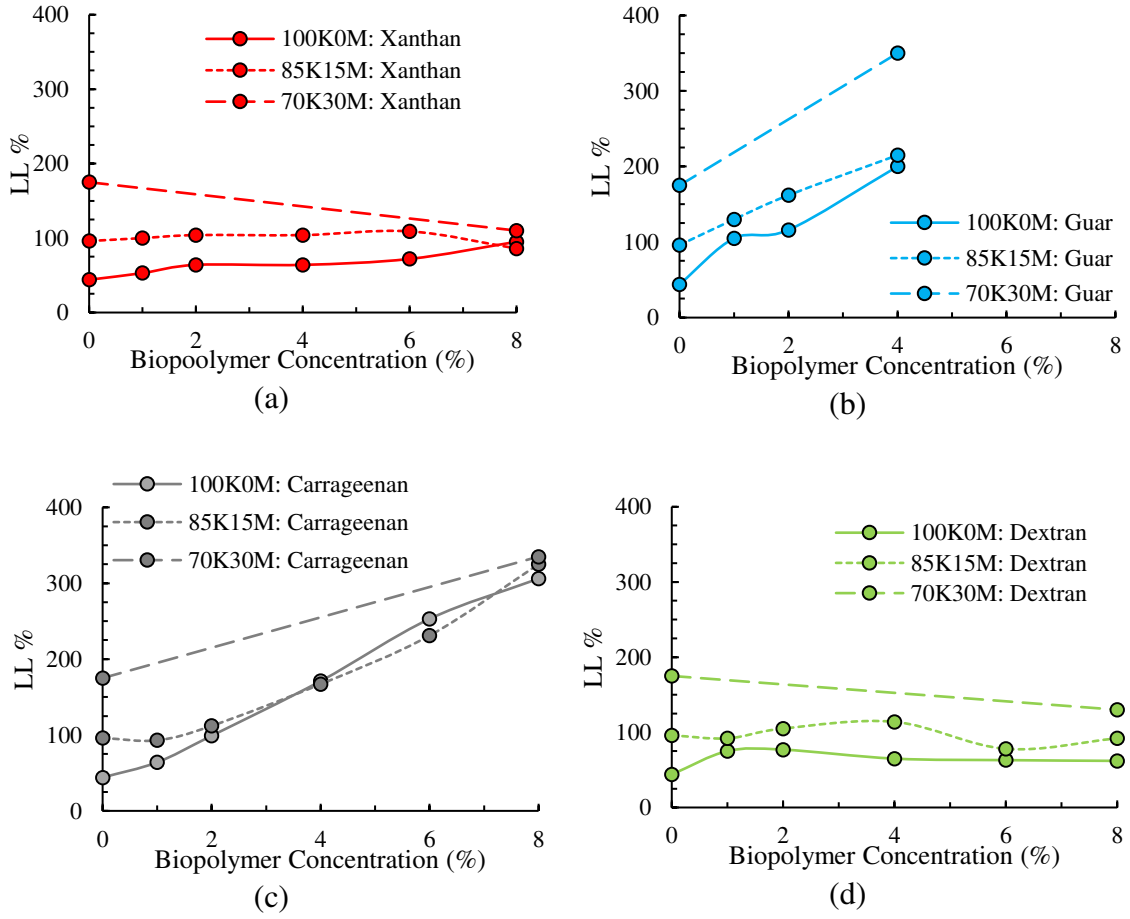

Figure 4.5: Results of biopolymer-soil liquid limit tests. Results show (a) xanthan in red, (b) guar in blue, (c) carrageenan in gray, and (d) dextran in green. 100K0M, 85K15M, and 70K30M soils are shown as solid, short-dashed, and long-dashed trend lines, respectively.

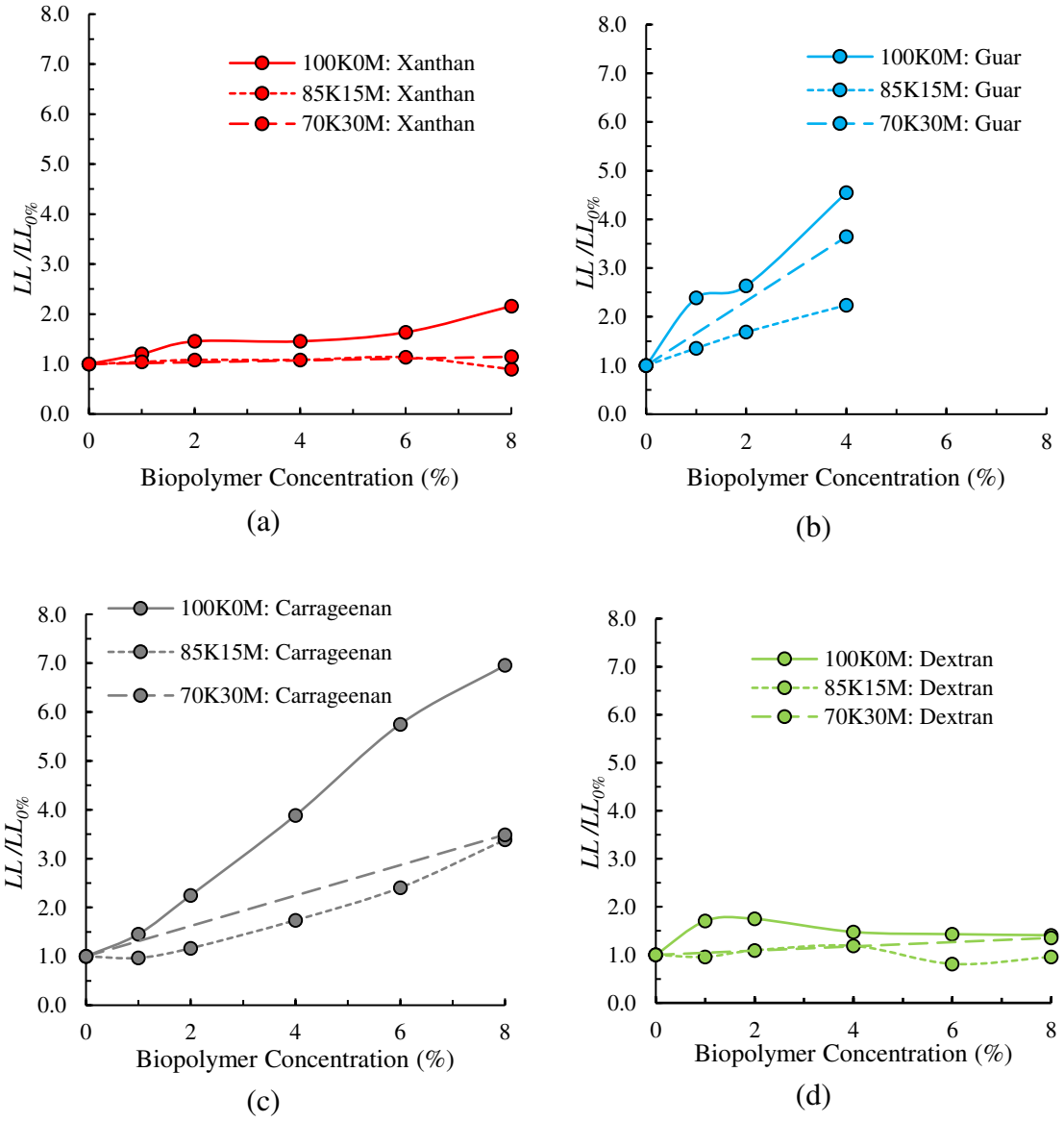

Figure 4.6: Normalized results for biopolymer-soil liquid limit testing. Results show (a) xanthan in red, (b) guar in blue, (c) carrageenan in gray, and (d) dextran in green. 100K0M, 85K15M, and 70K30M soils are shown as solid, short-dashed, and long-dashed trend lines, respectively.

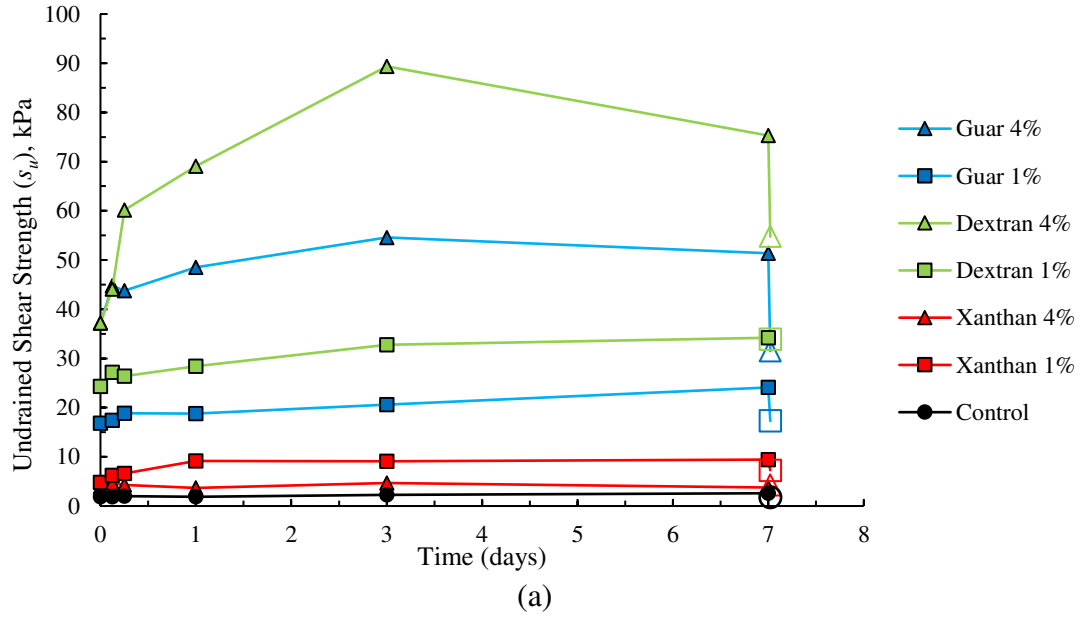

(a)

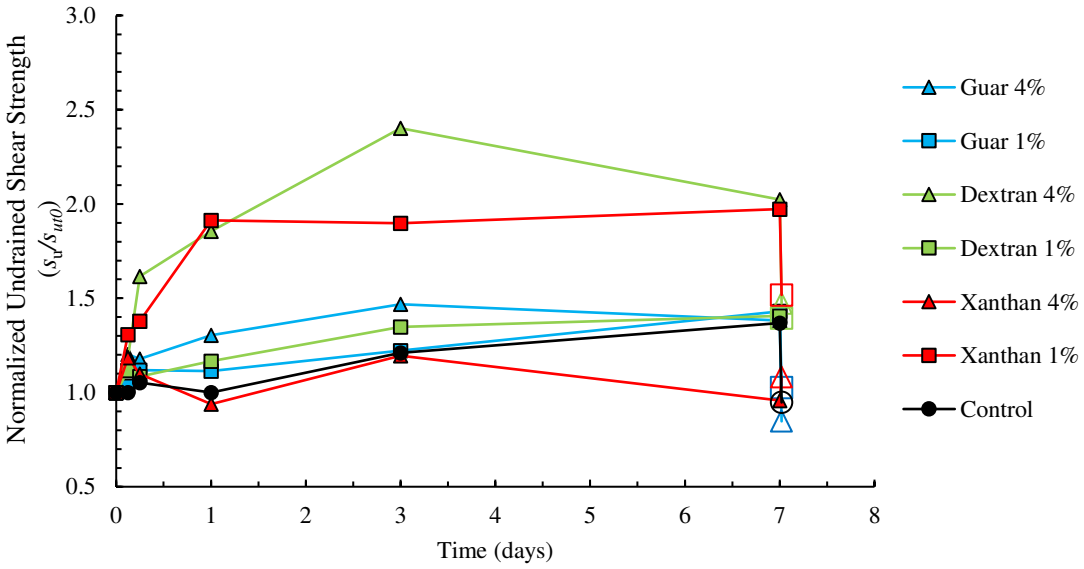

(b)

Figure 4.7: Fall Cone Results for 100K0M: (a) undrained shear strength values over time, (b) normalized undrained shear strength values s_u/s_{ut0}. Results show xanthan in red, guar in blue, dextran in green, and control in black. Concentrations of 1% and 4% are shown as squares and triangles, respectively. Open symbol represents test after remolding

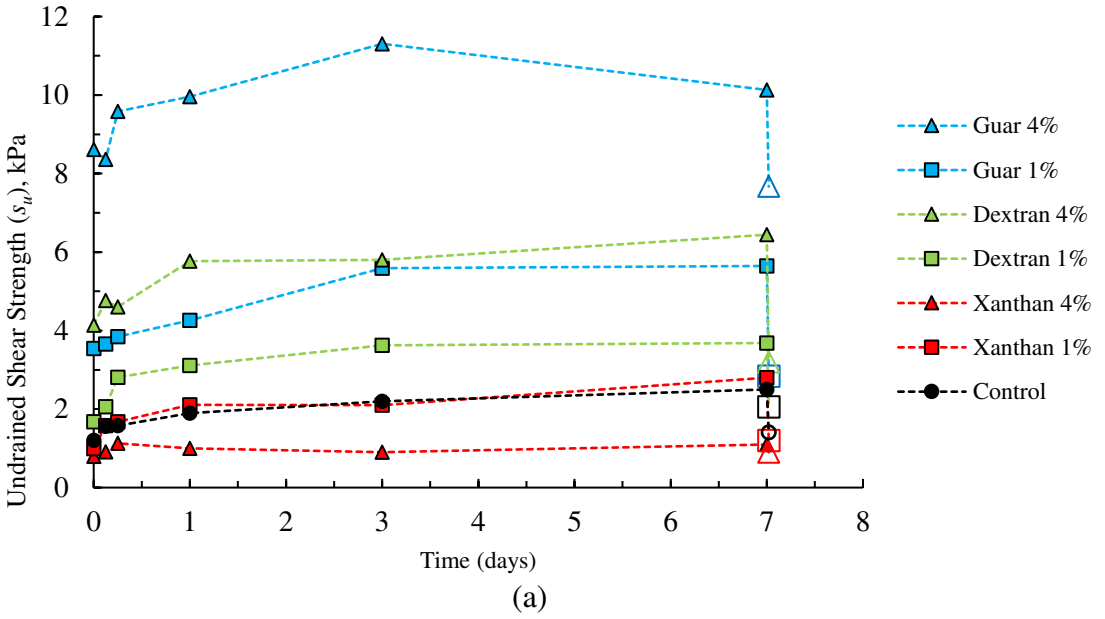

(a)

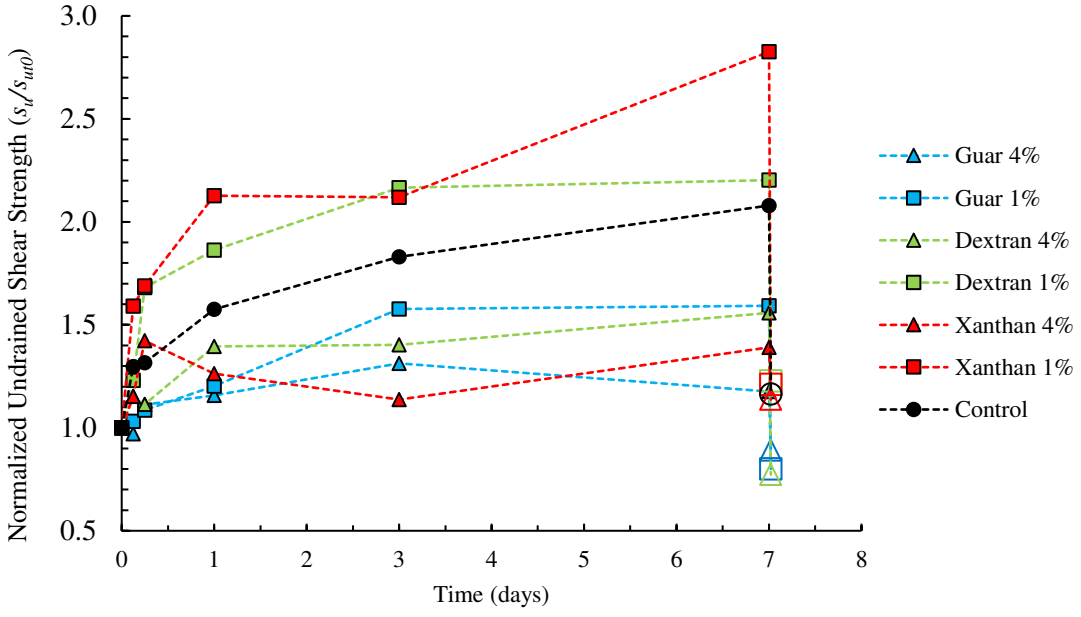

(b)

Figure 4.8: Fall Cone Results for 85K15M: (a) undrained shear strength values over time, (b) normalized undrained shear strength values. Results show xanthan in red, guar in blue, dextran in green, and control in black. Concentrations of 1% and 4% are shown as squares and triangles, respectively. Open symbol represents test after remolding

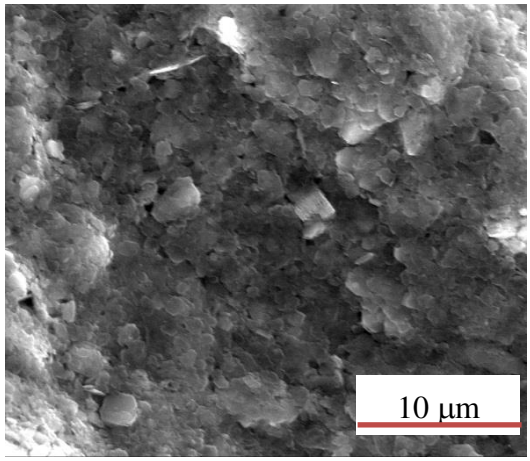

(a) Control – 0%

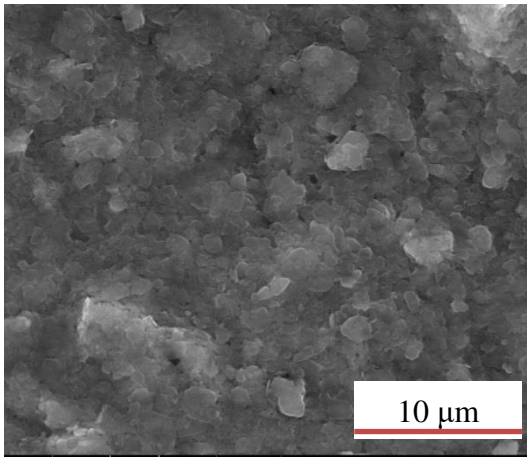

(b) Xanthan – 0.5%

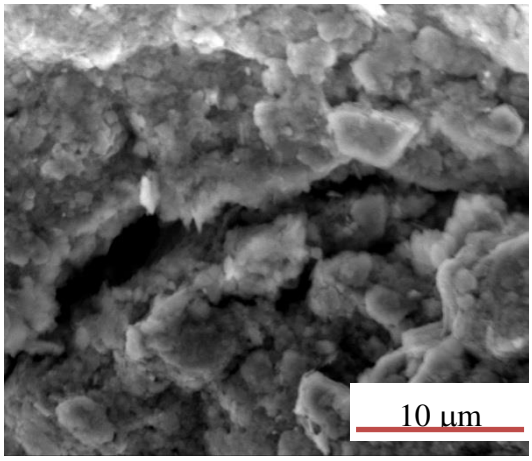

(c) Xanthan – 1%

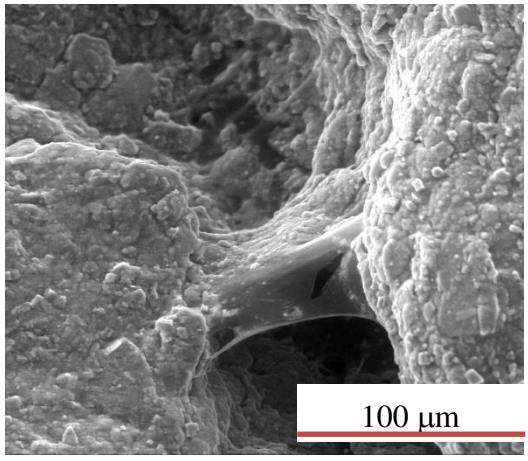

(d) Xanthan – 2%

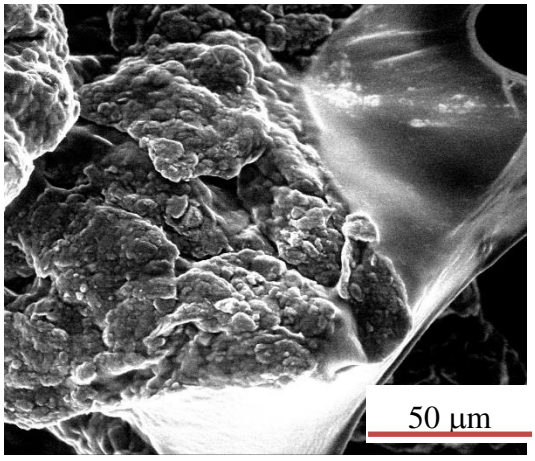

(e) Xanthan – 4%

Figure 4.9: ESEM Results for 100K0M, (a) is control, and (b) – (e) are increasing in xanthan concentration.

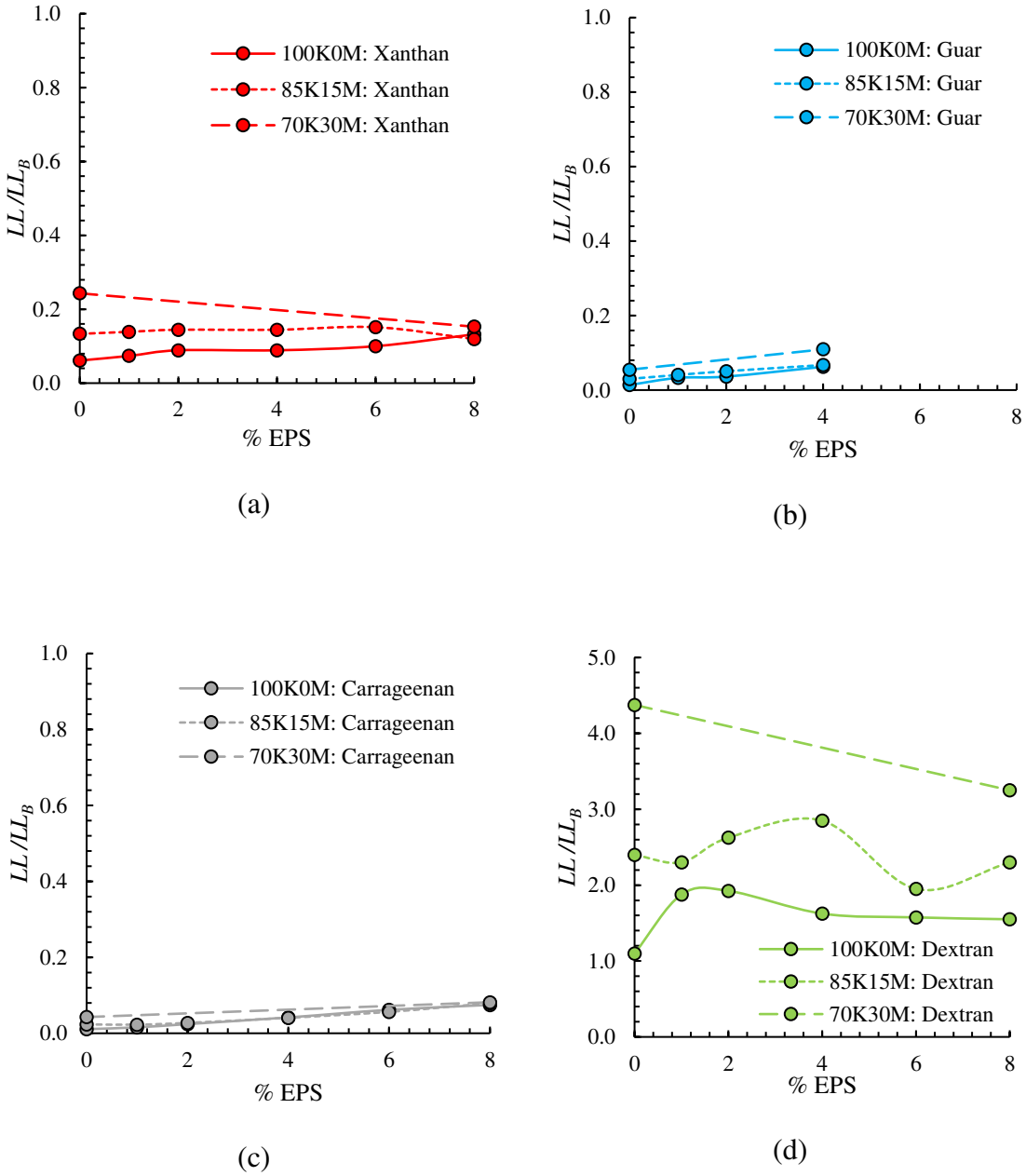

Figure 4.10: Liquid limit results normalized by biopolymer-only tests. Results show (a) xanthan in red, (b) guar in blue, (c) carrageenan in gray, and (d) dextran in green. Note: vertical scale for dextran is different than the other three biopolymers (xanthan, guar, and carrageenaan).

4.9 References

Abu-Zreig, M. (2006). "Control of Rainfall-Induced Soil Erosion with Various Types of Polyacrylamide (8 pp)." *Journal of Soils and Sediments,* 6(3), 137-144.

ASTM (2007). "ASTM D422 – 63: Standard Test Method for Particle-Size Analysis of Soils." ASTM International Committee D18 on Soil and Rock, Subcommittee D18.03 on Texture, Plasticity and Density Characteristics of Soils.

ASTM (2010). "ASTM D4318 – 10: Standard Test Methods for Liquid Limit, Plastic Limit, and Plasticity Index of Soils." ASTM International, Committee D18 on Soil and Rock, Subcommittee D18.03 on Texture, Plasticity and Density Characteristics of Soils.

Chang, I., Im, J., Prasidhi, A., and Cho, G. (2015). "Effects of Xanthan gum biopolymer on soil strengthening." *Construction & Building Materials,* 74 65-72.

Chang, I., Im, J., and Cho, G. (2016). "Introduction of Microbial Biopolymers in Soil Treatment for Future Environmentally-Friendly and Sustainable Geotechnical Engineering." *Sustainability* 8(251).

Chenu, C. (1993). "Clay- or sand-polysaccharide associations as models for the interface between micro-organisms and soil: water related properties and microstructure." *Geoderma,* 56(1), 143-156.

DeJong, J. (2015) "Sustainable Biogeotechnics." Geostrata, Published by the Geo-Institute, ASCE, September/October 2015.

Dontsova, K., and Bigham, J. (2005). "Anionic Polysaccharide Sorption by Clay Minerals." *Soil Science Society of America Journal*. 69:1026–1035.

FAO (1965). "Agar and Carrageenan Manual, Chapter 3: Properties, manufacture and application of seaweed polysaccharides agar, carrageenan and algin." Food and Agriculture Organization of the United Nations.

Grabowski, R.C., Droppo, I.G., and Wharton, G. (2011). "Erodibility of cohesive sediment: The importance of sediment properties." *Earth Science Reviews,* 105(3-4), 101-120.

Herrera, M. P. and Vasanthan, T. (2018). "Rheological characterization of gum and starch nanoparticle blends." *Food Chem.,* 243 43-49.

Holtz, R.D., Kovacs, W.D., and Sheahan, T.C. (2011). *An introduction to geotechnical engineering*. Pearson, Upper Saddle River, NJ.

ISO (2017). Geotechnical investigation and testing -- Laboratory testing of soil -- Part 6: Fall cone test, ISO 17892-6, Geneva, Switzerland.

McGill, H., McMahan, A., Wigodsky, H., and Sprinz, H. (1977). “Carrageenan in formula and infant baboon development.” *Gastroenterology*. 73: 512 – 517.

Meng, X., Jia, Y., Shan, H., Yang, Z. and Zheng J. (2012). "An experimental study on erodibility of intertidal sediments in the Yellow River delta." *IJSRC International Journal of Sediment Research,* 27(2), 240-249.

Mitchel, J. (1960). “Fundamental Aspects of Thixotropy in Soils.” *Journal of the Soil Mechanics and Foundations Division, Proceedings of the American Society of Civil Engineers*, June 1960.

Nugent, R., Zhang, G., and Gambrell, R. (2009). “Effect of exopolymers on the liquid limit of clays and its engineering implications.” *Transportation Research Record*, 2101, 34-43.

Or, D., Smets, B. F., Wraith, J. M., Dechesne, A., Friedman,S.P. (2007). "Physical constraints affecting bacterial habitats and activity in unsaturated porous media - a review." *Advances in Water Resources.,* 30(6-7), 1505-1527.

Partheniades, E. (1971). “River Mechanics, Chapter 25: Erosion and deposition of cohesive materials.” Edited and published by H.W. Shen, Fort Collings, CO, 1-46.

Samal, S., Dash, M., Moroni, L., van Blitterswijk, C., Samal, S. K., Dash, M., Van Vlierberghe, S., Dubruel, P., Kaplan, D. L., Chiellini, E., van Blitterswijk, C., and Moroni, L. (2012). "Cationic polymers and their therapeutic potential." *Chem.Soc.Rev.,* 41(21), 7147-7194.

Sharma, B. and Bora, P. (2003). “Plastic limit, liquid limit and undrained shear strength of soil—reappraisal.” *Journal of Geotechnical and Geoenvironmental Engineering*. August 2003, 129(8), 774 – 777.

Tabujew, I. and Peneva, K. (2015). “Functionalization of Cationic Polymers for Drug Delivery.” *Royal Society of Chemistry.* RSC Polymer Chemistry Series No. 13, Cationic Polymers in Regenerative Medicine.

Tolhurst, T.J., Black, K.S., Shayler, S.A., Mather, S., Black, I., Baker, K., and Paterson, D.M. (1999). "Measuring the in situ Erosion Shear Stress of Intertidal Sediments with the Cohesive Strength Meter (CSM)." *Estuarine, Coastal and Shelf Science Estuarine, Coastal and Shelf Science,* 49(2), 281-294.

Tolhurst, T.J., Defew, E.C., de Brouwer, J.F.C., Wolfstein, K., Stal, L.J., and Paterson, D.M. (2006). "Small-scale temporal and spatial variability in the erosion threshold and properties of cohesive intertidal sediments." *Cont.Shelf Res.,* 26(3), 351-362.

Watts, C.W., Tolhurst, T.J., Black, K.S., and Whitmore, A.P. (2003). "In situ measurements of erosion shear stress and geotechnical shear strength of the intertidal sediments of the experimental managed realignment scheme at Tollesbury, Essex, UK." *Estuarine Coastal & Shelf Science,* 58(3).

Whitcomb, P. J., Gutowski, J., and Howland, W. W. (1980). "Rheology of guar solutions." *J Appl Polym Sci,* 25(12), 2815.

Yu, W., Tong, D., Zhou, C., Lin, C. X., and Xu, C. (2013). "Adsorption of proteins and nucleic acids on clay minerals and their interactions: A review." *Appl.Clay.Sci.,* 80-81 443-452.

Yang, Z., Yang, H., and Yang, H. (2018). "Effects of sucrose addition on the rheology and microstructure of κ-carrageenan gel." *Food Hydrocoll.,* 75 164-173.

Zhang, G., Yin, H., Lei, Z., Reed, A., and Furukawa, Y. (2013). “Effects of exopolymers on particle size distributions of suspended cohesive sediments.” *Journal of Geophysical Research: Oceans*, Vol. 118, 1–17.

CHAPTER 5

DEVELOPMENT OF A PORTABLE ANNULAR FLUME FOR EVALUATING SOIL ERODIBILITY

5.1 Abstract

This chapter presents the design and fabrication of a portable annular flume that was first developed at the University of Massachusetts Amherst, hereafter termed UMass Amherst flume (UMAF). The purpose was to design and build a small portable device for the characterization of annular erosion of primarily very soft cohesive soils under varying tidal inundations, as well as granular sandy deposits. An infrared light sensor and sampling port were designed and installed to measure the total suspended sediment concentration (SSC). Numerical modeling was performed to assess the applied shear stress at the soil-water interface for varied flow velocities induced by the paddle rotation. The functionalities of the UMAF were validated by performing laboratory erosion tests on a series of samples consisting of very soft cohesive soils, coarse-grained soils, and two biopolymer-clay mixtures. Results indicated that the critical erosion threshold (CET) observed in the UMAF were similar to some prior findings but were generally lower than the values estimated from some empirical relationships. In addition, it was found that soils with similar undrained shear strengths may exhibit different CET, likely caused by differences in minerology. Finally, biopolymer admixtures can increase CET for very soft cohesive soils, suggesting their potential for practical applications in bio-inspired soil improvement.

5.2 Introduction

In the United States cohesive soils are prevalent in most major estuaries and bays, such as Boston Harbor, San Francisco Bay, the Delaware River estuary, and the New York City's Hudson River estuary (Nugent et al. 2009). Significant interests in observing and quantifying erosion, especially of cohesive soils, greatly developed circa 1950, with concerns of the stability and functionality of navigation channels (Partheniades 1971). Deposition of fine grained sediment within the nearshore channels can cause excessive "shoaling" (or filling in and shallowing) of such channels, making navigation difficult. Minimizing erosion of cohesive soils is important to the protection of United States coastlines in such events as flooding, coastal storms, surges, and hurricanes. Coastal wetlands in the U.S., for example, were estimated to provide $23.2 billion per year in storm protection services alone based on a regression model of 34 major hurricanes having landed on the U.S. coastal lines since 1980; a loss of 1 ha of wetland in the model corresponded with increased average storm damages of $33,000 from specific storms (Sutton-Grier et al. 2015).

A soil's vulnerability to erosion is generally quantified by considering there is a certain water flow velocity over a soil bed at which the induced shear forces acting on the sediment particles is sufficient to dislodge them from their equilibrium positions (Bohling, 2009). However, fine-grained soils (i.e., silts and clays) and coarse-grained soils (i.e., sands and gravels) erode in fundamentally different manners. This is illustrated well by the Hjulström diagram (Figure 5.1), which predicts a state of either sedimentation, transport, or erosion, based on particle size and respective flow velocity. While the terms "transport" and "erosion" are somewhat subjective based on the scale of the respective

investigation (Miller et al. 1977), it is generally understood that "transport" refers to an individual partial moving from point A to point B. "Erosion", on the other hand, refers to mass wasting of the soil bed (Boggs 2000). The velocity of flowing water at which transport occurs is therefore less than that at which erosion occurs. Likewise, a small amount of transport may be acceptable for practical purposes, whereas erosion is of greater concern to engineers, as the situation may warrant mitigation measures. Note that according to the Hjulström diagram, as the size of coarse-grained soil particles increases, the critical flow velocity also increases, which is reasonable due to the larger weight of the particle. For fine-grained soils, however, the flow velocity required for erosion increases as particle size decreases. This is due to physiochemical properties such as cohesion and other electrostatic interactions between particles. Moreover, the range of velocities at which erosion is expected to occur is larger for clays than sands and gravels, indicating greater uncertainty in assessing the erosion of soft clays. CET is often defined in terms of shear velocity of the fluid or as an applied shear stress at the soil-water interface. The general empirical relationship between shear velocity (u^*) and bed shear stress (τ_0) (regardless if it is high enough to surpass CET) is given by Equation 1 (Pope et al. 2006).

$$\tau_0 = \rho \times (u^*)^2 \qquad \textit{Eq. 1}$$

where:

τ_0 = erosion shear stress [Pa]

ρ = density of the fluid [kg/m3]

u^* = shear velocity [m/s]

In the event that the shear velocity of the fluid (or equivalate bed shear stress) is high enough reach the CET of the soil, the velocity and stress terms are instead denoted as u_c^* and τ_c, respectively.

While erosion is a heavily studied field, erosion of silts and clays is generally less well understood than erosion of sands. This is likely due to the fact that there are many complicated, interrelated, and poorly understood factors that affect the behavior of very soft cohesive soils, similar to those found in intertidal mudflats (Tolhurst et al. 1999). These factors may include (but are not limited to) stress history, compressibility, shear strength, plasticity, microbiology, organic matter content, and water holding capacity (Grabowski et al. 2011).

The most common methods to attempt to quantify a soil's vulnerability to erosion include: (1) Direct measurements using laboratory flumes (e.g., Pope et al. 2006), (2) estimation by empirical correlations based on soil parameters (such as particle size and undrained shear strength) (e.g., Clark and Wynn 2007), and (3) direct in situ measurements with a submerged flume or other devices (e.g., Tolhurst et al. 1999 and Bale et al. 2006). The general methodology by which erosion experiments are performed usually incorporates flowing water or a water jet exerted on the soil surface. The flow velocity (or jet pressure) is increased until the soil just begins to erode, which is referred to "incipient motion". Such a flow velocity at which the soil just begins to erode corresponds to the critical shear stress of surface erosion. There are many limitations and challenges regarding obtaining reliable measurements of soil erosion. In general, different erosion devices give inconsistent results, so there is no standardized method for measuring critical erosion shear stress (Widdows et al. 2007 and Tolhurst et al. 2000).

One of the commonly used erosion measurement devices is the Cohesive Strength Meter (CSM) (Tolhurst et al. 1999). The CSM is designed to measure critical erosion shear stress of intertidal sediments in situ and was used in several erosion studies (e.g., Perkins

et al. 2004, Prellwitz and Thompson 2014, Spears et al. 2008, Tolhurst et al. 2006, Watts et al. 2003, and Yallop et al. 2000). The CSM utilizes a vertical pressurized water jet to erode the sediment surface within a chamber pushed into the sediment surface. An infrared light path traverses the chamber above the sediment surface. Bed erosion is inferred from the drop in the transmission of infrared light across the chamber caused by the suspension of sediment (Tolhurst et al. 1999 and Widdows et al. 2007).

It is important to note that, according to Widdows et al. (2007), variations exist in results for similar soils among different erosion measurement devices. The CSM generates turbulent pressures downward perpendicular to the bed, whereas the annular flumes apply horizontal flows and hence bed shear stresses horizontally across the sediment. Annular flumes therefore tend to simulate the bed stresses induced by tidal currents, whereas the CSM vertical jet possibly produces a stress comparable to rainfall. Further, Widdows et al. (2007) found that the CSM may not be very effective in measuring the differences in erosion thresholds of soft estuarine sediments. Since annular flumes best represented stresses induced by tidal currents, and were better suited for soft estuarine sediments, the UMAF was designed as an annular flume (as opposed to a vertical jet).

In an annular flume, flow is generally driven through the use of rotating paddles and the water is recirculated in a circular path. The two key measured parameters are suspended sediment concentration and flow velocity. The main benefit of the annular flume (as opposed to jets or straight flumes) is that the flow has a potentially infinite path length, and therefore an individual particle can remain in motion for a long time. A challenge associated with annular flumes is that flow velocity varies in the x, y, and z directions. This makes measuring the velocity and sediment concentration, without

disrupting the flow field, particularly challenging. Further, techniques to measure bed shear stresses directly (e.g., using a shear plate) are very complex, especially under turbulent conditions. For these reasons, accurate flow measurement equipment can be technically challenging and expensive. An acoustic Doppler velocimeter (ADV), for example, quantifies flow velocity in three directions, but can be cost prohibitive to some projects (SonTek 2014).

Infrared light is traditionally used for suspended sediment concentration measurements because infrared light dissipates quickly over short distances in liquid water. Therefore, infrared light detected by a receiver was most likely generated by a nearby source, as opposed to ambient light (such as sunlight). In an optical backscatter sensor (OBS), infrared light is emitted from a source, reflected off soil particles, and returned to a receiver. In this manner, an increase in infrared light recorded by the receiver is proportionate to the amount of sediment in solution (Christie et al. 1997). Above a certain sediment concentration, the infrared light recorded by the receiver starts to decrease as the receiver is essentially blocked by sediment. Although, the concentration at which this occurs is typically above the point of critical erosion for fine grained soils. Optical Backscatter Sensors (OBS) are often purpose built for a specific project (example: Bale et al. 2006) and therefore require significant investment in time in research and development. These equipment challenges are further compounded when monitoring equipment is placed within the flow field, potentially disrupting the flow.

The design and construction of the University of Massachusetts Amherst Flume (UMAF) included an infrared light sensor and sampling port were developed to quantify the suspended sediment concentration (SSC). Explicit efforts were made to ensure the

following: (1) the device was small enough to be portable and operated onshore by one or two individuals, (2) the flow field was not disturbed by the environment during testing, and (3) fabrication costs were kept to a minimum as possible and the device was built with "off the shelf" parts whenever possible. Computational fluid dynamics modeling was performed to quantify the applied shear stress field at the soil-water interface under varied flow conditions. Performance of the UMAF was validated through a series of laboratory erosion tests on a several very soft cohesive soil samples, several coarse-grained soils, and two biopolymer-soil mixtures.

5.3 Small-Scale Annular Flume

Annular flume systems are extensively used to investigate the erosion of naturally formed and laboratory reproduced soils. In an annular flume, the fluid flow is fastest near the bottom surface of the paddles and, due to the frictional drag, slower near the soil-water interface. This creates a challenge for interpreting the critical erosion threshold (CET) velocity because critical erosion is dependent on the shear stress at the soil surface. Further, the flow is generally fastest at the outer portion of the flume and slower towards the center of the flume. This is due to the difference between angular velocity and linear velocity which is proportional to the radial distance measured from the center. Although there is an exception to this generality as the velocity immediately adjacent to the wall is slower because viscous drag forces start to dominate on the rough surface. This phenomenon is known as the "law of the wall" (Bohling, 2009). For these reasons, the flow field within an annular flume is nonuniform in the x, y, *and* z directions. This makes obtaining accurate direct measurements of the flow velocity and likewise shear stress challenging. Also,

laboratory tests which are performed in terms of paddle rotational velocity (RPM) must be converted into the shear stress exerted by the flowing water inside the chamber.

The Annular Flume (AF) developed by Pope et al. (2006) at the Plymouth Marine Laboratory (PML) has a 0.64 m outer diameter, 0.44 m inner diameter, and working volume of 60.0 L (Figure 5.2). Water flow was induced by rotating an annular drive cylinder with four paddles. Current velocities were increased in stepwise increments from 5 to 50 cm/s; each rotational speed was maintained for 15 – 20 min. Rotor speed was calibrated in terms of bed shear stress by employing a polyurethane foam cut to fit the annulus space and inserted into the base of the flume as a surrogate for smooth, muddy soil. A downward-looking 3D acoustic doppler velocimeter (ADV) probe (16 MHz Sontek MicroADV) was then inserted through the foam into the center of the track. Once filled with water, the flume was operated normally. Bed shear stress (τ_0) was then determined by applying the Turbulent Kinetic Energy (TKE) approach to the ADV data. Just downstream of the ADV was an optical backscatter sensor (OBS 3-M, D&A Instruments) flush mounted in the outer flume wall to measure the turbidity or the SSC of the flowing water throughout the entire testing. The OBS was periodically calibrated by samples collected via a sampling port in the outer chamber.

A similar but smaller annular flume was developed by Bale et al. (2006) (also affiliated with the PML), known as the Mini-Annular Flume (MAF). Its outer diameter was 200 mm with a 70 mm wide track, and the volume of water was 2.9 L. It was designed to be portable as it was used for field testing (Figure 5.3). The MAF operated in a similar general fashion as the AF, but with two important differences: The MAF did not have a sampling port, and the MAF had a miniature OBS housed within the flume between the

side edge of the paddles and flume wall. The MAF was calibrated using a similar method as the AF. Calibration of the MAF resulted in the following empirical relationships:

$$U = 0.00246(RPM) \quad \text{Eq. 2}$$

where:

U = average current velocity at mid channel [m/s]

RPM = rotor speed [rotations / min]

and

$$\tau_0 = 2.6038U^3 + 0.5562U^2 + 0.1759U + 0.008 \quad \text{Eq. 3}$$

5.4 UMass Amherst Flume (UMAF)

The UMAF design combined the benefits of both the AF of Pope et al. (2006) and the MAF of Bale et al. (2006). Specifically, the UMAF was scaled to be portable (similar to the MAF), adopted an inexpensive in-house designed and fabricated infrared light (IR) backscatter sensor in the flume wall combined with a sampling port (similar to the AF). In this manner, suspended sediment concentration (SSC) could be quantified continuously during testing using the IR sensor without disturbing the flow field. This also allowed for validation of the IR sensor operation by gravimetric analysis using the sampling port. As for measurement of flow velocity or bed shear stress, it was not possible to obtain expensive ADV instrumentation for this work and therefore a series of computational fluid dynamics (CFD) simulations were performed to quantify the fluid velocity distribution throughout the flume and the shear stress at the soil bed-water surface.

5.4.1 UMAF Structure

The UMAF has an outer tube with a 305 mm outer diameter, 13 mm thick wall, and a thin walled inner annular tube 76 mm diameter, making the flume track 102 mm wide. The walls are made of acrylic, with the bottom of the outer tube having a tapered edge for ease of insertion into the soil bed (Figure 5.4a). The flume chamber is 304 mm tall, and the flume was designed to be inserted about 114 mm into a natural soil bed, resulting in ~11 L of water in the chamber. Above the chamber is a 1/18 hp DC motor that rotates a drive shaft with four aluminum paddles spaced at 90 degrees at rotation velocities of 5 to 86 RPM. The paddle rotation velocity is directly proportional to the input voltage applied to the DC motor with a maximum obtainable rate of 86 RPM under a maximum input voltage of 20 V. Each paddle is 84 mm long, 61 mm high, and 6 mm thick. The motor is fastened on a metal top plate that covered the outer tube. A filling port, bubble level, and pair of handles are located on the top plate. The purpose of the bubble level and handles are to help ensure verticality while inserting the flume into the soil bed. Midway up the outer tube wall is the sampling port, and 180 degrees from the sampling port is the IR sensor.

Adding a sampling port to the flume wall that was both inexpensive and portable posed several challenges. It needed to be small and watertight, to prevent leakage and minimize possible disturbance to the flow inside the chamber. The final selection consisted of a septum pinned against a narrow opening in the outer tube by a set screw (12.7 mm long) with a vented opening of 1.57 mm in diameter. Such a device allows a hypodermic needle to pass through the vented set screw, pierce the septa to enter the flume chamber

and collect a soil suspension sample. Upon retrieval of the needle the septum can seal the opening and prevent leakage (Figure 5.4b)

An infrared optical backscatter sensor was designed for the UMAF using basic, inexpensive photodiodes. The UMAF IR sensor design was initially prototyped by trying a variety of different IR light emitters, IR light receivers, and resistors. The final design consists of four emitters that generate 950 nm IR light (manufacturer: Marktech Optoelectronics; Digi-Key Electronics part number: 1125-1156-ND; cost: approx. $8/ea) surrounding a single receiver (wavelength: 950 nm, spectral range: 870 nm to 1050 nm; viewing angle: 120 degrees; manufacturer: Vishay Semiconductor Opto Division; Digi-Key Electronics part number: 751-1008-ND; cost: approx. $1/ea). Two emitters are located about 12.7 mm above and below the receiver, while the other two are located about 19.1 mm on the two sides of the receiver (Figure 5.4c), measured as the arc distance along the outer wall of the flume. The entire assembly is installed in the outer flume wall. An excitation voltage of 5.0 V is applied to the system, 200 Ohm resisters are used for each of the emitters (to prevent the emitters from blowing out), and the actual voltage recorded is read across a 200 kOhm resister associated with the receiver (Figure 5.5). Readings are recorded digitally using a 22 bit digital-to-analog converter controlled by TestNet data acquisition software via a laptop.

The IR sensor functionality and range were validated by using sediment in suspension with known SSC of 0.1 to 15.0 g/L (Figure 5.6a). This range was specifically selected to allow sufficient readings both above and below the point of critical erosion, which was found to nominally occur at about 1.0 g/L for fine-grained soils (Bale et al. 2006). Two test soils were used for these measurements: a commercial, kaolinite rich,

white soil known as Prestige (Unimin Corporation) and a naturally occurring, illite rich gray soil known as Boston Blue Clay (BBC).

Table 5.1 presents the general index and classification properties of the two soils; index tests were performed in general accordance with pertinent ASTM standard methods (ASTM 2017). Based on the results presented in Figure 5.6b, it is clear that the soil type (grain size distribution, mineralogy, color, etc.) can play a significant role in infrared light results, even for the same concentration. Although in annular flume experiments the onset of erosion is determined from the break in the SSC versus flume RPM (or velocity) curve. Thus, when using IR readings as a proxy for direct measurement of SSC the relative change in voltage recorded by the sensor is important for a given soil and not the absolute values.

5.4.2 Estimation of Velocity and Soil Bed Shear Stress

The three-dimensional CFD model created for analyzing the UMAF flume was conducted using ANSYS Fluent version 17.2 which is a finite-volume method of analysis. The standard k-epsilon (k- ε) model (Launder and Spalding 1977) was used to account for the influence of turbulence. The k- ε model gives a general description of turbulence by means of two partial differential transport equations. The first transported variable is the turbulence kinetic energy (k). The second transported variable is the rate of dissipation of turbulence energy (ε).

The CFD model considered the general geometry of the flume including the cylindrical acrylic walls, annular space, four rotating paddles, and flat top. The flume and soil geometry external to the flow field were not considered. This enabled the meshing calculations to focus on the actual fluid flow volume. The top was considered a “slip”

surface whereas the acrylic side walls and the bottom at the soil-water interface were considered "no-slip stationary walls." The x, y, z coordinate system (Figure 5.7) considered the bottom of the paddles as a baseline elevation (El. 0.00 mm) with location above the paddles taken as positive and within this coordinate system the soil bed-water interface was set at El. -128 mm.

The ANSYS Fluent model was run using stepped increases in paddle rotation velocity, similar to the steps applied during erosion testing. The motion of the paddles was analyzed in terms of a Multiple Reference Frame (MRF) model which is a steady-state approximation in which individual cell zones move at different rotational and/or translational speeds. The flow in each moving cell zone is solved using the moving reference frame equations. At the interfaces between cell zones, a local reference frame transformation is performed to enable flow variables in one zone to be used to calculate fluxes at the boundary of the adjacent zone. The model was divided into two fluid regions, the upper "motion" region where the paddles are located and the lower "static" region below the paddles (Figure 5.7). The "motion" region has an input velocity equal to the rotational rate of the paddles (RPM), whereas the static region has an initial velocity of zero. In an MRF model, translational and rotational velocities are assumed to be constant (ANSYS, 2009). In this manner, the model represents a snapshot of the fluid after the paddles have been rotating long enough for the fluid flow to approach a steady state.

The CFD model was analyzed using a non-uniform mesh size which allowed for a finer mesh (and likewise more accurate results) near the soil bed-water interface while minimizing the required computing power. A mesh size of 3.8 mm, 5.1 mm and 2.5 mm was used for the motion region, the static region, and the soil bed-water interface areas,

respectively. The water was considered deionized, at room temperature, with a density of 998 kg/m^3 and a viscosity of 1.00x10^{-3} kg/m-s. The density of the water was considered constant throughout testing because the mass of suspended sentiment after erosion was minimal, and its impact on the overall fluid properties was negligible.

ANSYS uses two parameters to model boundary roughness effects: the roughness height K_s and the roughness constant C_s. The default roughness height K_s is zero which corresponds to smooth walls and this value was used for the vertical (acrylic) walls of the flume. For the soil bed-water interface, ANSYS recommends K_s be taken as equal to the mean soil grain diameter (d_{50}). The default roughness constant C_s is 0.5 which nominally represents a uniform sand grain with no irregular bed features; a non-uniform soil would have a higher value ($C_s \approx 0.5$ to 1.0). ANSYS provides little guidance beyond this; although a preliminary parametric analysis showed that unlike K_s, the C_s parameter has little influence on the results for the UMAF. As such, the soil bed-water interface in the UMAF was modeled as a boundary consisting of a generic soft clay with a roughness height K_s = 2.0x10^{-6} m and a roughness constant C_s = 0.40. Supplemental ANSYS models were performed to account for the high roughness of the three coarsest soils (two sands and one grave); these coarse soil models considered C_s = 0.5, and $K_s = d_{50}$ for the respective soil.

The side wall and most importantly the soil bed-water interface were modeled using the ANSYS default standard wall functions for turbulent flow conditions. These functions are based on Launder and Spalding (1977) and are a collection of semi-empirical formulas and functions that link the solution variables at the near-wall cells and the corresponding quantities on the wall (ANSYS 2009). The walls are taken as no-slip boundaries and the laws-of-the-wall approach was utilized to determine the mean velocity. While the flow

conditions were considered turbulent, even if this was not the case for low RPMs, the solution approach was also valid for laminar flow conditions.

ANSYS runs were performed with motor rotation speeds ranging from 5 to 86 RPM; each run took about 10 to 14 hours of computation time using a desktop PC. Figure 5.8 presents an example set of results for the velocity profile as a function of radial distance from the center of the flume (x axis) within the static water region for a paddle rotational velocity of 86 RPM (the inner flume extends to x = 38 mm). As expected, given the flume construction and geometry, the velocity is greatest at the location of the paddles and increases with radial distance (x direction) from the center of the flume while it decreases with vertical distance below the paddles (y direction) down towards the soil bed-water interface. Furthermore, close to the vertical boundaries (i.e., the smooth acrylic walls) the velocity rapidly drops off to zero; likewise at the soil bed-water interface. The discontinuity in the velocity plot at the base of the paddles is because the paddles do not extend all the way to the inner tube wall. Figure 5.9 plots an example of computed velocity depth profiles at the mid-track location for several RPMs and Figure 5.10 plots the depth averaged value for each profile versus RPM. Figure 5.11 plots the resulting shear stress at the soil bed-water interface versus radial distance for the paddle rotational velocity of 86 RPM. As also expected, the shear stress reaches a maximum within the flume track and approaches zero at both the inner and outer lateral boundaries. Figure 5.12 plots the maximum and average shear stress (across the width of the soil bed) versus the full range of motor RPMs.

Table 5.2 presents a summary of the CFD flow conditions over a range of RPMs for the assumed conditions of a clay soil bed surface with $K_s = 2.0 \times 10^{-6}$ m and a roughness constant $C_s = 0.40$. The Reynolds number (R_e) of the flow is computed assuming a cylindrical vessel stirred by a central rotating paddle (Başbuğ et al. 2017) as

$$R_e = ND^2/\nu \qquad \textit{Eq. 4}$$

where:

N = rotation velocity of the paddles (rotations/second)

D = diameter of the agitator

ν = kinematic viscosity of the fluid

The system is fully turbulent for R_e values above 10,000.

If the velocity profile is assumed to be logarithmic in the region immediately above the soil bed-water interface as described by the von Karmen–Prandtl equation (Pope et al. 2006), the normalized velocity is computed as

$$u/u^* = (1/K)\ln(z/z_0) \qquad \textit{Eq. 5}$$

where

u = velocity at the height (z) above the bed

u^* = friction velocity

K = von Karmen constant

z = height above bed of interest

z_0 = roughness length

and the bed shear stress is computed using the general form of Equation 1.

The CFD simulations provide the value of $\tau_{0,max}$ for a given RPM. Thus u^* was computed from Equation 1 which in turns allows for the roughness Reynolds number to be computed as Equation 6 (Bohling 2009).

$$R_e^* = u^* d_{50}/\nu \qquad Eq.\ 6$$

where

d_{50} = mean grain size (m)

ν = kinematic viscosity of water

and the corresponding roughness length (Dade et al. 2001) as

$$z_0 = k_s[1 - exp(R_e^*/28) + 10/(3R_e^*)]/30 \qquad Eq.\ 7$$

where

k_s = the effective bed roughness, which can be estimated for a flat non-rippled bed with $k_s = 2.5d_{50}$ (Soulsby 1997, Bolhing 2009)

Given that no direct measurements of field velocity were possible in the UMAF, the CFD results were validated using the experimental data collected in the MAF by Bale et al. (2006). The MAF was modeled in the same way as described above for the UMAF and Figure 5.13 plots the Bale et al. (2006) determined relationship between flume rotation rate and soil bed-water interface (Equations 2 and 3) together with that predicted from the ANYSIS Fluent model. The close match between the two indicated that the ANSYS Fluent modelling methods, assumptions, and results for the UMAF were reasonable. The soil bed shear stress values for the two flumes are very similar at low RPMs but then start to deviate significantly above around 60 RPM. The MAF had a 200 mm diameter, whereas the UMAF had a 280 mm diameter and therefore at the same RPM the UMAF has a higher equivalent

linear velocity at the paddles and greater flow turbulence, especially at higher RPMs, resulting in a higher soil bed shear stress.

5.5 Test Methods

The UMAF was validated in terms of its ability to quantify critical erosion shear stress for very soft cohesive soils (i.e., undrained shear strength less than about 10 kPa) through a series of laboratory experimental erosion tests. Test samples of Prestige kaolin and BBC were mixed with deionized water to water contents relative to the liquid limit and then placed in a 380 x 380 x 150 mm acrylic box which was lined with a geotextile at the base and had several holes in the bottom to allow consolidation drainage. Filter paper lined both the top and bottom of the soil. A metal top plate was incrementally loaded with dead weights to consolidate the soil (Figure 5.14a). In this manner, a very soft soil bed was produced with a uniform consistency (minimal air bubbles) and a horizontal surface.

The undrained shear strength of the consolidated soil bed was measured using three different methods: miniature full flow penetrometers, miniature motorized laboratory vane (MLV), and fall cone (FC). The miniature full-flow penetrometers consisted of both a mini-T-bar and a mini-ball and were advanced into the soil bed using a computer controlled GeoJac loading system (Figure 5.15), which is described in more detail in Boscardin (2013). The major advantage of using the full-flow penetrometers was that a depth profile of undrained shear strength can be obtained and in addition to testing at different lateral locations the overall spatial uniformity of the test soil could be assessed. To this end the full-flow penetrometers would typically be performed in each corner of the test bed. The full-flow penetrometers also provided the option to evaluate the sensitivity of the soil by

conducting a cyclic test which would progressively degrade the soil shear strength down to its remolded state. The miniature motorized laboratory vane consisted of a 38 mm by 19 mm four bladed vane, driven by a computer-controlled servo motor at a constant rate of rotation of 60 degrees/minute (ASTM D4648). The MLV test was typically performed in the center of the test bed and the developed rotation force was measured with a torque transducer. This test procedure also had the advantage of being able to measure the sensitivity of the soil by conducting multiple fast rotations of the vane after the initial intact strength test was computed and then measuring the resulting undrained shear strength after remolding. The disadvantage of the MLV test was that according to ASTM D4648 the vane must be penetrated at least one vane diameter into the test bed and hence does not measure the near surface undrained shear strength. It is also not possible to obtain a continuous profile of undrained shear strength. The third measurement method was the fall cone (ISO 17892-6:2017), which consisted of free penetration a 60 g/60 degree or 100 g/30 degree polished stainless steel cone into the surface of the soil for 5 seconds. The undrained shear strength was determined using the empirical correlations presented in ISO (2017). The major advantage of the FC was that the test was easy and quick to perform and also tested the soil at soil bed surface.

Once the soil bed was ready for erosion testing, the flume was inserted into the soil bed surface (Figure 5.14b) together with the inner tube, filled with deionized water via a filling port, and monitored continuously using the infrared light sensor (obtaining readings every 2 seconds). For erosion testing, the IR sensor data acquisition program was initiated and thereafter the paddle RPM was incrementally increased and held for at least 10 minutes at each RPM increment to allow for steady state conditions to be achieved. In most cases,

a 20 mL gravimetric sample was obtained via the septa sampling port just before increasing the RPM for the next increment. To minimize disturbance to the flow field, gravimetric samples were only obtained at the end of an incremental rotation step, after the flow field approached steady state. Capturing the early, low values of suspended sediment concentration (SSC) was important to clearly define the subsequent onset of erosion. Therefore, gravimetric analysis was performed using a balance with a resolution of 0.0001 g. At the completion of each test, the sampling port septa was discarded and replaced with a new one. The Prestige soil bed was tested two additional times, consecutively, to the examine what impact, if any, rinsing the soil surface had on the results.

Additional tests were performed on Prestige and BBC at various water contents (for a range of undrained shear strength), four coarse grained soils, and two biopolymer-soil mixtures. For these subsequent tests, the outer flume wall remained in place and the soil in the track was replaced. The inner tube was then inserted into the soil bed of interest. The tank was then filled with DI by slowly pouring water onto a donut shaped sheet of bubble wrap that was placed on the soil bed surface to avoid any filling flow induced erosion. Once several centimeters of water filled the flume the bubble wrap was removed and filling continued at a faster flow rate. Finally, the motor and paddles were attached to the outer flume wall. This approach was particularly necessary for testing the coarse-grained soils, as is minimized potential leakage under the flume wall.

Due to the different manners in which fine- and coarse-grained soils erode, it is necessary to have clear definitions of transport and erosion, as well as sedimentation, of the respective particles. Therefore, for the purposes of this investigation, the following definitions were considered for the applicable soils:

- Transport
    - Fine-grained: Unable to be detected by infrared sensor.
    - Coarse-grained: One or two stray particles moving such as bouncing or rolling along bed. Movement is discontinuous.
- Erosion
    - Fine-grained: Break in the curve from the infrared sensor. Generally speaking, a concentration of around 1 g/L suspended at least 1 in above bed surface.
    - Coarse-grained: Many particles moving along bed surface continuously for a distance of at least 6 inches.
- Sedimentation
    - Fine-grained: No particles in suspensions.
    - Coarse-grained: No visible movement on bed surface.

Regarding the coarse-grained soils test specifically, three sands and one gravel were tested in the flume. These soils are referred to (in order of increasing d_{50}) as: fine Ottawa sand, medium Ottawa sand, filter pack sand, and river gravel. These coarse-grained soils were selected because they each were free of fines and had a uniform grain size distribution. A summary table of coarse grained soil properties is provided in Table 5.3. The coarse-grained tests were performed by gradually increasing the RPM of the paddles to observe the point at which mass wasting of the bed occurred (as defined as "erosion" above). The coarse-grained tests provided several benefits including: (1) they allowed the flume to be tested at high CET, (2) mass wasting was directly observed without clouding up the tank, and (3) the tests provided direct comparison to literature in order to confirm reasonableness of results, such as the Hjulström diagram.

The biopolymer-soil mixtures consisted of combining carrageenan with Prestige clay in one of two ways. (See Chapter 4 for additional information regarding carrageenan

and biopolymer-soil mixtures.) The first consisted of mixing a relatively thick biopolymer-DI water solution into soil which already had a water content of 30%. This was referred to as the "biopolymer to wet prestige test." The second test consisted of mixing a more dilute biopolymer-DI water solution to air dried Prestige (in powder form) and was referred to as the "biopolymer to dry prestige test." In both cases, the final target water content (after solution was mixed in) was 44% (i.e. near the liquid limit if the biopolymer had no effect on the soil). The biopolymer/soil ratio was 1% for both mixes, i.e., for each 100 grams of dry prestige, there was 1 gram of dry biopolymer. In this manner, the effect the biopolymer solution had on the soil could be directly compared to the control test, Prestige, 2 kPa, Test 1.

5.6 Analysis of Results

Results from the mini full flow penetrometer and mini lab vane are presented in Figure 5.16 and Figure 5.17, respectively for a sample of Prestige prepared from a slurry and consolidated. These results show that the bed had undrained strength near (or slightly below) 2 kPa, as is expected near the liquid limit. Furthermore, based on the t-bar and ball tests the sample appeared to be relatively uniform both laterally and vertically. For the majority of the follow-on tests, which were conducted by placing test soil directly into the flume with it already in the soil box, it was much easier and quicker to perform the undrained shear strength measurements using the fall cone.

One of the main goals of the coarse-grained tests was to compare results to published values. The Hjulström diagram (Figure 5.1) was originally based on observations of stream erosion and considers the velocity at a location approximately 1 meter and greater

above the stream bed. Hjulström (1935) does note that velocities near the bottom of the stream would be approximately 10 to 20 cm/s less that those given in Figure 5.1. The velocity in the UMAF varies 3 dimensionally, a location within the flume flow field was selected (both laterally and vertically) to approximate a reasonable flow velocity (as determined by the ANSYS model). The location selected was the base of the paddles, at the mid-track for which the critical velocity for the coarse-grained soils were (in order of increasing d_{50}): 20, 28, 41, and 68 cm/s. Clearly as the particle diameter increases, the CET velocity also increases, which is reasonable. Figure 5.18 plots these results on the Hjulström diagram.

The CET for the fine-grained soils was determined by the break in the curve produced by plotting the results from the infrared light sensor, relative to the corresponding average shear stress for the respective paddle rotational velocity. Similarly, a break in the curve of gravimetric SSC values (obtained from the hypodermic needle port grab samples) relative to corresponding shear stress, was also considered when determining CET. Two examples of the manner in which CET was determined for IR and SSC results are presented in Figure 5.19 and Figure 5.20, respectively. Figure 5.19 clearly shows three phases of testing: 1) the early phase (Phase I) shows little change in IR voltage (recall that backscatter IR sensor voltage was proportionate to suspended sediment concentration (SSC)), which indicate that the corresponding shear stress is below the critical erosion threshold (CET), 2) the second phase (Phase II) shows a rapid increase in IR sensor results (SSC) and hence sustainable erosion is ongoing, and 3) the last phase (Phase III) shows the IR sensor results (SSC) beginning to plateau or even decline, showing that the CET was

well exceeded, and the test started to exceed the upper limits of the sensor. The CET was interpreted as the break in the curve between Phase I and Phase II.

The IR sensor results for all of the fine-grained soils tested (without biopolymer) is presented in Figure 5.21 and the interpretation of CET is summarized in Table 5.4. The CET shear stress values as interpreted by infrared light sensor ranged from 0.008 to 0.022, with BBC eroding at a higher shear stress than Prestige for a similar undrained shear strength. Select erosion tests also included gravimetric analysis presented in Figure 5.22 and CET summarized in Table 5.4. Finally, a graph comparing the CET obtained from IR sensor to SSC is presented in Figure 5.23. It is clear from this figure that the results obtained from IR sensor are very nearly similar to that from the SSC gravimetric samples.

The undrained shear strength (by fall cone) of the Biopolymer to Wet Prestige mix was 7 kPa, while the Biopolymer to Dry Prestige mix had an undrained shear strength of 12 kPa. The results of the biopolymer-soil mixture erosion test are presented Figure 5.24. These results show a CET with the biopolymer as about 0.0125 Pa (regardless of mixing method), compared to the control which had a CET of only 0.008 Pa. Finally, a graph was plotted comparing undrained shear strength (by fall cone), and CET shear stress for soils both with and without biopolymers (Figure 5.25). A summary table of fine grained soil tests, and respective flow conditions and critical shear stress properties is provided in Table 5.5.

5.7 Discussion

The fine-grained soil CET values obtained in this investigation were low relative to empirical relationships between CET and undrained shear strength presented in the

literature (e.g. Watts et al. 2003 and Clark and Wynn 2007). However, Bale et al. (2006) tested fine grained soils and obtained CET values as low as 0.02 – 0.03 Pa and as such the values obtained in this investigation are considered reasonable considering that the UMAF and MAF are similar in size and the means of inducing flow on the soil. Furthermore, this work tested young laboratory consolidated test samples undergoing erosion for the first time and are likely to be more erodible than aged in situ soils.

One interesting observation from this investigation is that the BBC eroded at a higher CET than the Prestige, despite the fact that the soil beds were prepared to the same undrained shear strength, and the soils had similar plasticity indexes. This indicates that while undrained shear strength may be one factor in CET shear stress, there are other factors to consider. The most likely explanation for this observation is that the erosion resistance is also related to mineralogy and pore water chemistry. Specifically, the BBC consists predominantly of illite whereas Prestige consist predominantly of kaolin. It is possible that the soil particles of illite are more attracted to each other (more prone to form flocs) than kaolin, and therefore less prone to erosion.

While it is generally understood that resistance to erosion increases with increased undrained shear strength, this investigation did not show this as a strong, clear overall trend (Figure 5.25) – although the data set is limited. This may be due to a couple of factors. First, the undrained shear strengths tested in this investigation did not cover a large enough range to provide confidence in this relationship. Also, as discussed, the difference in minerology between BBC and Prestige may play a role in erosion resistance, regardless of undrained shear strength.

Another interesting observation is that the CET did not change significantly for the various Prestige 2 kPa tests (Prestige Test 1 was a fresh bed, whereas the beds in Test 2 and 3 were rinsed prior to testing). However, the slope of the curve from the IR sensor plot decreased with each subsequent rinsing. This indicates that once erosion started to occur in Test 1, the erosion was more aggressive than in Tests 2 and 3. The likely cause of this is loose particles initially on the soil surface (potentially from adhering to the filter paper) that were eroded during Test 1. Those loose particles were then not available for erosion in subsequent tests. This issue may not arise in erosion tested performed by some straight flumes, as some straight flumes do not recirculate the test fluid. Therefore, the soil surface in a straight flume is perpetually rinsed as the testing continues, and those initial loose particles are removed from the test early on. This observation indicates that pre-rinsing a bed should be considered when performing annular flume studies, particularly on young, soft soils made in the laboratory.

The biopolymers increased the CET of the Prestige by about 50%, which is notable. Even if based on only two tests, it indicates that biopolymers are a potential soil additive to improve in situ soil erosion conditions. While the CET was the same between the wet and dry mixes, the slope of the curve (IR sensor) for the wet mix was slightly steeper than that of the dry mix. This may indicate that the wet mix soil eroded as flocs, and likewise, the wet mix may have not been as uniform a soil as the dry mix; albeit this difference was subtle. Therefore, additional studies are needed to better understand the most effective means to incorporate biopolymer into field soils.

Additional studies are recommended to further validate the flume. These additional studies include both laboratory flume tests and field studies. Specifically, additional

investigations should be performed using the flume on beds with substantially higher undrained shear strengths. Also, as discussed, gaining a better understanding of the influence minerology has on CET results is critical. Finally, it is recommended that the flume be tested in the field; this is feasible because the flume was specifically scaled to be portable.

5.8 Summary and Conclusions

This investigation presented the development and validation of a portable annular flume, UMAF, for the evaluation of erodibility of both cohesive and coarse-grained soils. An annular flume design was chosen because its lateral circular flow is most consistent with tidal inundation (as opposed to a jet erosion device). The UMAF design combined the benefits of Annular Flume (AF) presented by Pope et al. (2006) and the Miniature Annular Flume (MAF) presented by Bale et al. (2006). A wall mounted infrared light sensor and sampling port were developed to quantify suspended sediment concentration. Computational fluid dynamics numerical modeling was performed using ANSYS Fluent to quantify flow conditions without interrupting the flow field. The UMAF was then validated by performing laboratory erosion tests on a series of very soft cohesive sediment, several coarse-grained soils, and two biopolymer-soil mixtures. Important conclusions drawn from this investigation are as follows:

- The CET values observed in the UMAF were generally similar to CET values demonstrated by Bale et al. (2006), particularly for the soils tested by Bale et al. (2006) with density values below than 1200 kg/m^3.

- The CET values observed in the UMAF were generally much lower than values suggested by other empirical relationships based on undrained shear strength (e.g. Watts et al. 2003 and Clark and Wynn 2007). This is likely due to the fact that the empirical relationships were developed using different erosion measurement devices involving different physical mechanisms and/or testing soils that have aged considerably or demonstrate a higher undrained shear strength.
- The newly developed flume included an innovative infrared sensor system that provided total SSC (or turbidity) without disrupting the flow field.
- A hypodermic needle port allowed for collection of grab samples for direct SSC measurements via gravimetric analysis at the end of each increment.
- Interpretation of CET either indirectly (via the IR sensor) or directly (via hypodermic needle port) resulted in similar CET values.
- The functionalities of the new device were validated for both fine-grained and coarse-grained soils, and results were comparable with prior studies (e.g. Bale et al. 2006 and Hjulström 1935).
- Two different soft soils (BBC and Prestige) possessed similar undrained shear strengths and similar index properties; yet yielded different CET values. Such a difference was likely associated with different minerology and pore water chemistry, although additional studies are warranted.
- Biopolymers increased CET for very soft cohesive sediments, suggesting their potential for practical applications in bio-inspired soil improvement. The CET did not vary significantly for the two methods of mixing (wet or dry), although the wet

mixing method may have produced more flocs due to uneven distribution of the biopolymer (as compared to the dry mixing method).

- Additional flume validation tests were recommended. Specifically, future testing should include cohesive soil beds at higher undrained shear strength as well as testing suitability of the flume to in situ field testing. In situ field testing is feasible because the flume was specifically scaled to be portable.

5.9 Acknowledgments

The authors would like to thank Ms. Siyan Lin (undergraduate student in electrical engineering, UMass Amherst) for her assistance in prototyping the infrared light sensor and Mr. Lenny Czerwonka for his machining work to construct the flume. The authors also want to thank Dr. Jon Woodruff (Professor, Geosciences, UMass Amherst) for serving as interdisciplinary PhD committee member.

The authors also want to acknowledge several sources of funding which made this research possible including: The Boston Society of Civil Engineers Section (BSCES) of the American Society of Civil Engineers (ASCE) Leo Casagrande Memorial Scholarship, the National Science Foundation Research Collaboration Network (RCN), Science, Engineering and Education for Sustainability (SEES) Grant: "RCN-SEES: Sustainable Adaptive Gradients in the Coastal Environment (SAGE): Reconceptualizing the Role of Infrastructure in Resilience," Award Number: ICER-1338767, and several sources of support provided by UMass Amherst such as the Graduate School Dissertation Research Grant, Charles Perrell Fellowship, and Edith Robinson Fellowship.

5.10 Tables

Table 5.1: Summary of the index properties and classification of the tested fine-grained soils

Soil Sample	*LL* (%)	*PL* (%)	*PI* (%)	Clay fraction (%)	USCS	Activity	Primary clay minerals
Prestige	44	23	21	63	CL	0.33	kaolinite
BBC	45	24	21	54	CL	0.39	illite

Note: LL = liquid limit, PL = plastic limit, clay fraction (CF) = % < 0.002 mm, Activity = PI/CF, USCS = Unified Soil Classification System

Table 5.2: CFD computation results for flow conditions in the UMAF over a fine-grained soil bed.

N	Velocity	R_e	τ_0		u^* for $\tau_{0,max}$	R_e^*	z_0
			Mean	Max			
RPM	(cm/s)	-	(Pa)	(Pa)	(cm/s)	-	(cm)
5	7.2	6200	0.009	0.012	0.35	6.96E-03	7.98E-03
9	12.9	11200	0.011	0.015	0.38	7.63E-03	7.28E-03
13	18.7	16200	0.013	0.017	0.42	8.37E-03	6.64E-03
21	30.1	26200	0.018	0.025	0.50	1.01E-02	5.52E-03
30	43.1	37500	0.028	0.038	0.62	1.24E-02	4.49E-03
38	54.6	47500	0.040	0.055	0.74	1.49E-02	3.73E-03
47	67.5	58700	0.060	0.084	0.92	1.83E-02	3.03E-03
57	81.8	71200	0.094	0.133	1.15	2.31E-02	2.41E-03
64	91.9	80000	0.130	0.183	1.36	2.71E-02	2.05E-03
74	106.2	92500	0.204	0.291	1.71	3.41E-02	1.63E-03
86	123.5	107500	0.352	0.506	2.25	4.50E-02	1.23E-03

Notes: $\rho = 998.2$ kg/m^3 , $\mu = 1.002\text{x}10^{-3}$ kg/m-s, $\nu = 1.00\text{x}10^{-6}$ m^2/s, $K_s =$ 2.0x10-6 m, $C_s = 0.40$

Table 5.3: Coarse-Grained Soil Properties

Soil	Median Grain Size, d_{50} *(mm)*	Coefficient of Uniformity, C_u	Coefficient of Curvature, C_c
Fine Ottawa Sand	0.3	1.4	1.0
Medium Ottawa Sand	0.6	1.7	0.8
Filter Pack Sand	3.0	1.6	1.0
River Gravel	10.0	1.7	1.0

Table 5.4: Summary of average critical erosion threshold shear stress, as interpreted by infrared light sensor and SSC.

Test	*CET (Pa)*	
	IR Sensor	SSC
Prestige, s_u = 2 kPa, Test 1	0.008	0.008
Prestige, s_u = 2 kPa, Test 2	0.008	0.010
Prestige, s_u = 2 kPa, Test 3	0.010	0.010
BBC, s_u = 2 kPa	0.014	0.016
BBC, s_u = 4 kPa	0.022	0.022
Prestige, s_u = 7 kPa	0.015	0.018
Prestige, s_u = 11 kPa	0.013	-

Table 5.5: Summary of flume test soils and flow conditions at critical shear stress

Test Description	*N*	Velocity	R_e	τ_0		u^* for $\tau_{0,max}$	R_e^*	z_0
				Mean	Max			
-	RPM	(cm/s)	-	(Pa)	(Pa)	(cm/s)	-	(cm)
Prestige, 2 kPa, Test 1	2	2.9	2500	0.008	0.011	0.32	6.49E-03	8.55E-03
Prestige, 2 kPa, Test 2	2	2.9	2500	0.008	0.011	0.32	6.49E-03	8.55E-03
Prestige, 2 kPa, Test 3	7	10.0	8700	0.010	0.013	0.36	7.29E-03	7.62E-03
BBC, 2 kPa	15	21.5	18700	0.014	0.019	0.44	8.76E-03	6.34E-03
BBC, 4 kPa	25	35.9	31200	0.022	0.030	0.55	1.10E-02	5.03E-03
Prestige, 7 kPa	16	23.0	20000	0.015	0.020	0.45	8.97E-03	6.19E-03
Prestige, 11 kPa	13	18.7	16200	0.013	0.017	0.42	8.37E-03	6.64E-03
Biopolymer to Wet Prestige, 7 kPa	13	18.7	16200	0.013	0.017	0.42	8.37E-03	6.64E-03
Biopolymer to Dry Prestige, 12 kPa	13	18.7	16200	0.013	0.017	0.42	8.37E-03	6.64E-03
Medium Ottawa Sand	27	38.8	33700	0.046	0.035	0.59	3.57E+00	5.27E-03
Filter Pack Sand	41	58.9	51200	0.161	0.308	1.76	5.27E+01	2.28E-02
River Gravel	67	96.2	83700	0.440	0.833	2.89	2.89E+02	8.43E-02

5.11 Figures

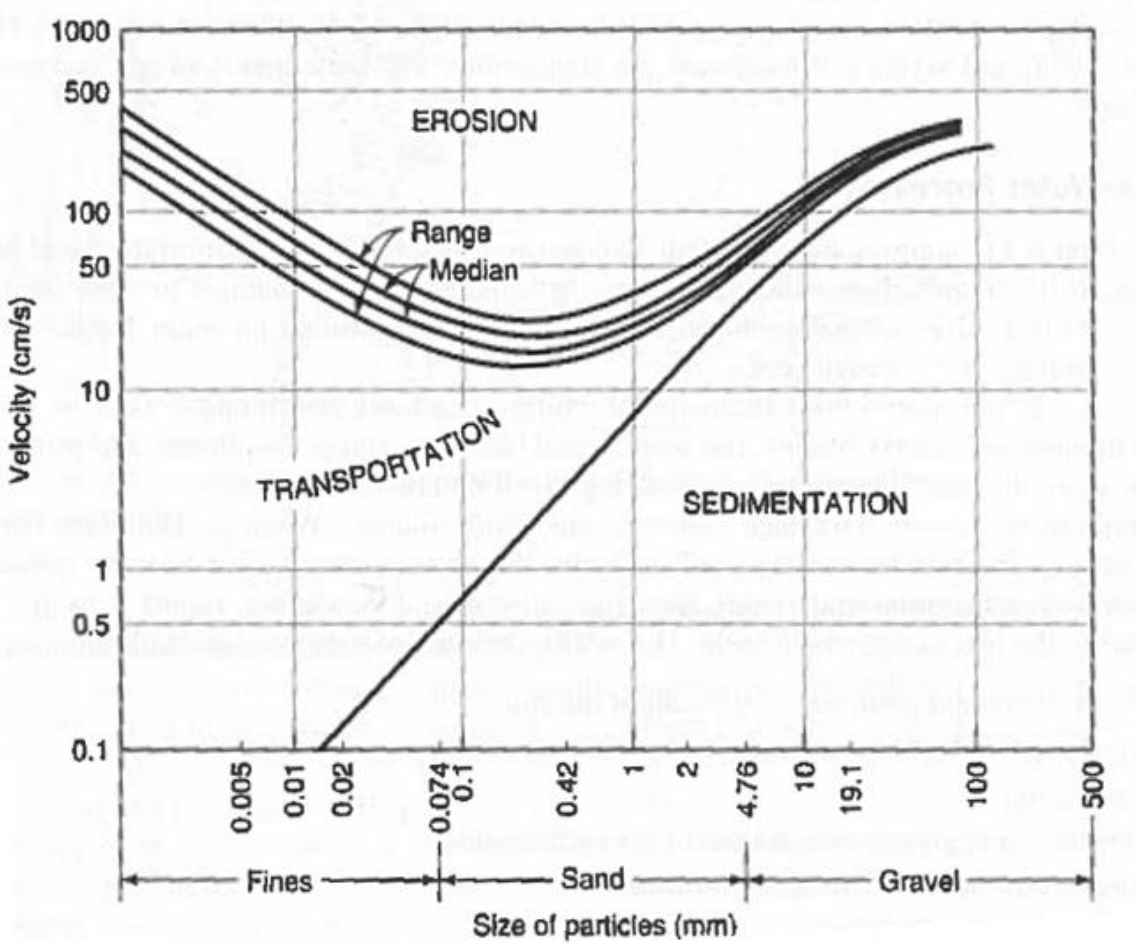

Figure 5.1: Hjulström diagram of flow velocity and particle sizes required for erosion, transportation, and deposition (after Hjulström 1935)

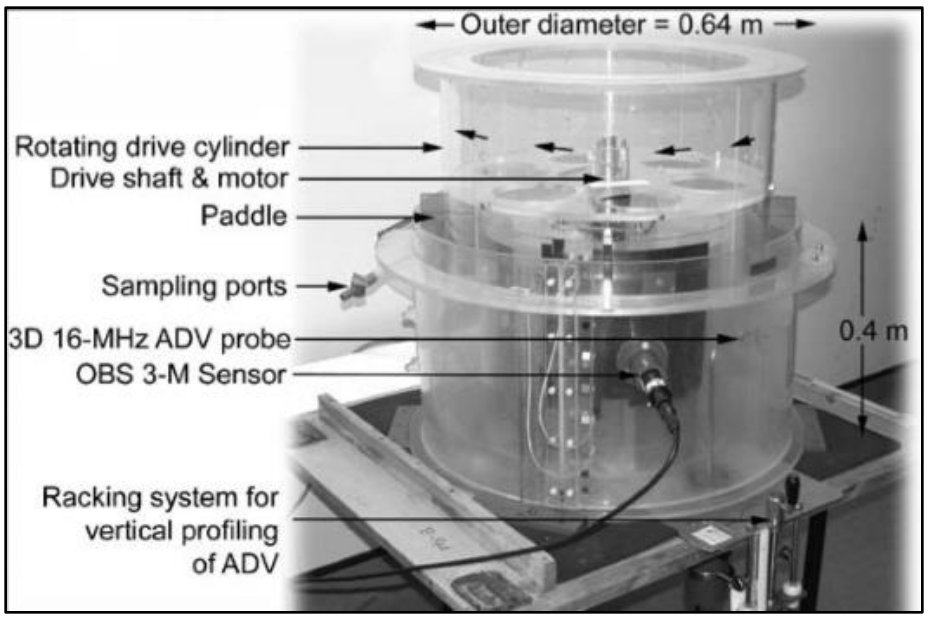

Figure 5.2**:** Annular Flume (AF) components, after Pope et al (2006)

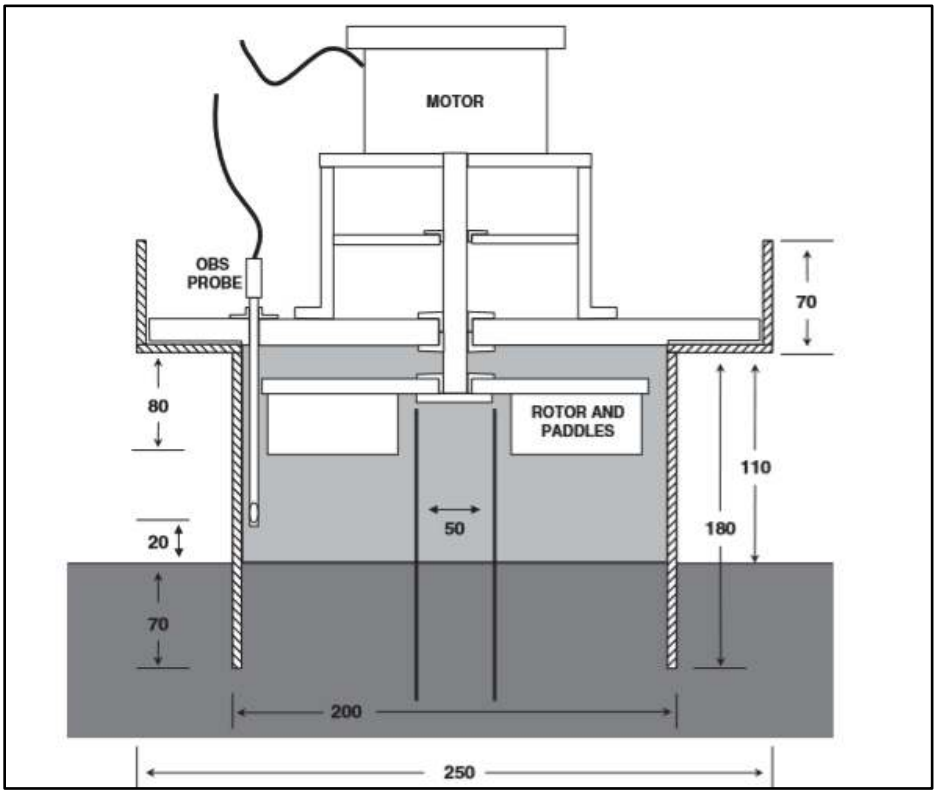

Figure 5.3: Schematic of Mini-Annular Flume (MAF), from Bale et al (2006), all dimension in millimeters.

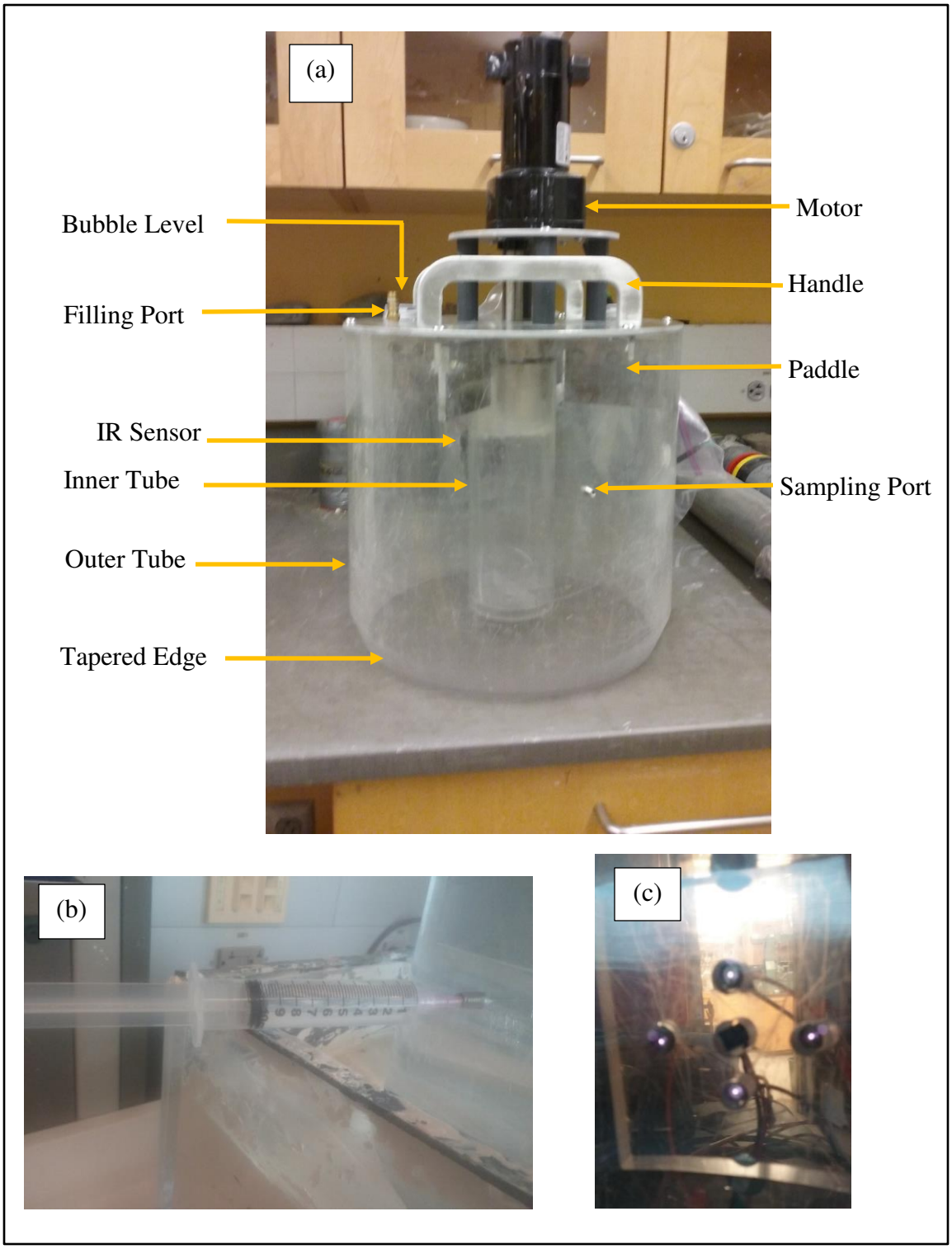

Figure 5.4: UMass Amherst Flume (UMAF) components (a) general assembly, flume outer diameter is 305 mm, (b) 10 mL hypodermic needle passing through vented set screw into flume chamber, and (c) IR sensor arrangement, emitters are spaced 12.7 mm above and below receiver, and 19.1 mm on either side of receiver.

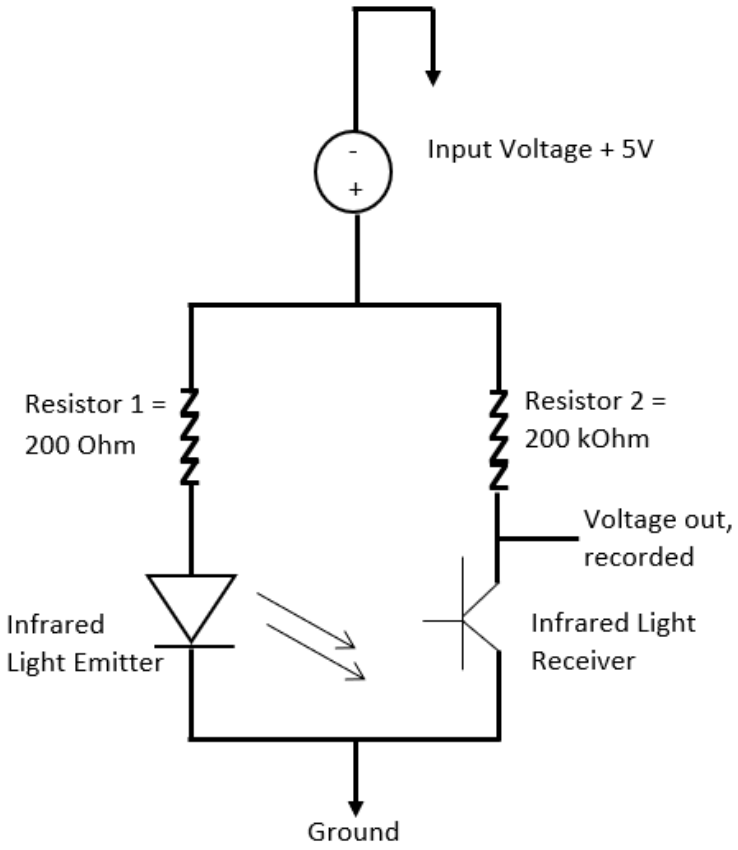

Figure 5.5: Infrared light circuit diagram

(a)

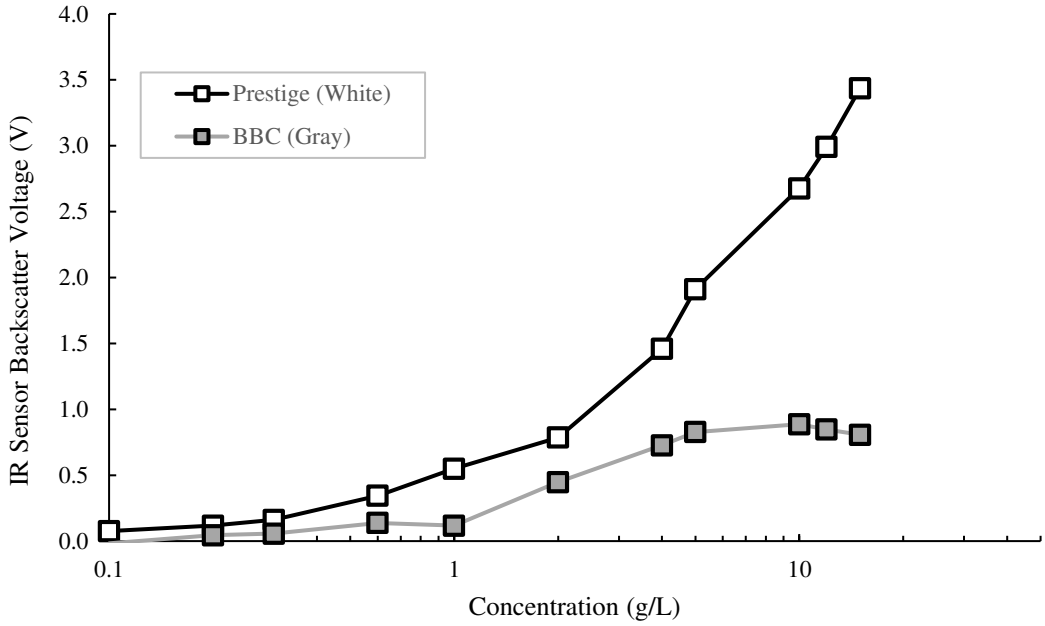

(b)

Figure 5.6: IR sensor validation: (a) solutions of Prestige at known concentrations ranging from 0.1 to 15.0 g/L, (b) results of Prestige versus Boston Blue Clay.

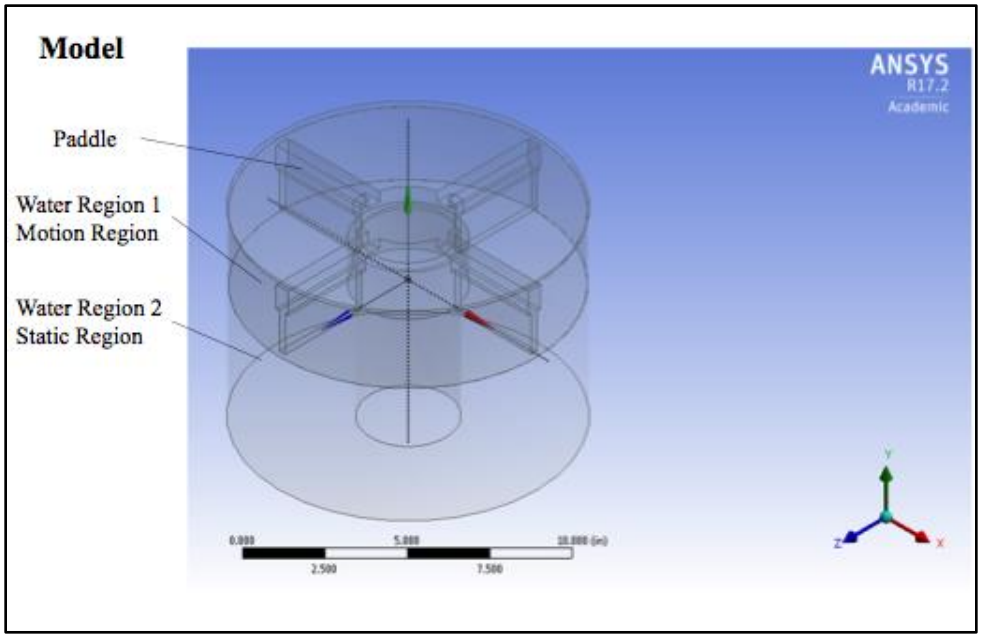

Figure 5.7: Geometry of UMAF using Computational Fluid Dynamics in ANSYS Fluent Modeling.

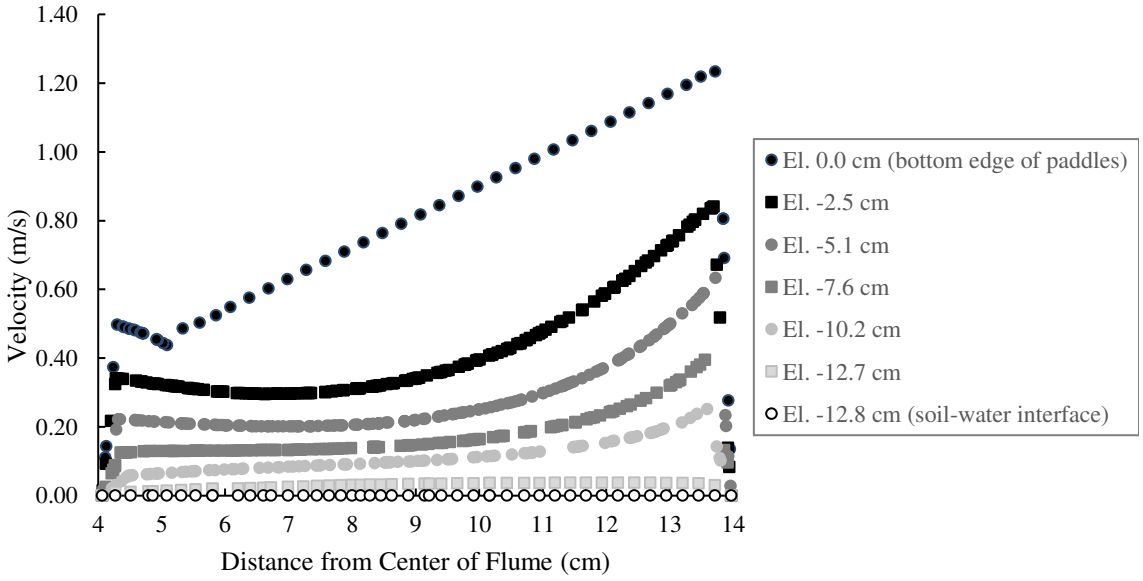

Figure 5.8: Velocity Profile from ANSYS Fluent Model at 86 RPM test

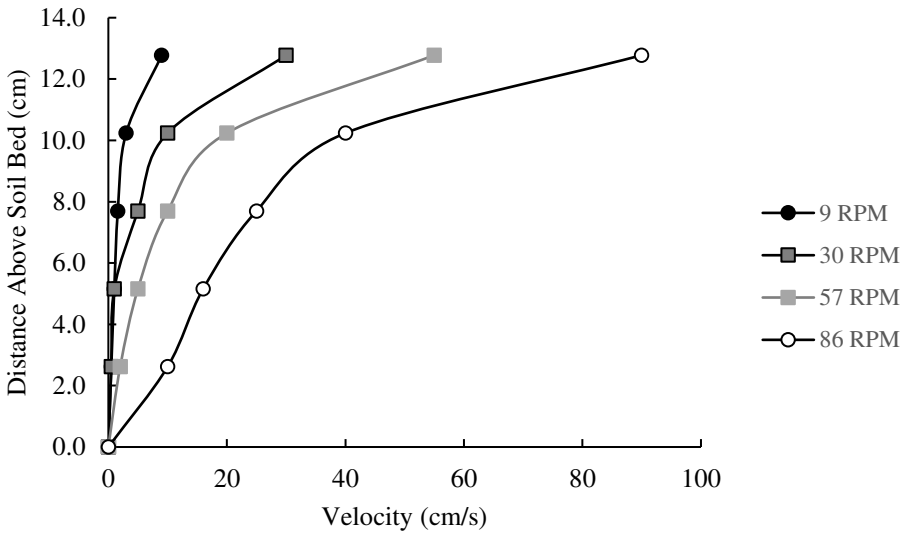

Figure 5.9: Fluid velocity profile at mid-track for a range of paddle rotational velocities

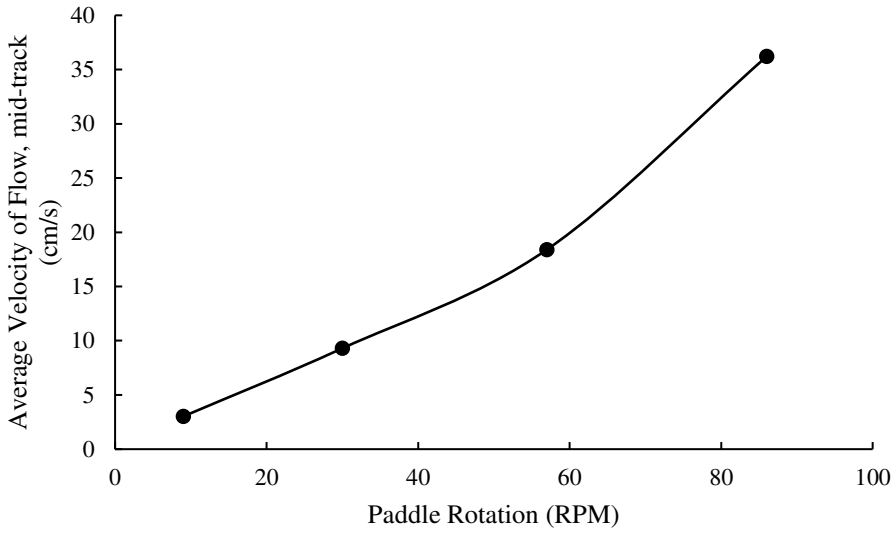

Figure 5.10: Depth averaged velocity for a range of paddle rotational velocities

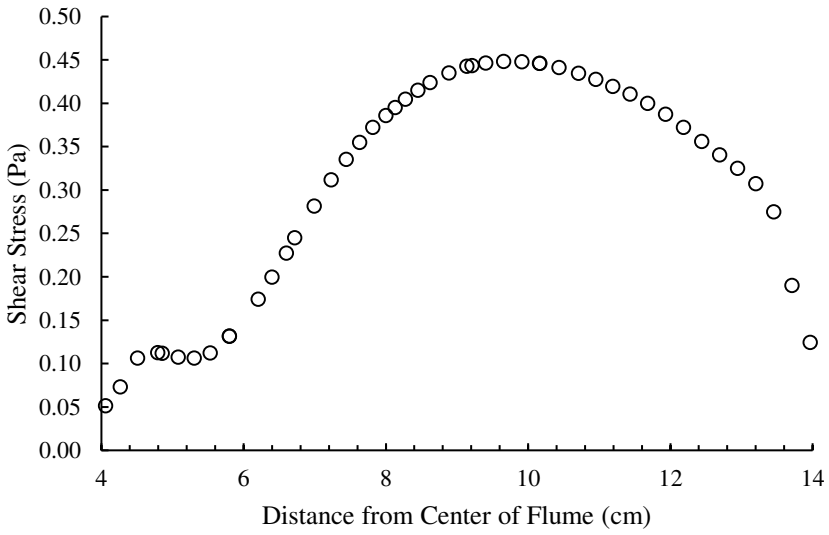

Figure 5.11: Shear Stress at Soil-Water Interface from ANSYS Fluent Model for 86 RPM

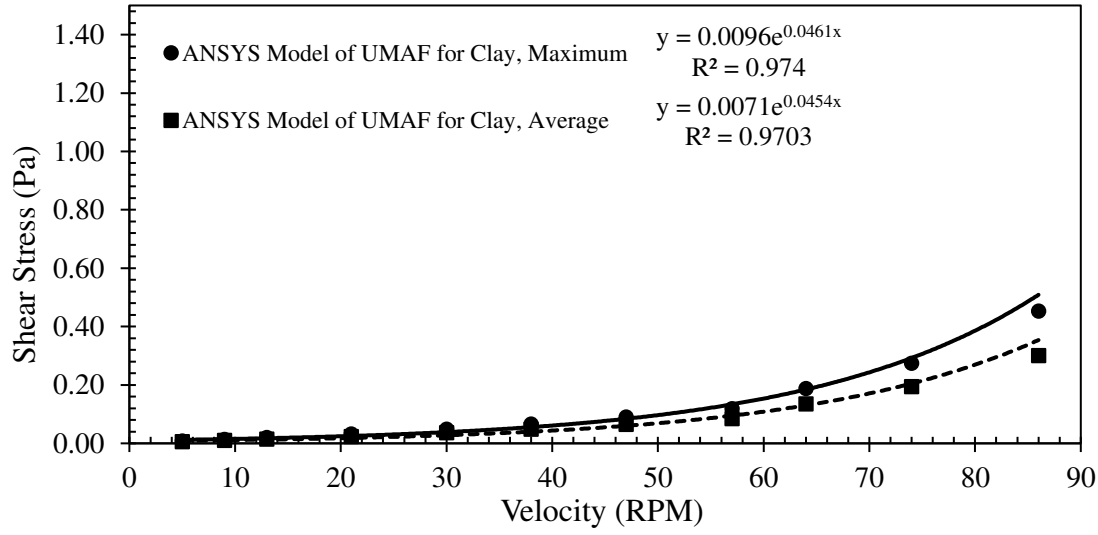

(a)

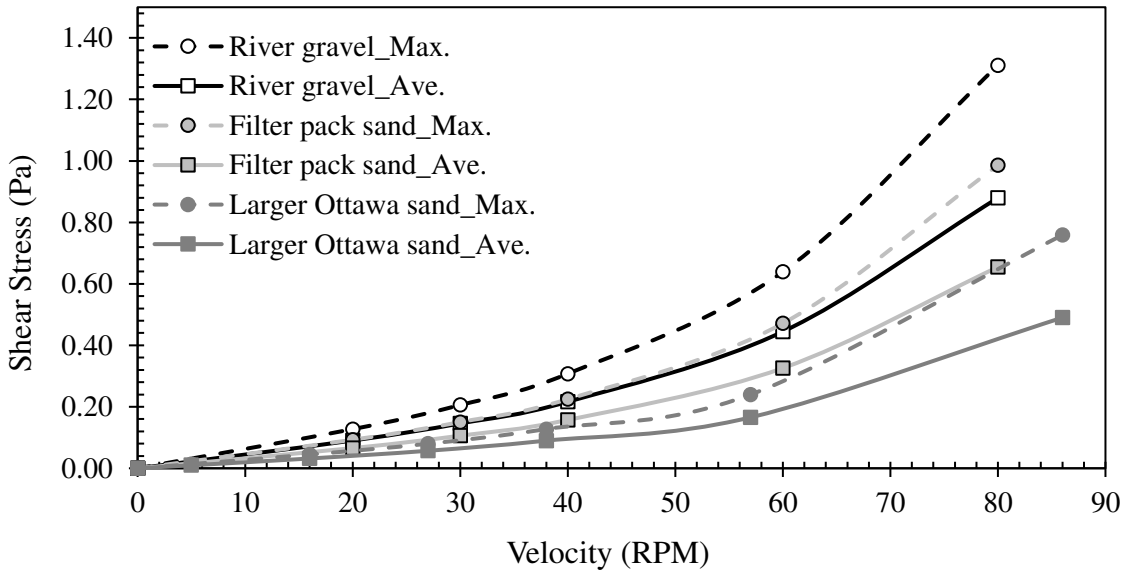

(b)

Figure 5.12: Average and maximum shear stress for UMAF from ANSYS Model (a) results for clay including empirical relationships, (b) coarse grained soil results

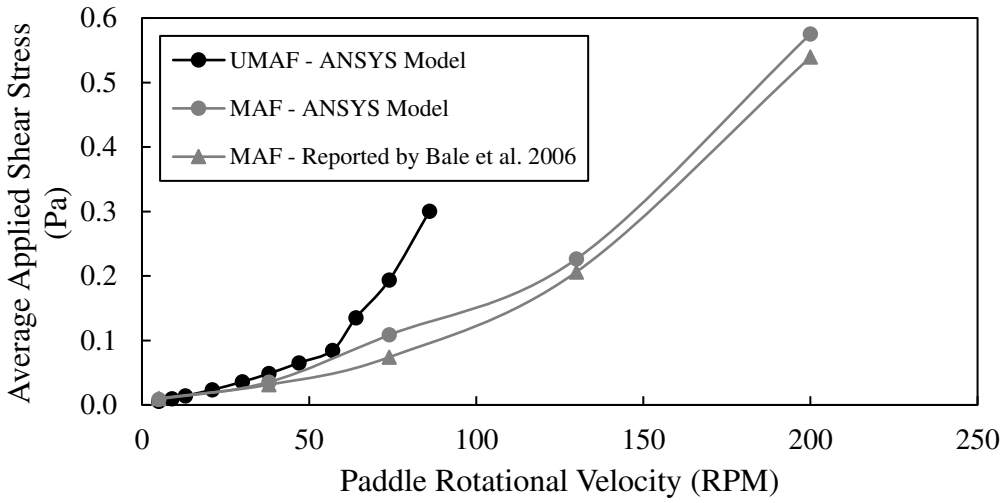

Figure 5.13: Comparison of ANSYS Modeling to empirical equation presented by Bale et al (2006).

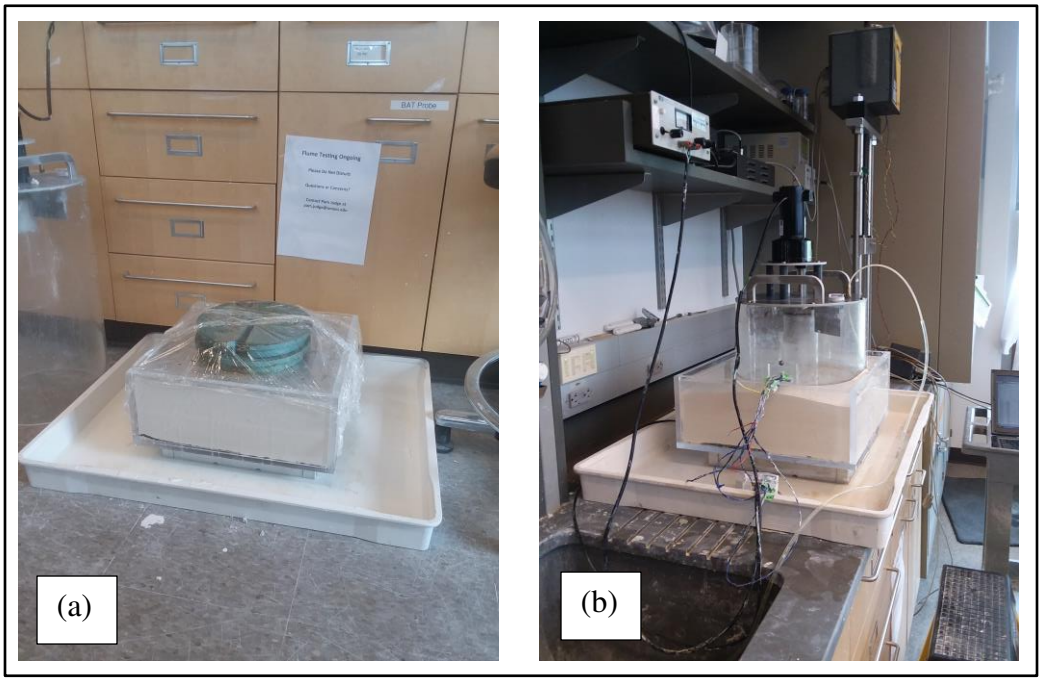

Figure 5.14: Experimental validation of UMAF: (a) Consolidation of soil bed, inside dimension of box: 380 x 380 x 150 mm (b) UMAF inserted into soil prior to testing, outer diameter of flume: 305 mm.

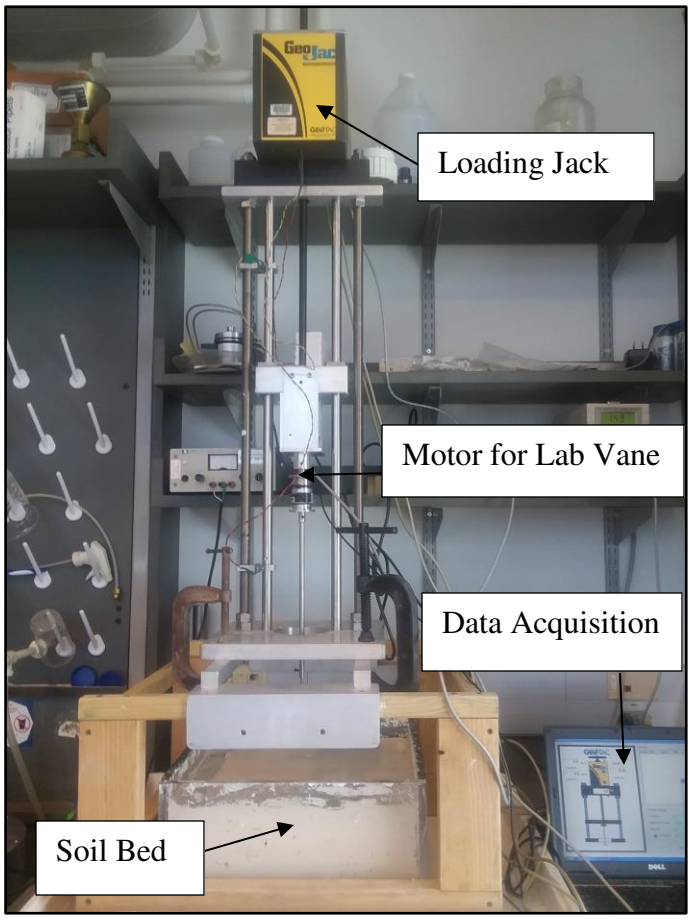

Figure 5.15: Penetrometer testing set-up for undrained shear strength of clay bed.

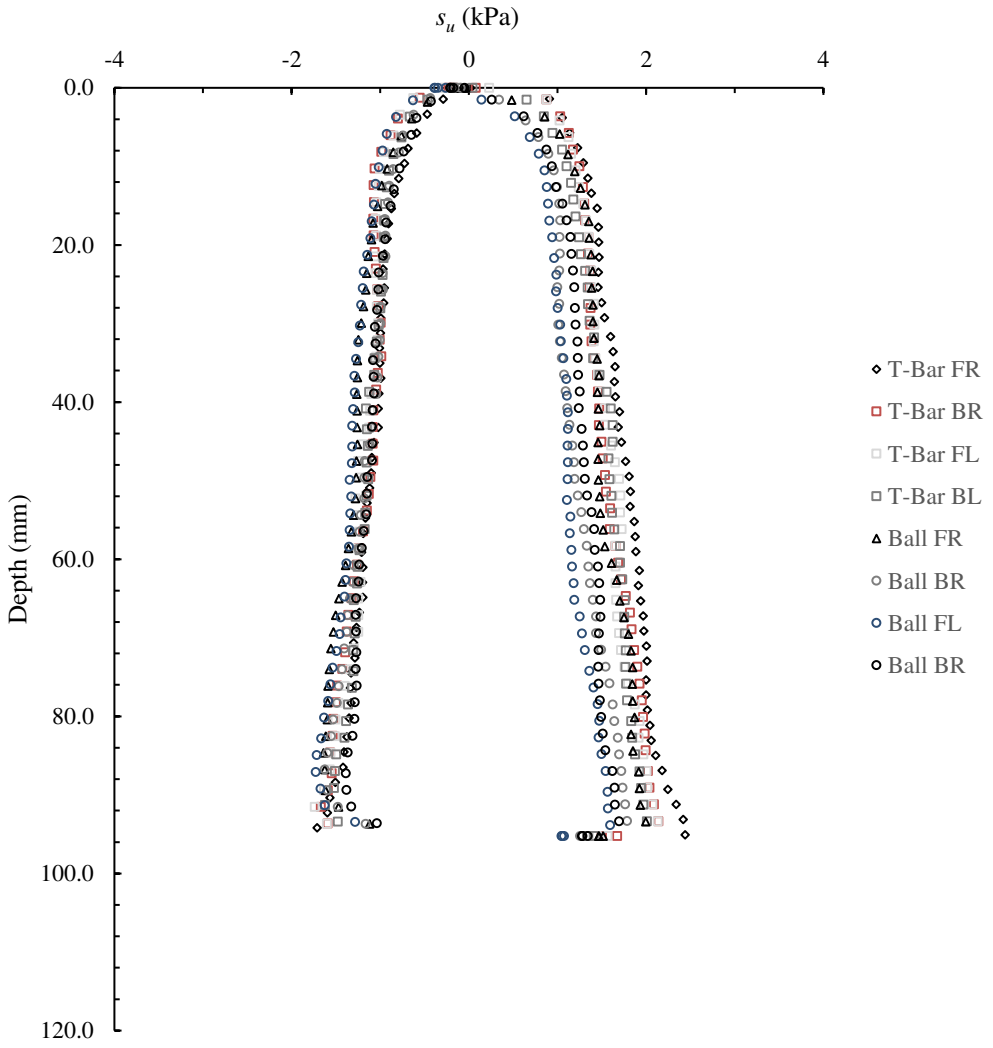

Figure 5.16: Results of Miniature Full Flow Penetrometer Testing.

Note 1: F, B, R, and L indicate direction of coner of box where test was performed (F = Front, B = Back, R = Right, and L = Left).

Note 2: Factor used to convert penetrometer resistance to undrained shear strength = 9.

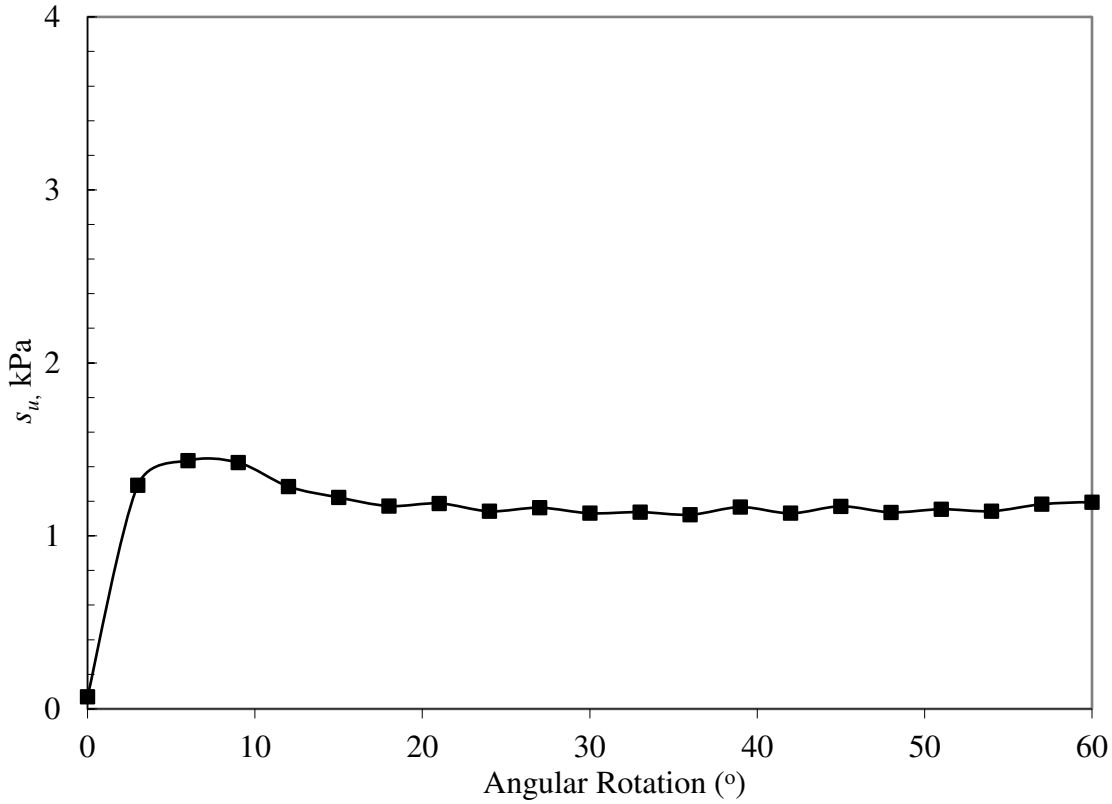

Figure 5.17: Results from miniature motorized laboratory vane. Test was performed at center of soil bed. Vane was four bladed, 38 mm tall by 19 mm wide.

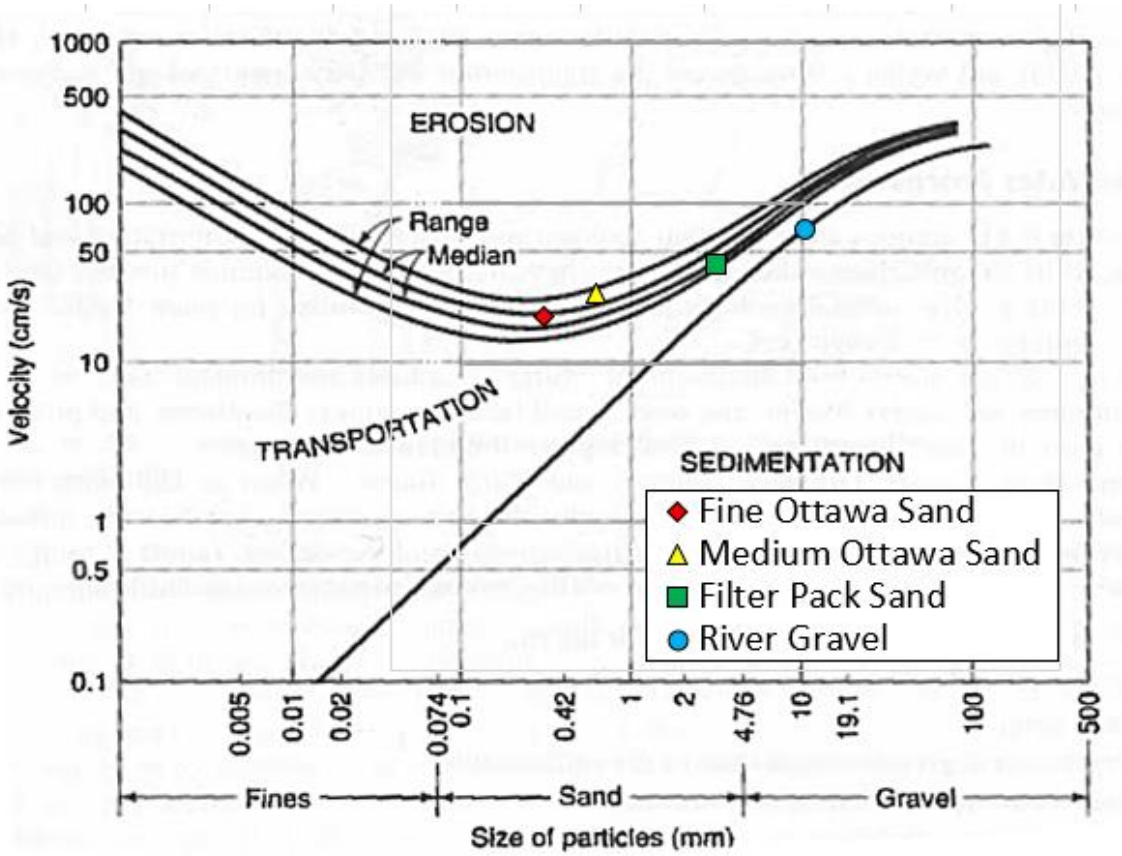

Figure 5.18: Comparison of coarse grained soils to Hjulström diagram.

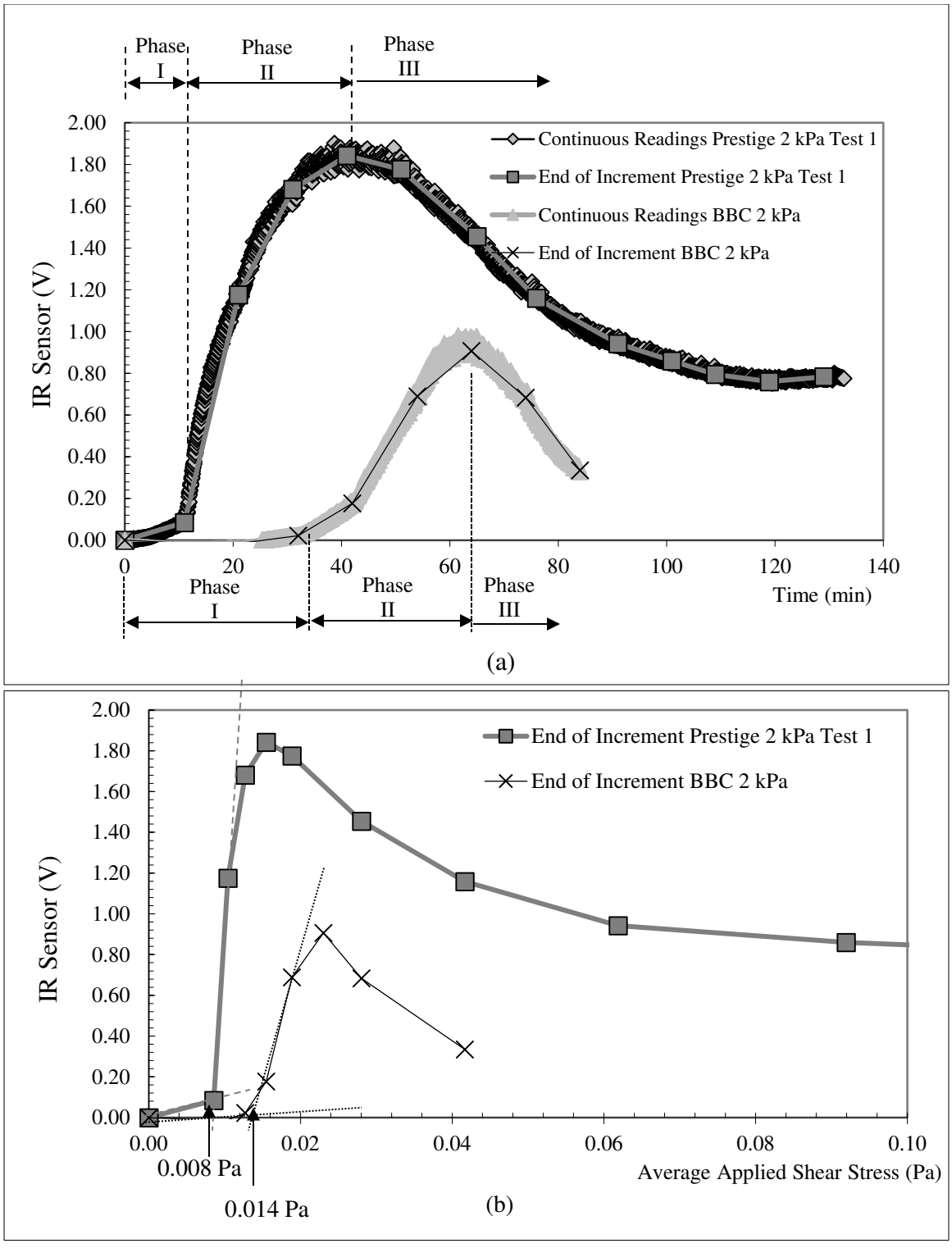

Figure 5.19: Two example results of infrared sensor from experiential tests (one Prestige and one BBC test): (a) continuous readings obtained every 2 seconds and end of increment values (b) average applied shear stress (obtained from CFD modeling) and interpretation of critical erosion shear stress.

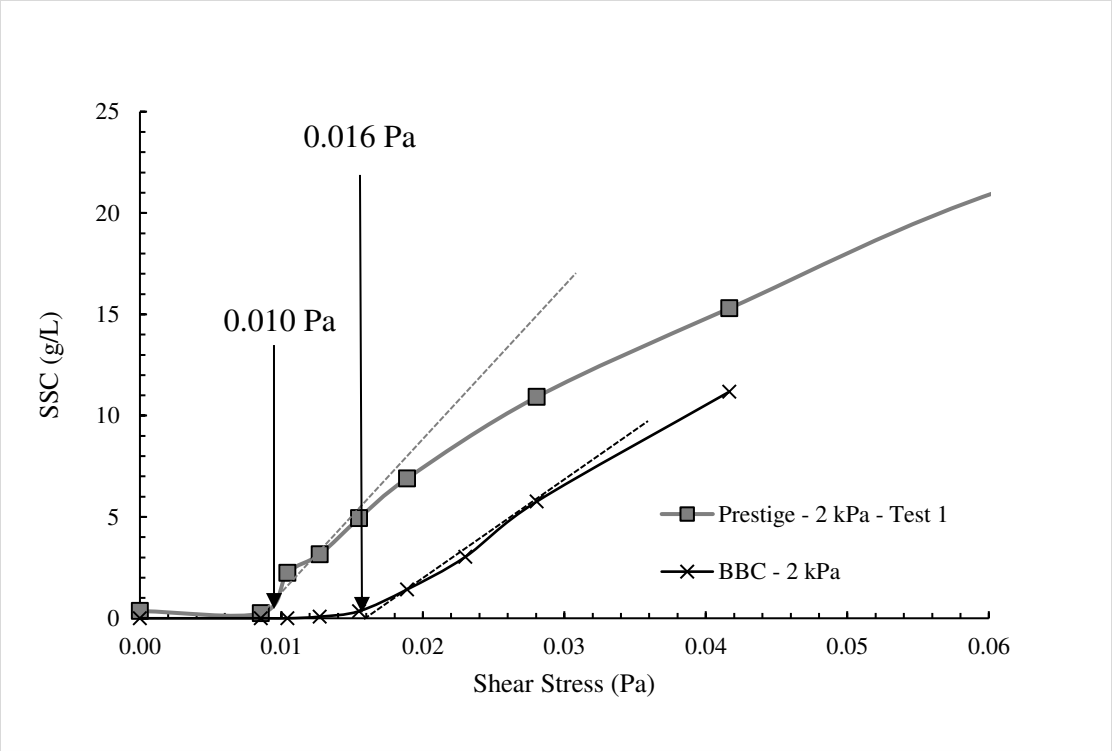

Figure 5.20: Two example results for gravimetric analysis via sampling port.

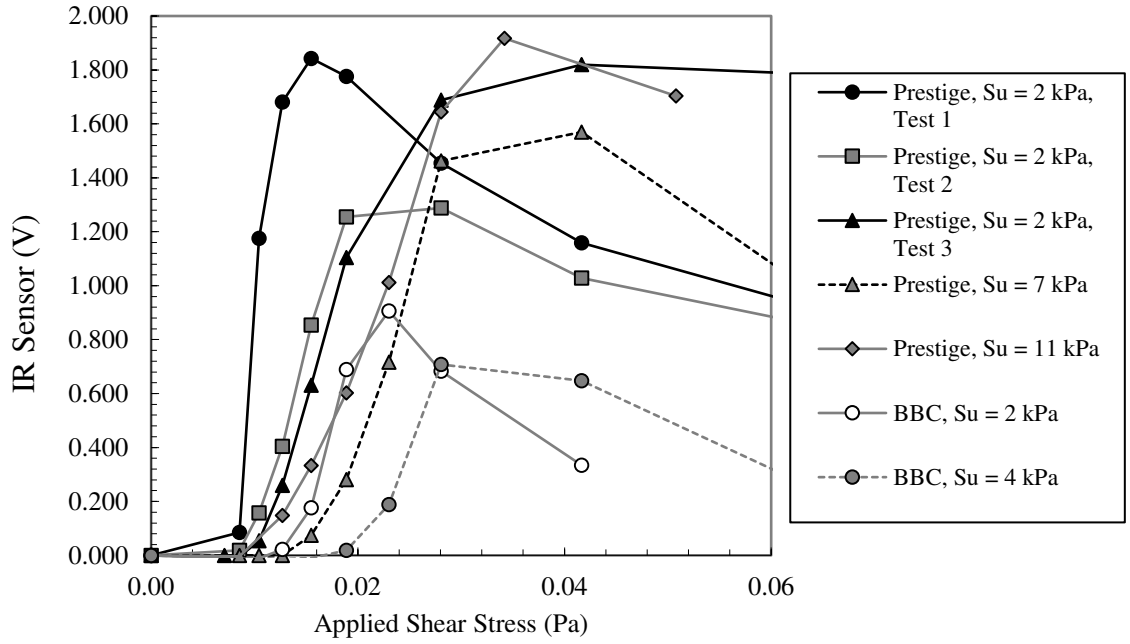

Figure 5.21: Infrared light sensor results for all fine-grained soils tested without biopolymers

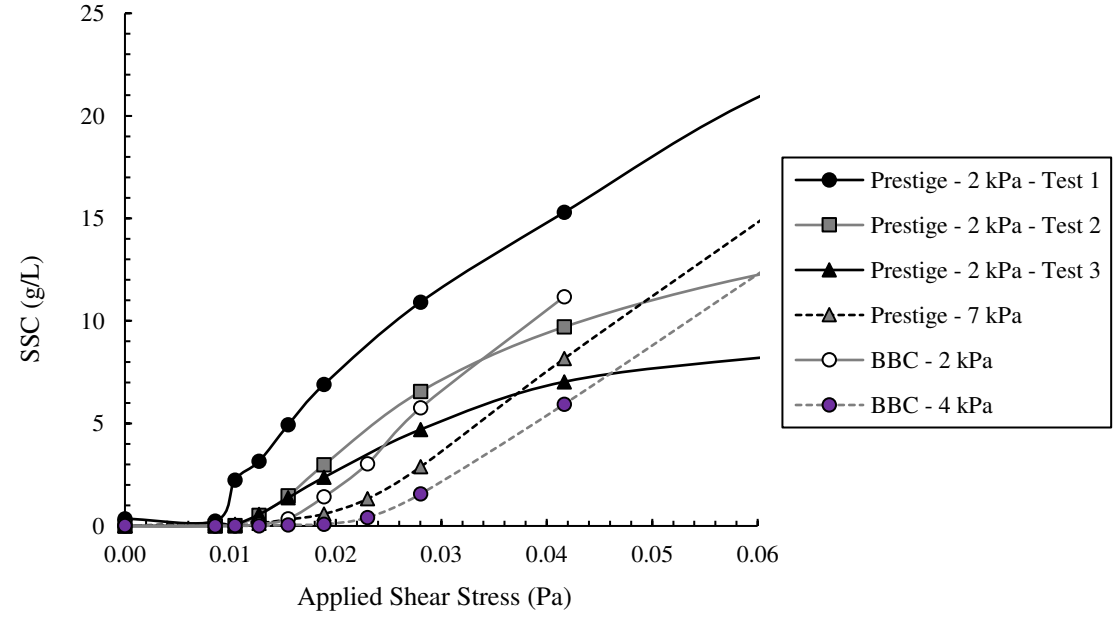

Figure 5.22: Suspended sediment concentration results for fine grained soils tested without biopolymers.

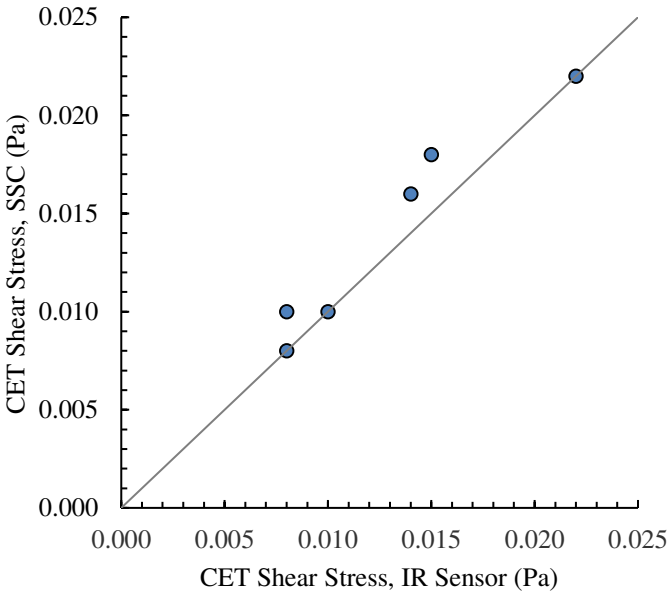

Figure 5.23: CET shear stress for infrared light sensor as compared to suspended sediment concentration for same fine-grained soil test.

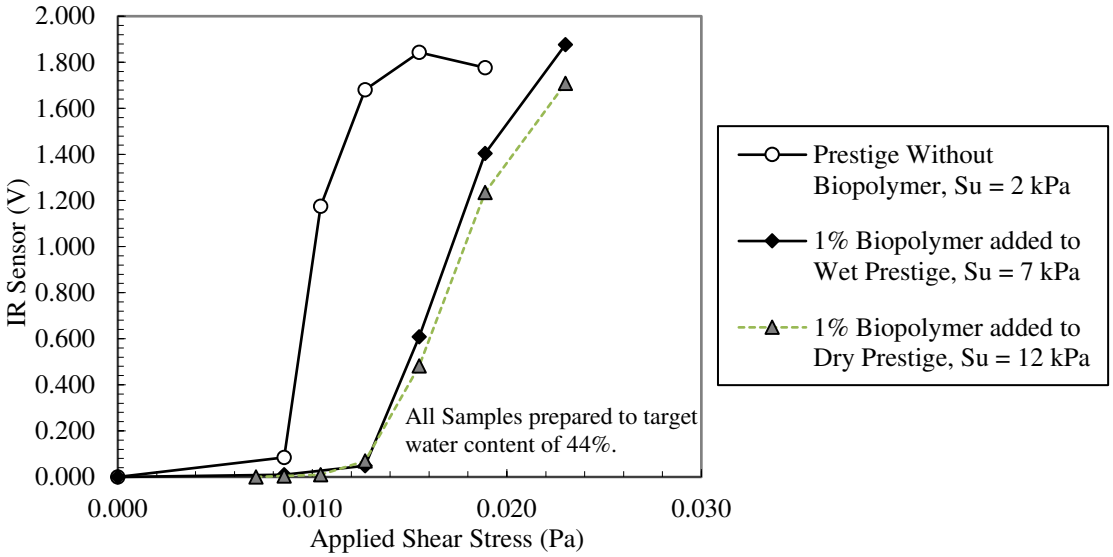

Figure 5.24: Results of erosion tests on biopolymer-soil mixtures.

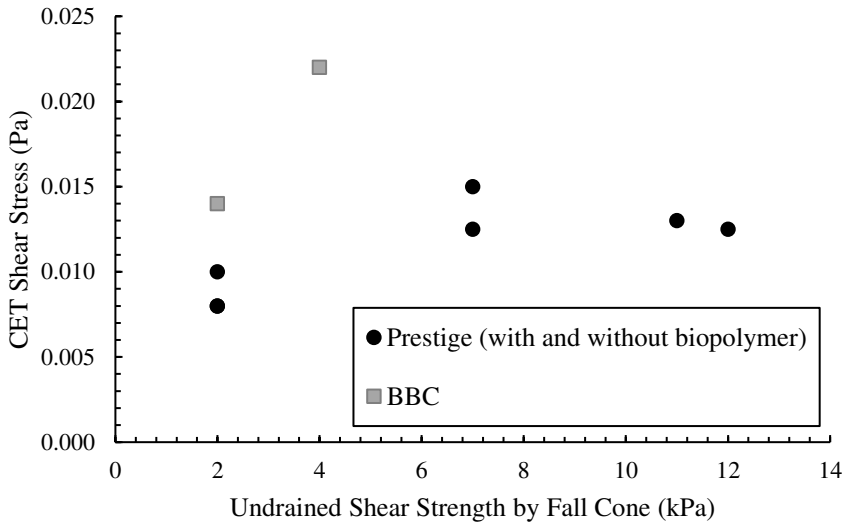

Figure 5.25: Plot of CET shear stress for each of the flume tests performed of fine grained soils relative to respective undrained shear strength by fall cone.

5.12 References

ANSYS (2009). "Wall Boundary Conditions." *ANSYS Fluent Version 12.0 User Guide.*

ASTM (2017). Annual Book of ASTM Standards, vol 4.80, Soil and Rock (I): D421-D5876.

Başbuğ, S., Papadakis, G., and Vassilicos, J.C. (2017). "DNS investigation of the dynamical behaviour of trailing vortices in unbaffled stirred vessels at transitional Reynolds numbers." *Physics of Fluids,* 29, 064101.

Boggs, S. (2000). "Principles of Sedimentology and Stratigraphy, 3rd Edition." Prentice Hall, Chapter 2.

Bohling, B. (2009). "Measurements of threshold values for incipient motion of sediment particles with two different erosion devices." *Journal of Marine Systems*, 75(3-4), 330-335.

Boscardin, A. (2013). "Development of miniature full flow and model pipeline probes for testing of box core samples of surficial seabed sediments." Doctoral Thesis, University of Massachusetts, Amherst, Massachusetts.

Christie, M. C., Dyer, K. R., Quartley, C.P. (1997). "The development of the POST system for in-situ intertidal measurements." *IEE Conference Publication*, (439), 39-45.

Clark, L. A., and Wynn, T. M. (2007). "Soil & Water - Methods for Determining Streambank Critical Shear Stress and Soil Erodibility: Implications for Erosion Rate Predictions." *Transactions of the ASAE.,* 50(1), 95.

Dade, W.B., Hogg, J.A., Boudreau, B.P. (2001). "Physics of flow above the sediment–water interface." In: Boudreau, B.P., Jørgensen, B.B. (Eds.), The Benthic Boundary Layer. Oxford University Press, New York, pp. 4–43.

Faas, R.W., Christian, H.A., Daborn, G.R., and Brylinsky, M. (2013). "Biological control of mass properties of surficial sediments: An example from Starr's Point Tidal Flat, Minas Basin, Bay of Fundy." Nearshore and Estuarine Cohesive Sediment Transport, 360-377.

Grabowski, R.C., Droppo, I.G., and Wharton, G. (2011). "Erodibility of cohesive sediment: The importance of sediment properties." *Earth Science Reviews,* 105(3-4), 101-120.

Hjulström, F. (1935). "Transportation of Detritus by Moving Water." Geographical Institute, University of Upsala, Sweden, Translated from Swedish to English by Trask, P.D, 1938.

ISO (2017). "Geotechnical investigation and testing – laboratory testing of soil – Part 6: Fall cone test." Standard No. 17892-6:2017, Geneva, Switzerland.

Launder, B.E., Spalding, D.B. (1974). "The numerical computation of turbulent flows". *Computer Methods in Applied Mechanics and Engineering*. 3 (2): 269–289

Miller, M.C., McCabe, I.N., and Komar, P.D. (1977). "Threshold of sediment motion under unidirectional currents." *Sedimentology* 24, 507-527.

Nugent, R. Zhang, G., and Gambrell, R. (2009). "Effect of exopolymers on the liquid limit of clays and its engineering implications." *Transportation Research Record*, 2101, 34-43.

Partheniades, E. (1971). "River Mechanics, Chapter 25: Erosion and deposition of cohesive materials." Edited and published by H.W. Shen, Fort Collings, CO, 1-46.

Perkins, R.G., Paterson, D.M., Sun, H., Watson, J., and Player, M.A. (2004). "Extracellular polymeric substances: quantification and use in erosion experiments." *Continental Shelf Research*, 24(15), 1623-1635.

Pope, N.D., Widdows, J., Brinsley, M.D. (2006). "Estimation of bed shear stress using the turbulent kinetic energy approach - A comparison of annular flume and field data." *Continental Shelf Research*, 26(8), 959-970.

Prellwitz, S.G., and Thompson. A. M. (2014). "Biota and hydrology influence soil stability in constructed wetlands." *Ecological Engineering*, 64, 360-366.

Spears B.M., Saunders J.E., Davidson I., and Paterson D.M. (2008). "Microalgal sediment biostabilisation along a salinity gradient in the Eden Estuary, Scotland: Unravelling a paradox." *Marine and Freshwater Research*, 59(4), 313-321.

SonTek (2014). Personal email correspondence and quote regarding "16 MHz MicroADV Splash Proof system" September.

Sutton-Grier, A., Wowka, K., and Bamford, H. (2015) "Future of our coasts: The potential for natural and hybrid infrastructure to enhance the resilience of our coastal communities, economies and ecosystems." *Environmental Science and Policy,* 51, 137-148.

Tolhurst, T.J., Black, K.S., Shayler, S.A., Mather, S., Black, I., Baker, K., and Paterson, D.M. (1999). "Measuring the in situ Erosion Shear Stress of Intertidal Sediments with the Cohesive Strength Meter (CSM)." *Estuarine, Coastal and Shelf Science*, 49(2), 281-294.

Tolhurst, T.J., Defew, E.C., de Brouwer, J.F.C., Wolfstein, K., Stal, L.J., and Paterson, D.M. (2006). "Small-scale temporal and spatial variability in the erosion threshold and properties of cohesive intertidal sediments." *Continental Shelf Research*, 26(3), 351-362.

Watts, C.W., Tolhurst, T.J., Black, K.S., and Whitmore, A.P. (2003). "In situ measurements of erosion shear stress and geotechnical shear strength of the intertidal sediments of the experimental managed realignment scheme at Tollesbury, Essex, UK." *Estuarine, Coastal & Shelf Science,* 58(3), 611-620.

Widdows, J., Friend, P.L., Bale, A.J., Brinsley, M.D., Pope, N.D., and Thompson, C.E.L. (2007). "Inter-comparison between five devices for determining erodability of intertidal sediments." *Continental Shelf Research*, 27(8), 1174-1189.

Yallop, M. L., Paterson, D. M., and Wellsbury, P. (2000). "Interrelationships between rates of microbial production, exopolymer production, microbial biomass, and sediment stability in biofilms of intertidal sediments." *Microbial Ecology*, 39, 116-127.

CHAPTER 6

SUMMARY AND CONCLUSIONS

The main objective of this dissertation was to increase the uptake of natural and nature-based infrastructure within the coastal civil engineering community, while providing quantitative information for natural and nature-based coastal protection techniques. Specifically, this research addresses preservation of cohesive intertidal mudflat soils; intertidal mudflats could prove beneficial to the engineering community as a means of providing space for attenuation of wave energy, and protection of near shore properties and businesses in the event of potential flood inundation. This objective was met through the research presented in three chapters that summarize the results of an extensive series of field trips, workshops, laboratory testing programs, and computational analyses. A brief overview of the most important results of these three chapters are presented below.

Chapter 3 presented the results of the Adaptive Gradients Framework. The framework was developed through a collaborative four-year process undertaken by the SAGE network which included fieldtrips and workshops in New York (2014), Jamaica (2015), Boston (2016) and Barbados (2018). SAGE was an NSF-funded network of thirty academics and practitioners across the domains of engineering, ecology, and social science, and included representation from the US Northeast and the Caribbean, with several members from Europe.

The resulting Adaptive Gradients framework consisted of eight gradients which covered the most relevant socio-economic and biophysical variables. The eight gradients included: exposure reduction, cost efficiency, intuitional capacity, ecological enhancement, adaption over time, greenhouse gas reduction, participatory process, and

social benefits. The framework was tested using the Harlem River Park case study which illustrated implementation of the evaluation method. This case study ultimately led to a multi-step implementation process by an interdisciplinary evaluation team and was supported by analysis with three additional case studies.

Chapter 4 presented the results of a series of laboratory tests which investigated the strength, micromorphology, and microstructure of a variety of soft clays amended by four biopolymers (xanthan gum, guar gum, carrageenan, and dextran). Tests soil minerology was predominantly kaolin with lesser amounts of montmorillonite. The effectiveness of different biopolymers and their interactions with different clay minerals were assessed over a range of biopolymer concentrations. Test methods included liquid limit (LL) measurement, fall cone (FC) penetration, and environmental scanning electron microscope (ESEM). The effects of biopolymer-clay interactions on the temporal development of intact strength and the remolded strength are investigated.

Fall cone results demonstrated both an immediate strength gain and a time-dependent strength gain induced by biopolymers for the clay samples studied. Some of the biopolymers demonstrated a saturation point. The results showed guar and carrageenan behave fundamentally differently than xanthan and dextran, likely due to the high LL_B values demonstrated by guar and carrageenan. Xanthan did not provide considerable improvement to soil properties, relative to the other biopolymers investigated. Finally, dextran and guar resulted in relatively similar improvements in undrained shear strength of soil, although guar also produced a more viscous solution and required considerable mixing effort.

Chapter 5 presented the design and construction of the University of Massachusetts Amherst Flume (UMAF). The purpose of this investigation was to design and construct a small laboratory annular erosion measurement device intended specifically for very soft cohesive soils under varying tidal inundations. An infrared light sensor and sampling port were developed to quantify suspended sediment concentration. Numerical modeling was performed to quantify applied shear stress at the soil-water interface at the critical erosion threshold (CET). The UMAF was validated by performing laboratory erosion tests on a series of very soft cohesive sediment, several coarse-grained soils, and two biopolymer-soil mixtures, and results were comparable to prior studies.

The newly developed flume included an innovative infrared sensor system that provided total SSC (or turbidity) without disrupting the flow field. A hypodermic needle port allowed for collection of grab samples for direct SSC measurements via gravimetric analysis at the end of each increment. Interpretation of CET by either indirectly (via the IR sensor) or directly (via hypodermic needle port) resulted in similar CET values.

The CET values observed in the UMAF were generally similar to CET values demonstrated by Bale et al. (2006), particularly for the soils tested by Bale et al. (2006) with density values below than 1200 kg/m^3. The CET values observed in the UMAF were generally much lower than values suggested by other empirical relationships based on undrained shear strength. This is likely due to the fact that the empirical relationships were developed using different erosion measurement devices involving different physical mechanisms and/or testing soils that have aged considerably or demonstrate a higher undrained shear strength.

Two different soft soils (BBC and Prestige) possessed similar undrained shear strengths and similar index properties; yet yielded different CET values. Such a difference was likely associated with different minerology and pore water chemistry, although additional studies are warranted. Biopolymers increased CET for very soft cohesive sediments suggesting their potential for practical applications in bio-inspired soil improvement. The CET did not vary significantly for the two methods of mixing (wet or dry), although the wet mixing method may have produced more flocs due to uneven distribution of the biopolymer (as compared to the dry mixing method). Additional flume validation tests were recommended. Specifically, future testing should include cohesive soil beds at higher undrained shear strength as well as testing suitability of the flume to in situ field testing.

BIBLIOGRAPHY

Abunnasr, Y.; Hamin, E. M.; Brabec, E. (2015). "Windows of opportunity: addressing climate uncertainty through adaptation plan implementation." *J. Environ. Planning Manage. 58*, 135–155.

Abu-Zreig, M. (2006). "Control of Rainfall-Induced Soil Erosion with Various Types of Polyacrylamide (8 pp)." *Journal of Soils and Sediments,* 6(3), 137-144.

Adger, W. N.; Hughes, T. P.; Folke, C.; Carpenter, S. R.; Rockström J. (2005). "Social-ecological resilience to coastal disasters." *Science*, *309*, 1036–1039.

Adger, W. N. (2016). "Place, well-being, and fairness shape priorities for adaptation to climate change." *Glob. Environ. Change*, *38*, A1–A3.

Ahern, J. (2011). From fail-safe to safe-to-fail: Sustainability and resilience in the new urban world. *Landsc. Urban Plan.*, *100*, 341–343.

Aldrich, D. P.; Meyer, M. A. (2015). "Social Capital and Community Resilience." *Am. Behav. Sci.*, *59*, 254–269.

Allen, K. M. (2006). "Community-based disaster preparedness and climate adaptation: local capacity-building in the Philippines." *DISA Disasters, 30*, 81–101.

ANSYS (2009). "Wall Boundary Conditions." *ANSYS Fluent Version 12.0 User Guide.*

Aragon, C., Hamin, E. & Buxton, J. (2017). "The Role of Landscape Installations in Climate Change Visualization" (Manuscript).

Arnstein, S. R. (1969). "A Ladder Of Citizen Participation." *J. Am. Inst. Plann. 35*, 216–224.

ASTM (2007). "ASTM D422 – 63: Standard Test Method for Particle-Size Analysis of Soils." ASTM International Committee D18 on Soil and Rock, Subcommittee D18.03 on Texture, Plasticity and Density Characteristics of Soils.

ASTM (2010). "ASTM D4318 – 10: Standard Test Methods for Liquid Limit, Plastic Limit, and Plasticity Index of Soils." ASTM International, Committee D18 on Soil and Rock, Subcommittee D18.03 on Texture, Plasticity and Density Characteristics of Soils.

ASTM (2017). Annual Book of ASTM Standards, vol 4.80, Soil and Rock (I): D421-D5876.

Barnett, J.; O'Neill, S. (2010). "Maladaptation." *Glob. Environ. Change*, *20*, 211–213.

Başbuğ, S., Papadakis, G., and Vassilicos, J.C. (2017). "DNS investigation of the dynamical behaviour of trailing vortices in unbaffled stirred vessels at transitional Reynolds numbers." *Physics of Fluids,* 29, 064101.

Becker, A.; Chase, N. T. L.; Fischer, M.; Schwegler, B.; Mosher, K. (2016). "A method to estimate climate-critical construction materials applied to seaport protection." *Glob. Environ. Change*, *40*, 125–136.

Bierbaum, R.; Smith, J. B.; Lee, A.; Blair, M.; Carter, L.; Chapin, F. S.; Fleming, P.; Ruffo, S.; Stults, M.; McNeeley, S.; Wasley, E.; Verduzco, L. (2013). "A comprehensive review of climate adaptation in the United States: more than before, but less than needed." *Mitig Adapt Strateg Glob Change Mitigation and Adaptation Strategies for Global Change : An International Journal Devoted to Scientific, Engineering, Socio-Economic and Policy Responses to Environmental Change*, *18*, 361–406.

Boggs, S. (2000). "Principles of Sedimentology and Stratigraphy, 3rd Edition." Prentice Hall, Chapter 2.

Bohling, B. (2009). "Measurements of threshold values for incipient motion of sediment particles with two different erosion devices." *Journal of Marine Systems*, 75(3-4), 330-335.

Boscardin, A. (2013). "Development of miniature full flow and model pipeline probes for testing of box core samples of surficial seabed sediments." Doctoral Thesis, University of Massachusetts, Amherst, Massachusetts.

Boulton, E. (2016). "Climate change as a "hyperobject": a critical review of Timothy Morton's reframing narrative." *WIREs Clim Change*, *7*, 772–785.

Brown, C.; Ghile, Y.; Laverty, M.; Li, K. (2012). "Decision scaling: Linking bottom-up vulnerability analysis with climate projections in the water sector." *Water Resour. Res.*, *48*.

Brown, H. (2014). "*Next generation infrastructure : principles for post-industrial public works."* Island Press: Washington; Covelo; London.

CEQ (2014). "*Revised Draft Guidance for Federal Departments and Agencies on Consideration of Greenhouse Gas Emissions and the Effects of Climate Change in NEPA Reviews."* Council on Environmental Quality, Vol. 79.

Chang, I., Im, J., Prasidhi, A., and Cho, G. (2015). "Effects of Xanthan gum biopolymer on soil strengthening." *Construction & Building Materials,* 74 65-72.

Chang, I., Im, J., and Cho, G. (2016). "Introduction of Microbial Biopolymers in Soil Treatment for Future Environmentally-Friendly and Sustainable Geotechnical Engineering." *Sustainability* 8(251).

Chen, L.C., Liu, Y.C., & Chan, K.C. (2006). “Integrated Community-Based Disaster Management Program in Taiwan: A Case Study of Shang-An Village. Nat Hazards Natural Hazards.” *Journal of the International Society for the Prevention and Mitigation of Natural Hazards*, *37*, 209–223.

Chenu, C. (1993). "Clay- or sand-polysaccharide associations as models for the interface between micro-organisms and soil: water related properties and microstructure." *Geoderma,* 56(1), 143-156.

Christie, M. C., Dyer, K. R., Quartley, C.P. (1997). "The development of the POST system for in-situ intertidal measurements." *IEE Conference Publication*, (439), 39-45.

Clark, L. A., and Wynn, T. M. (2007). "Soil & Water - Methods for Determining Streambank Critical Shear Stress and Soil Erodibility: Implications for Erosion Rate Predictions." *Transactions of the ASAE.,* 50(1), 95.

Collins, K., Ison, R. (2009). Jumping off Arnstein’s ladder: social learning as a new policy paradigm for climate change adaptation. *Environmental Policy and Governance*, *19*, 358–373.

Cornwall, A. (2008). “Unpacking “Participation”: models, meanings and practices.” *Community Dev. J.*, *43*, 269–283.

Cutter, S. L.; Barnes, L.; Berry, M.; Burton, C.; Evans, E.; Tate, E.; Webb, J. (2008). “A place-based model for understanding community resilience to natural disasters.” *Glob. Environ. Change*, *18*, 598–606.

Cutter, S. L.; Boruff, B. J.; Shirley, W. L. (2003). “Social vulnerability to environmental hazards.” *Soc. Sci. Q.*, *84*, 242–261.

Cutter, S. L.; Finch, C. (2008). “Temporal and spatial changes in social vulnerability to natural hazards.” *Proc. Natl. Acad. Sci. U. S. A.*, *105*, 2301–2306.

Dade, W.B., Hogg, J.A., Boudreau, B.P. (2001). “Physics of flow above the sediment–water interface.” In: Boudreau, B.P., Jørgensen, B.B. (Eds.), The Benthic Boundary Layer. Oxford University Press, New York, pp. 4–43.

DeJong, J. (2015) “Sustainable Biogeotechnics.” Geostrata, Published by the Geo-Institute, ASCE, September/October 2015.

Di Risio, M., Bruschi, A., Lisi, I., Pesarino, V., & Pasquali, D. (2017). Comparative Analysis of Coastal Flooding Vulnerability and Hazard Assessment at National Scale. Journal of Marine Science and Engineering, 5(4), 51.

Dontsova, K., and Bigham, J. (2005). “Anionic Polysaccharide Sorption by Clay Minerals.” *Soil Science Society of America Journal*. 69:1026–1035.

Duguma, L. A.; Minang, P. A.; van Noordwijk, M. (2014). "Climate Change Mitigation and Adaptation in the Land Use Sector: From Complementarity to Synergy." *Environ. Manage.*, *54*, 420–432.

Ellen, I. G.; Yager, J.; Hanson, M.; Bosher, L. (2016). Planning for an Uncertain Future Can Multicriteria Analysis Support Better Decision Making in Climate Planning? *Journal of Planning Education and Research*, *36*, 349–362.

EPA Guidelines for Preparing Economic Analyses Available online: https://www.epa.gov/environmental-economics/guidelines-preparing-economic-analyses#download (accessed on Oct 3, 2017).

Faas, R.W., Christian, H.A., Daborn, G.R., and Brylinsky, M. (2013). "Biological control of mass properties of surficial sediments: An example from Starr's Point Tidal Flat, Minas Basin, Bay of Fundy." Nearshore and Estuarine Cohesive Sediment Transport, 360-377.

FAO (1965). "Agar and Carrageenan Manual, Chapter 3: Properties, manufacture and application of seaweed polysaccharides agar, carrageenan and algin." Food and Agriculture Organization of the United Nations.

Goodin, R. E. (1995). "*Utilitarianism as a public philosophy."* Cambridge University Press: Cambridge; New York.

Grabowski, R.C., Droppo, I.G., and Wharton, G. (2011). "Erodibility of cohesive sediment: The importance of sediment properties." *Earth Science Reviews,* 105(3-4), 101-120.

Haasnoot, M.; Kwakkel, J. H.; Walker, W. E.; ter Maat, J. (2013). "Dynamic adaptive policy pathways: A method for crafting robust decisions for a deeply uncertain world." *Glob. Environ. Change* , *23*, 485–498.

Hallegatte, S. (2009). "Strategies to adapt to an uncertain climate change." *Glob. Environ. Change*, *19*, 240–247.

Hallegatte, S.; Corfee-Morlot, J. (2011). "Understanding climate change impacts, vulnerability and adaptation at city scale: an introduction." *Clim. Change*, *104*, 1–12.

Hamin, E. M.; Gurran, N.; Emlinger, A. M. (2014). "Barriers to municipal climate adaptation: examples from coastal Massachusetts' smaller cities and towns." *J. Am. Plann. Assoc.*, *80*, 110–122.

Head, B. W. (2007). "Community Engagement: Participation on Whose Terms?" *Aust. J. Polit. Sci.*, *42*, 441–454.

Heltberg, R.; Siegel, P. B.; Jorgensen, S. L. (2009). "Addressing human vulnerability to climate change: Toward a "no-regrets" approach." *Glob. Environ. Change*, *19*, 89–99.

Herrera, M. P. and Vasanthan, T. (2018). "Rheological characterization of gum and starch nanoparticle blends." *Food Chem.,* 243 43-49.

Hjulström, F. (1935). "Transportation of Detritus by Moving Water." Geographical Institute, University of Upsala, Sweden, Translated from Swedish to English by Trask, P.D, 1938.

Holtz, R.D., Kovacs, W.D., and Sheahan, T.C. (2011). *An introduction to geotechnical engineering.* Pearson, Upper Saddle River, NJ.

Innes, J. E.; Booher, D. E. (2010). "*Planning with Complexity: An Introduction to Collaborative Rationality for Public Policy*." Routledge, ISBN 9781135194277.

IPCC (2014). *Climate Change 2014: Synthesis Report. Contribution of Working Groups I, II and III to the Fifth Assessment Report of the Intergovernmental Panel on Climate Change*; Core Writing Team, R.K. Pachauri and L.A. Meyer., Ed.; IPCC: Geneva, Switzerland.

IPCC (2014). *Climate Change 2014: Impacts, Adaptation, and Vulnerability Summaries, Frequently Asked Questions, and Cross-Chapter Boxes, A Contribution of Working Group II to the Fifth Assessment Report of the Intergovernmental Panel on Climate Change*; Field, C.B., V.R. Barros, D.J. Dokken, K.J. Mach, M.D. Mastrandrea, T.E. Bilir, M. Chatterjee, K.L. Ebi, Y.O. Estrada, R.C. Genova, B. Girma, E.S. Kissel, A.N. Levy, S. MacCracken,P.R. Mastrandrea, and L.L. White, Ed.; World Meteorological Organization, Geneva, Switzerland.

IPCC (2012). *Managing the Risks of Extreme Events and Disasters to Advance Climate Change Adaptation. A Special Report of Working Groups I and II of the Intergovernmental Panel on Climate Change*; Field, C.B., V. Barros, T.F. Stocker, D. Qin, D.J. Dokken, K.L. Ebi, M.D. Mastrandrea, K.J. Mach, G.-K. Plattner, S.K. Allen, M. Tignor, and P.M. Midgley, Ed.; IPCC: Cambridge, United Kingdom and New York, NY, USA.

ISO (2017). Geotechnical investigation and testing -- Laboratory testing of soil -- Part 6: Fall cone test, ISO 17892-6, Geneva, Switzerland.

Jones, L.; Champalle, C.; Chesterman, S.; Cramer, L.; Crane, T. A. (2016). "Constraining and enabling factors to using long-term climate information in decision-making." *Clim. Policy* , *17*, 551–572.

Jongman, B.; Ward, P. J.; Aerts, J. C. J. H. (2012). "Global exposure to river and coastal flooding: Long term trends and changes." *Glob. Environ. Change*, *22*, 823–835.

Keeley, M.; Koburger, A.; Dolowitz, D. P.; Medearis, D.; Nickel, D.; Shuster, W. (2013). "Perspectives on the Use of Green Infrastructure for Stormwater Management in Cleveland and Milwaukee." *Environ. Manage.*, *51*, 1093–1108.

Kelman, I.; Gaillard J C Lewis; Mercer, J. (2016). "Learning from the history of disaster vulnerability and resilience research and practice for climate change." *Nat. Hazards*, *82*, S129–S143.

Kenney, M. A.; Hamin, E. M.; Sheahan, T. C. (2014). "Reconceptualizing the Role of Infrastructure in Resilience." *Eos Trans. Amer. Geophys. Union*, *95*, 298–298.

Kenney, M. A.; Janetos, A. C.; Lough, G. C. (2016). "Building an integrated U.S. National Climate Indicators System." *Clim. Change*, *135*, 85–96.

Klein, R. J. T.; Midgley, G. F.; Preston, B. L.; Alam, M.; Berkhout, F. G. H.; Dow, K.; Shaw, M. R.(2014). "Adaptation opportunities, constraints, and limits." *Climate Change 2014: Impacts, Adaptation, and Vulnerability. Part A: Global and Sectoral Aspects. Contribution of Working Group II to the Fifth Assessment Report of the Intergovernmental Panel on Climate Change*; Field, C.B., V.R. Barros, D.J. Dokken, K.J. Mach, M.D. Mastrandrea, T.E. Bilir, M. Chatterjee, K.L. Ebi, Y.O. Estrada, R.C. Genova, B. Girma, E.S. Kissel, A.N. Levy, S. MacCracken, P.R. Mastrandrea, and L.L. White, Ed.; Cambridge University Press, pp. 899–943.

Launder, B.E., Spalding, D.B. (1974). "The numerical computation of turbulent flows". *Computer Methods in Applied Mechanics and Engineering*. 3 (2): 269–289

Lutz, W.; Muttarak, R. (2107). "Forecasting societies' adaptive capacities through a demographic metabolism model." *Nat. Clim. Chang.*, *7*, 177–184.

Matthews, T.; Lo, A. Y.; Byrne, J. A. (2015). "Reconceptualizing green infrastructure for climate change adaptation: Barriers to adoption and drivers for uptake by spatial planners." *Landsc. Urban Plan.*, *138*, 155–163.

McDaniels, T.; Chang, S.; Cole, D.; Mikawoz, J.; Longstaff, H. (2018). "Fostering resilience to extreme events within infrastructure systems: Characterizing decision contexts for mitigation and adaptation." *Glob. Environ. Change*, *18*, 310–318.

McGill, H., McMahan, A., Wigodsky, H., and Sprinz, H. (1977). "Carrageenan in formula and infant baboon development." *Gastroenterology*. 73: 512 – 517.

Meadow, A. M.; Ferguson, D. B.; Guido, Z.; Horangic, A.; Owen, G.; Wall, T. (2015). "Moving toward the Deliberate Coproduction of Climate Science Knowledge." *Weather, Climate, and Society*, *7*, 179–191.

Mendoza, G. A.; Martins, H. (2006). "Multi-criteria decision analysis in natural resource management: A critical review of methods and new modelling paradigms." *For. Ecol. Manage.*, *230*, 1–22.

Meng, X., Jia, Y., Shan, H., Yang, Z. and Zheng J. (2012). "An experimental study on erodibility of intertidal sediments in the Yellow River delta." *IJSRC International Journal of Sediment Research,* 27(2), 240-249.

Miller, M.C., McCabe, I.N., and Komar, P.D. (1977). "Threshold of sediment motion under unidirectional currents." *Sedimentology* 24, 507-527.

Mimura, N.; Pulwarty, R. S.; Duc, D. M.; Elshinnawy, I.; Redsteer, M. H.; Huang, H. Q.; Nkem, J. N.; Sanchez Rodriguez, R. A. (2014). "Adaptation Planning and Implementation." *Climate Change 2014: Impacts, Adaptation, and Vulnerability. Part A: Global and Sectoral Aspects. Contribution of Working Group II to the Fifth Assessment Report of the Intergovernmental Panel on Climate Change*; Field, C.B., V.R. Barros, D.J. Dokken, K.J. Mach, M.D. Mastrandrea, T.E. Bilir, M. Chatterjee, K.L. Ebi, Y.O. Estrada, R.C. Genova, B. Girma, E.S. Kissel, A.N. Levy, S. MacCracken, P.R. Mastrandrea, and L.L. White, Ed.; Cambridge University Press; pp. 869–898.

Mitchel, J. (1960). "Fundamental Aspects of Thixotropy in Soils." *Journal of the Soil Mechanics and Foundations Division, Proceedings of the American Society of Civil Engineers*, June 1960.

Moser, S. C.; Boykoff, M. T. (2013). *Successful Adaptation to Climate Change: Linking Science and Policy in a Rapidly Changing World*; Routledge; ISBN 9781135071301.

Moser, S. C.; Dilling, L. (2007). *Creating a Climate for Change: Communicating Climate Change and Facilitating Social Change*; Cambridge University Press; ISBN 9781139461085.

Moser, S. C.; Ekstrom, J. A. (2010). "A framework to diagnose barriers to climate change adaptation." *Proc. Natl. Acad. Sci. U. S. A.*, *107*, 22026–22031.

Muttarak, R.; Pothisiri, W. (2013). "The role of education on disaster preparedness: case study of 2012 Indian Ocean earthquakes on Thailand's Andaman Coast." *Ecology & Society*http://paperpile.com/b/N2Ugn1/xkDEP, *18*, 1–16.

Mycoo, M. (2013). Sustainable tourism, climate change and sea level rise adaptation policies in Barbados. *Nat. Resour. Forum*, *38*, 47–57.

National Research Council (2011). Division on Earth and Life Studies; Board on Atmospheric Sciences and Climate; America's Climate Choices: Panel on Adapting to the Impacts of Climate Change *Adapting to the Impacts of Climate Change*; National Academies Press; ISBN 9780309145916.

Neuman, M. (2006). “Infiltrating infrastructures: On the nature of networked infrastructure.” *Journal of Urban Technology*, *13*, 3–31.

NOAA (2015). *Guidance for Considering the Use of Living Shorelines*; National Oceanic and Atmospheric Administration, U.S. Department of Commerce.

Nordenson, G.; Seavitt, C. (2015). “Structures of coastal resilience: Designs for climate change.” *Soc. Res.*, *82*, 655–671.

Nugent, R., Zhang, G., and Gambrell, R. (2009). “Effect of exopolymers on the liquid limit of clays and its engineering implications.” *Transportation Research Record*, 2101, 34-43.

NYC (2013). “Coastal climate resilience: urban waterfront adaptive strategies.” *Department of City Planning, City of New York,* June 2013, www.nyc.gov/uwas.

Or, D., Smets, B. F., Wraith, J. M., Dechesne, A., Friedman,S.P. (2007). "Physical constraints affecting bacterial habitats and activity in unsaturated porous media - a review." *Advances in Water Resources.,* 30(6-7), 1505-1527.

Partheniades, E. (1971). “River Mechanics, Chapter 25: Erosion and deposition of cohesive materials.” Edited and published by H.W. Shen, Fort Collings, CO, 1-46.

Pelling, M.; Uitto, J. I. (2001). “Small island developing states: natural disaster vulnerability and global change.” *Global Environmental Change Part B: Environmental Hazards*, *3*, 49–62.

Perkins, R.G., Paterson, D.M., Sun, H., Watson, J., and Player, M.A. (2004). "Extracellular polymeric substances: quantification and use in erosion experiments." *Continental Shelf Research*, 24(15), 1623-1635.

Pope, N.D., Widdows, J., Brinsley, M.D. (2006). "Estimation of bed shear stress using the turbulent kinetic energy approach - A comparison of annular flume and field data." *Continental Shelf Research*, 26(8), 959-970.

Prellwitz, S.G., and Thompson. A. M. (2014). "Biota and hydrology influence soil stability in constructed wetlands." *Ecological Engineering*, 64, 360-366.

Rawls, J. (2009). “*A Theory of Justice*.” Harvard University Press: Cambridge, MA.

Raymond, C. M.; Frantzeskaki, N.; Kabisch, N.; Berry, P.; Breil, M.; Nita, M. R.; Geneletti, D.; Calfapietra, C. (2017). “A framework for assessing and implementing the co-benefits of nature-based solutions in urban areas.” *Environ. Sci. Policy*, *77*, 15–24.

Rosenzweig, C.; Solecki, W. (2014). “Hurricane Sandy and adaptation pathways in New York: Lessons from a first-responder city.” *Glob. Environ. Change*, *28*, 395–408.

Samal, S., Dash, M., Moroni, L., van Blitterswijk, C., Samal, S. K., Dash, M., Van Vlierberghe, S., Dubruel, P., Kaplan, D. L., Chiellini, E., van Blitterswijk, C., and Moroni, L. (2012). "Cationic polymers and their therapeutic potential." *Chem.Soc.Rev.,* 41(21), 7147-7194.

Sandifer, P. A.; Sutton-Grier, A. E.; Ward, B. P. (2015). "Exploring connections among nature, biodiversity, ecosystem services, and human health and well-being: Opportunities to enhance health and biodiversity conservation." *Ecosystem Services*, *12*, 1–15.

Scannell, L.; Gifford, R. (2013). "Climate Change Engagement Questionnaire. *PsycTESTS Dataset*.

Serban Scrieciu, S.; Belton, V.; Chalabi, Z.; Mechler, R.; Puig, D. (20140. "Advancing methodological thinking and practice for development-compatible climate policy planning." *Mitig Adapt Strateg Glob Change*, *19*, 261–288.

Sharma, B. and Bora, P. (2003). "Plastic limit, liquid limit and undrained shear strength of soil—reappraisal." *Journal of Geotechnical and Geoenvironmental Engineering*. August 2003, 129(8), 774 – 777.

Shi, L.; Chu, E.; Anguelovski, I.; Aylett, A.; Debats, J.; Goh, K.; Schenk, T.; Seto, K. C.; Dodman, D.; Roberts, D.; Roberts, J. T.; VanDeveer, S. D. (2016). :Roadmap towards justice in urban climate adaptation research." *Nat. Clim. Chang.*, *6*, 131–137.

Silva, S.F.; Martinho, M.; Capitão, R.; Reis, T.; Fortes, C.J.; Ferreira, J.C. (2017). "An index-based method for coastal-flood risk assessment in low-lying areas (Costa de Caparica, Portugal)". *Ocean Coast. Manag*., 144, 90–104.

Smit, B.; Wandel, J. (2006). "Adaptation, adaptive capacity and vulnerability." *Glob. Environ. Change*, *16*, 282–292.

Smith, J. B.; Klein, R. J. T.; Huq, S. (2003). *Climate change, adaptive capacity and development*; Imperial College Press: London.

SonTek (2014). Personal email correspondence and quote regarding "16 MHz MicroADV Splash Proof system" September.

Spears B.M., Saunders J.E., Davidson I., and Paterson D.M. (2008). "Microalgal sediment biostabilisation along a salinity gradient in the Eden Estuary, Scotland: Unravelling a paradox." *Marine and Freshwater Research*, 59(4), 313-321.

Sutton-Grier, A., Wowka, K., and Bamford, H. (2015) “Future of our coasts: The potential for natural and hybrid infrastructure to enhance the resilience of our coastal communities, economies and ecosystems.” *Environmental Science and Policy,* 51, 137-148.

Tabujew, I. and Peneva, K. (2015). “Functionalization of Cationic Polymers for Drug Delivery.” *Royal Society of Chemistry.* RSC Polymer Chemistry Series No. 13, Cationic Polymers in Regenerative Medicine.

Tolhurst, T.J., Black, K.S., Shayler, S.A., Mather, S., Black, I., Baker, K., and Paterson, D.M. (1999). "Measuring the in situ Erosion Shear Stress of Intertidal Sediments with the Cohesive Strength Meter (CSM)." *Estuarine, Coastal and Shelf Science Estuarine, Coastal and Shelf Science,* 49(2), 281-294.

Tolhurst, T.J., Defew, E.C., de Brouwer, J.F.C., Wolfstein, K., Stal, L.J., and Paterson, D.M. (2006). "Small-scale temporal and spatial variability in the erosion threshold and properties of cohesive intertidal sediments." *Cont.Shelf Res.,* 26(3), 351-362.

TRS (2014). “Resilience to extreme weather.” *The Royal Society, Science Policy Center*, London, Report 02/14, Chapter 3.

USACE (2013). “Coastal risk reduction and resilience: using the full array of measures.” *Directorate of Civil Works, US Army Corps of Engineers*, CWTS 2013-3.

USACE (2015). “Use of Natural and Nature-Based Features (NNBF) for Coastal Resilience, Final Report.” *Engineer Research and Development Center, US Army Corps of Engineers*, ERDC-SR-15-1

USGS Structured Decision Making for Management of Warm-Water Habitat of Manatees Available online: https://www.usgs.gov/centers/wetland-and-aquatic-research-center-warc/science/structured-decision-making-management-warm?qt-science_center_objects=1#qt-science_center_objects (accessed on Oct 3, 2017).

Watts, C.W., Tolhurst, T.J., Black, K.S., and Whitmore, A.P. (2003). "In situ measurements of erosion shear stress and geotechnical shear strength of the intertidal sediments of the experimental managed realignment scheme at Tollesbury, Essex, UK." *Estuarine, Coastal & Shelf Science,* 58(3), 611-620.

Whitcomb, P. J., Gutowski, J., and Howland, W. W. (1980). "Rheology of guar solutions." *J Appl Polym Sci,* 25(12), 2815.

Widdows, J., Friend, P.L., Bale, A.J., Brinsley, M.D., Pope, N.D., and Thompson, C.E.L. (2007). "Inter-comparison between five devices for determining erodability of intertidal sediments." *Continental Shelf Research*, 27(8), 1174-1189.

Yallop, M. L., Paterson, D. M., and Wellsbury, P. (2000). "Interrelationships between rates of microbial production, exopolymer production, microbial biomass, and sediment stability in biofilms of intertidal sediments." *Microbial Ecology*, 39, 116-127.

Yang, Z., Yang, H., and Yang, H. (2018). "Effects of sucrose addition on the rheology and microstructure of κ-carrageenan gel." *Food Hydrocoll.,* 75 164-173.

Younger, M.; Morrow-Almeida, H. R.; Vindigni, S. M.; Dannenberg, A. L. (2008). "The built environment, climate change, and health: opportunities for co-benefits." *Am. J. Prev. Med.*, *35*, 517–526.

Yu, W., Tong, D., Zhou, C., Lin, C. X., and Xu, C. (2013). "Adsorption of proteins and nucleic acids on clay minerals and their interactions: A review." *Appl.Clay.Sci.,* 80-81 443-452.

Zaidi, A.; Timothy, D. T. M. Incorporating Natural Infrastructure and Ecosystem Services in Federal Decision-Making Available online: https://www.whitehouse.gov/blog/2015/10/07/incorporating-natural-infrastructure-and-ecosystem-services-federal-decision-making (accessed on Nov 20, 2016).

Zhang, G., Yin, H., Lei, Z., Reed, A., and Furukawa, Y. (2013). "Effects of exopolymers on particle size distributions of suspended cohesive sediments." *Journal of Geophysical Research: Oceans*, Vol. 118, 1–17.

.